Spring 2011

Absorbing state transitions in clean and disordered lattice models

Man Young Lee

Department: Physics

ABSORBING STATE TRANSITIONS IN CLEAN AND DISORDERED LATTICE MODELS

by

MAN YOUNG LEE

A DISSERTATION

Presented to the Faculty of the Graduate School of the

MISSOURI UNIVERSITY OF SCIENCE AND TECHNOLOGY

In Partial Fulfillment of the Requirements for the Degree

DOCTOR OF PHILOSOPHY

in

PHYSICS

2011

Approved by

Dr. Thomas Vojta, Advisor
Dr. Gerald Wilemski
Dr. Julia E. Medvedeva
Dr. Paul E. Parris
Dr. Uwe C. Tauber

PUBLICATION DISSERTATION OPTION

This dissertation contains two parts, a general introduction (section 1) and preprints of four research papers (sections 2-5) that have already been published or that are submitted for publication. The introductory chapter is written in normal dissertation style. Section 2 is published in Phys. Rev. Lett, vol. 96, p. 035701, 2006. Section 3 is published in Phys. Rev. E, vol. 79, p. 041112, 2009. Section 4 is published in Phys. Rev. E, vol. 81, p. 061128, 2010. Section 5 is accepted for publication in Phys. Rev. E. All articles are written in the style (REVTEX4) of the American Physical Society.

ABSTRACT

Nonequilibrium systems can undergo continuous phase transitions between different steady states. These transitions are characterized by collective fluctuations over large distances and long times similar to the behavior of equilibrium critical points. They also can be divided into different universality classes according to their critical behavior.

This dissertation considers two types of nonequilibrium transitions. First study concerns absorbing state transitions on a randomly diluted lattice. Second study deals with nonequilibrium models with several absorbing states. We investigate two specific nonequilibrium lattice models, i.e., the contact process and the generalized contact process by means of both theoretical and computational approaches.

In section 1, we introduce the basic arguments and theories to support our investigations for both problems. In sections 2 and 3, we investigate nonequilibrium phase transitions of the contact process and the generalized contact process on a percolating lattice, focusing on the transition across the lattice percolation threshold. In this study, we show that the interplay between geometric criticality due to percolation and dynamical fluctuations of the nonequilibrium system leads to a new universality class. The critical point is characterized by ultra-slow activated dynamical scaling and accompanied by strong Griffiths singularities. We support our theory by extensive Monte-Carlo simulations. In sections 4 and 5, we investigate the generalized contact process on one and two-dimensional lattices. We treat the creation rate of active sites between inactive domains as an independent parameter. It turns out that this model has an unusual phase diagram with two different nonequilibrium phase transitions. The special point separating them shares some characteristics with a multicritical point. For one dimension, a small boundary rate takes the system from the directed percolation universality class to the parity-conserved class. For two dimensions, the critical behavior on the generic transition line is of mean-field type with logarithmic corrections suggesting that the two-dimensional generalized contact process is in the generalized voter universality class.

ACKNOWLEDGMENT

First of all, I sincerely thank to Dr. Thomas Vojta. His name was very big and admirable to me during past six years. His passionate teaching led me to physics and his affectionate supports were able to make me study in Rolla. It was impossible to finish my doctorate program without him. I owe a deep gratitude to him and his family. Many Thanks to my advisor Dr. Vojta again.

My gratitude goes to my committee members: Dr. Gerald Wilemski, Dr. Julia E. Medvedeva, Dr. Paul E. Parris, and Dr. Uwe C. Tauber. I took many helps from Dr. Parris, Dr. Wilemski, and Dr. Medvedeva. Their advices for physics inspired me and their suggestions were valuable enough to finish my doctorate program. Dr. Tauber is one of master maestros in my research field. It was really good to me that he was one of my committee member. Thanks for your joining from Virginia. Many thanks to all committee again.

I wish to thank our chairman, Dr. George D. Waddill, and staffs: Ellen Marie Kindle, Pamela J. Crabtree, and Russell L. Summers. They helped and took care of me for my school life. Thanks very much! Also I want to thank Dr. Jose Hoyos, Chetan Kotabage, Ben Payne, and Dr. Vojta's research group members. It was very useful and joyful to discuss with them concerning about physics and other interesting topics.

Finally, many thanks go to my parents for their endless love and support. Their true love and strong trust made me always to keep my faith and road. I owe a deep gratitude and love to them. I really want to say in here that *I love you and I devote my doctoral degree to you.* I wish to thank my brother, Cheonyoung, and my sister's family: Jisook, Giyeol, and their children: Yeonseo and Yejoon are the source of my smile. Their concerns for an elder brother have allowed me to sustain over long time. I love my family (Sarang hapnida woori gajokeul.....).

TABLE OF CONTENTS

LIST OF ILLUSTRATIONS

LIST OF TABLES

1. INTRODUCTION

1.1. EQUILIBRIUM PHASE TRANSITIONS

Phase transitions are fundamental processes that have been detected in nature. What is a phase transition? A phase transition can be defined as the singularity of the free energy and other thermodynamic variables that occurs if a system transforms from one state to a qualitatively different one. One of the examples is the phase transition of water from liquid to vapor. If water is heated at atmospheric pressure, the temperature increases until the evaporation temperature ($T = 373.15K$) is reached. At this point, further heating does not increase the temperature, but only turns the liquid water into vapor. This heat is called *latent heat* which overcomes the attractive forces between the water molecules in the liquid state. When all of the liquid has evaporated, then the temperature rises again. This phenomenon formally corresponds to an infinite heat capacity

$$C_p = T\frac{\partial S}{\partial T}|_p, \tag{1}$$

at the evaporation temperature [1]. If the entropy S is discontinuous at the transition temperature, the transition is called a *first-order phase transition.* In contrast a phase transition at which the entropy is continuous, is called a *second-order phase transition* or *critical point.* In other words, 1st order phase transitions involve latent heat, while continuous transitions do not.

The phase transition of liquid to vapor at atmospheric pressure is of 1st order, characterized by a large jump in density. If one follows the phase boundary to higher T, this density difference goes to zero at a critical point, at $T_c = 647\,K$ for water. This behavior of the density difference means that a second order phase transition occurs at the critical point.

Systematic investigations of phase transitions started, perhaps, in 1869 when T. Andrews discussed the liquid-gas critical point in CO_2 [2, 3]. In 1894, van der Waals suggested the equation of state $(P + a/V^2)(V - N_A b) = RT$ for a fluid of volume V, pressure P, and temperature T. It provided one of the first theoretical explanations of phase transition phenomena. In 1895, P. Curie noticed the similarity of the magnetic critical point in iron to the liquid-gas critical point. After that, magnetism became one of major topics in phase transition phenomena research. After the Ising model (1925) was introduced, L.D. Landau (1937) suggested his general theory for phase

transitions [4, 5]. We now know that Landau theory is not exact because it does not contain fluctuation effects. Nonetheless, Landau theory remains a valuable starting point for the investigation of critical phenomena. The modern area of phase transition research started in 1944, when L. Onsager [6] solved the two dimensional Ising model exactly and found behavior different from Landau theory.

1.1.1. Phase Transitions in Magnetism. From the early 20th century to the present, many physicists have tried to understand and solve the phase transition phenomena in magnetic materials. The most basic theoretical model, called the Ising model, was introduced by Lenz and Ising [7, 8] who were studying the phase transition of *ferromagnets* at the Curie temperature. This model consists of a lattice in which each site is occupied by a binary "*spin*" variable $s_i = \pm 1$. Each spin interacts with its neighbors. If no external field exists, the Hamiltonian is given by

$$H(s_1, s_2, \ldots, s_N) = -J \sum_{<ij>} s_i s_j, \tag{2}$$

where J is an interaction energy. For $J > 0$ spins prefer to be parallel, leading to ferromagnetic behavior while $J < 0$ leads to antiparallel spin configurations (antiferromagnet). For $J > 0$ and sufficiently low temperature $T < T_c$, where T_c is the critical temperature, all spins align parallel to a common axis and this phase is called a ferromagnetic phase. If $T > T_c$, the parallel alignment is destroyed by thermal motion. This phase is called a paramagnetic phase. The two phases can be distinguished via the magnetization $m =< s_i >$, which is the *order parameter* of the transition; $m = 0$ corresponds to the paramagnetic phase, and $m \neq 0$ corresponds to the ferromagnetic phase. This is illustrated in the left panel of Fig. 1.1. The ferromagnet has two equivalent states ($m > 0$ and $m < 0$) at low temperature. As the external field $H \rightarrow 0^+$, the magnetization m approaches a non-zero positive value. However, when H changes sign at $H = 0$, m has same magnitude but different sign. Crossing the $H = 0$ line at $T < T_c$ is thus a first-order phase transition. From $T \geq T_c$, m is continuous at $H = 0$. Thus, as in the liquid-gas case the critical point at $T = T_c$ is the end point of the line of first-order phase transitions, as is illustrated in the right panel of Fig. 1.1.

1.1.2. Landau Theory. Early theoretical approaches to phase transitions were of the *mean-field theory* (MFT) type. The MFT is an approximative method and is broadly used in many-body problems. This theoretical method is based on the assumption that neighboring spins affect a selected spin only via their average field. Thus, the problem is reduced to a one-body problem with an effective field.

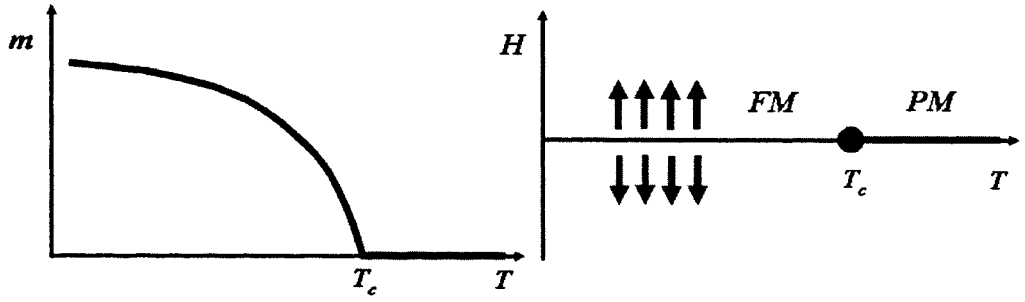

Figure 1.1. Phase transition in a ferromagnet. Left: Behavior of the order parameter. Right: Phase diagram of the ferromagnet as function of temperature and external magnetic field. When the external field $H = 0$, a continuous (second-order) phase transition occurs at $T = T_c$.

Landau introduced a generalization of earlier MFT, now called the *Landau theory*. The significant assumption of Landau theory is that in the vicinity of the critical point, one may expand the free energy in a power series in the order parameter [9]. Thus the free energy F is a function[1] of the magnetization m, and the external magnetic field h,

$$F \backsimeq -hm + am^2 + bm^3 + cm^4 \cdots , \tag{3}$$

where a, b, and c are system parameters. The stable physical state is given by the minimum of F. In this section we shall only consider the symmetric case, therefore we can set $b = 0$ (In the case of $b \neq 0$, a first-order transition would occur).

If no external field exists ($h = 0$), the critical point of Landau theory is easily explained. When $T > T_c$, $m = 0$ gives a minimum of F. When $T < T_c$, two minima of F appear (see Fig. 1.2) and are corresponding to

$$m = \pm\sqrt{\frac{-a}{2c}}. \tag{4}$$

In the Fig. 1.2, the two inner dashed parabolas are corresponding to $T > T_c$ and the outer dashed parabolas represent the condition $T < T_c$. Thus $a > 0$ corresponds to the paramagnetic phase, $a < 0$ corresponds to the ferromagnetic phase. Close to

[1]It is known as the *Landau function* equal to the Gibbs free energy.

T_c we can thus write $a = a_0(T - T_c)$ with a positive constant a_0. The *singularity* in Eq. (4) is an example of the critical singularities generally occurring in the vicinity of a critical point, i.e.,

$$m(T) \sim |T - T_c|^{\beta}, \tag{5}$$

$$\chi(T) \sim |T - T_c|^{-\gamma}, \tag{6}$$

$$C(T) \sim |T - T_c|^{-\alpha}, \tag{7}$$

and

$$m_c(T_c, h) \sim h^{1/\delta}, \tag{8}$$

where $\chi(T)$ is the magnetic susceptibility, $C(T)$ is the specific heat, and m_c is the magnetization at $T = T_c$. As follows from Eq. (4), the critical exponent for the magnetization m in Landau theory is $\beta = 0.5$. The other exponents take the values $\alpha = 0$, $\gamma = 1$, and $\delta = 3$ in Landau theory [9, 10]. For example, by using the minimization property $(\partial F/\partial m) = 0$, we obtain a nonlinear equation for m. The magnetic susceptibility is then given by $\chi(T) = (\partial h/\partial m)_T^{-1}$. If $T > T_c$ under the condition of $m \longrightarrow 0$, $\chi(T) = 1/2a(T)$. If $T < T_c$, $\chi(T) = -1/4a(T)$. These two power-laws give a critical exponent $\gamma = 1$.

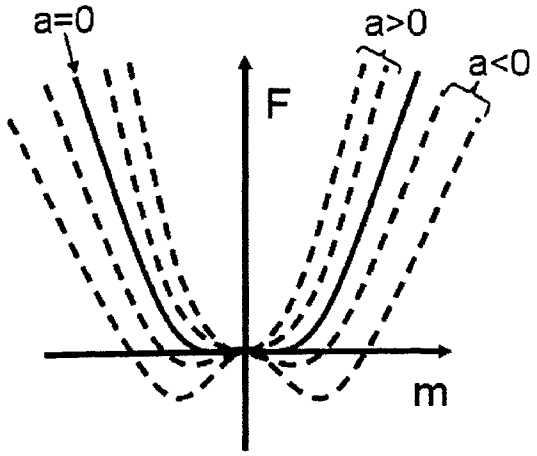

Figure 1.2. Landau free energy for a sequence of temperatures with $a = a_0(T - T_c)$ and $b = 0$. The two inner dashed parabolas correspond to $T > T_c$ and the outer dashed parabolas represent the condition $T < T_c$.

The Landau free energy depends only on the average value of the order parameter, it does not contain any space dependence. Landau theory can be generalized by making m a function of position and adding a gradient term to the free energy. The minimum condition $\partial F/\partial m(\vec{r}) = 0$ then reads

$$-D\nabla^2 m - h + 2bm + 4cm^3 \cdots = 0. \tag{9}$$

By expanding m and h about their averages, $m_0 + \delta m(\vec{r})$ and $h_0 + \delta h(\vec{r})$, where m_0 and h_0 are constants, one can find the δm-δm correlation function $G(\vec{r}) \sim exp(-r/\xi)$. The correlation length $\xi(T)$ diverges as

$$\xi(T) \sim \mid T - T_c \mid^{-\nu}, \tag{10}$$

at the critical point where the correlation length critical exponent is $\nu = 1/2$.

1.1.3. Fluctuations and Ginzburg Criterion. A crucial question for the validity of Landau theory is the strength of the order parameter fluctuations. In the original Landau theory, Eq. (3), they have been neglected, and even in the generalized form leading to Eq. (9), they have been assumed to be small. In this subsection we discuss under what conditions this assumption is fullfilled. The long-range fluctuations are described by correlation functions

$$G(\vec{x_1} - \vec{x_2}) = \langle m(\vec{x_1})\, m(\vec{x_2}) \rangle - \langle m(\vec{x_1}) \rangle \langle m(\vec{x_2}) \rangle, \tag{11}$$

where $\vec{x_1} - \vec{x_2} = \vec{r}$ is the distance and $m(\vec{x})$ is the order parameter. In a ferromagnet fluctuations can be considered small, if

$$\frac{\int d^d\vec{r}\, G(\vec{r})}{\int d^d\vec{r}\, m^2} \ll 1, \tag{12}$$

where the integrals are taken over a correlation volume. Statistically the numerator represents the variance of the order parameter fluctuation and it is compared with the mean-square value of the order parameter. Close to the critical point, $G(\vec{r})$ takes the general form [3]

$$G(\vec{r}) \simeq \frac{1}{\vec{r}^{d-2+\eta}} exp(-\frac{\vec{r}}{\xi}), \tag{13}$$

where ξ represents the correlation length. The critical exponent is $\eta = 0$ in Landau theory. Evaluating Eq. (12) leads to

$$|T - T_c|^{d\nu - 2\beta - 2\nu} \ll const \tag{14}$$

for $T \rightarrow T_c$, and the exponent must satisfy the condition

$$d\nu - 2\beta - 2\nu > 0. \tag{15}$$

Inserting the mean field values $\nu = 1/2$, $\beta = 1/2$ gives $d > 4$. The effects of fluctuations must therefore be considered for $d < d_c^+ = 4$ to describe the critical behavior correctly. In contrast, for $d > d_c^+$, we can expect Landau theory to give the correct critical behavior. d_c^+ is called the upper critical dimension, and the condition (15) is the *Ginzburg criterion* [11].

1.1.4. Landau-Ginzburg-Wilson Theory. In order to adequately describe the order parameter fluctuations, one needs to generalize the Landau free energy function (3) to a functional that depends on a spatially varying order parameter field $\phi(x)$. Expanding in both ϕ and its gradient yields the so-called *Landau-Ginzburg-Wilson* (LGW) theory [12, 13, 14]

$$S\left[\phi\left(\vec{x}\right)\right] = \int d^d x \left[t\phi^2\left(\vec{x}\right) + c\left(\nabla\phi\left(\vec{x}\right)\right)^2\right] + u\int d^d x \phi^4\left(\vec{x}\right). \tag{16}$$

In contrast to the original Landau theory, the LGW theory is a nontrivial many-body problem which cannot be solved in closed form. Understanding critical phenomena based on the LGW theory was made possible by the development of the renormalization group by K.G. Wilson [12, 13] who was awarded the 1982 Nobel Prize in physics.

Wilson's renormalization group (RG) is based on the earlier idea of *Kadanoff scaling* [3, 9, 15]. The crucial idea is that at a critical point the correlation length diverges and therefore the system effectively looks scale invariant. We shall explore these scaling ideas in Subsec 1.2.

1.1.5. Universality Class. Critical phenomena are characterized by sets of critical exponents and systems can be classified according to the values of these exponents. Interestingly, the critical exponents of several physical systems are exactly identical. Thus, we can aggregate these models and label them as being in

same *universality class* [9, 10]. Usually, critical exponents depend on the spatial dimensionality[2] d, and on the symmetry of the order parameter. For example, the $3d$ Ising model and the $2d$ Ising model do not have the same critical exponents. The Heisenberg model also should not be described by critical exponents of the $3d$ Ising model: although the two models have the same dimensionality, they have different order parameter symmetries ($O(3)$ vs $Z(2)$). The universality class is independent of microscopic details such as the geometric structure of the lattice (triangular, square, and hexagonal lattice) [9, 10]. Critical exponents for low dimensional Ising models are shown in the Table 1.1.

Table 1.1. The critical exponents of the Ising model. MF: Mean-field solution; Onsager solution (1944): Exact solution of two-dimensional Ising model without a field; Ising ($d = 3$): Results of computational experiments.

	MF	Onsager solution ($d = 2$)	Ising ($d = 3$)
α	0	0	0.110(5)
β	1/2	1/8	0.325±0.0015
γ	1	7/4	1.2405±0.0015
δ	3	15	4.82(4)
ν	1/2	1	0.630(2)
η	0	1/4	0.032±0.003

1.2. SCALING THEORY

In this section, we shall introduce the *scaling theory* [3, 9, 10] for equilibrium phase transitions. The scaling theory is based on the assumption that the only relevant length close to a critical point is the correlation length [16]. As shown previously, physical quantities are characterized by power-laws in the vicinity of the critical point and these power-laws mathematically have the implicit property of scale invariance. In order to define the concept of scaling, we introduce the Widom scaling [17] assumption and the Kadanoff block-spins [15] which illustrate a schematic example for scaling properties near the critical point.

1.2.1. Scaling Properties Near the Critical Point. Consider a system of interacting spins on a lattice of lattice constant r_0, distance from criticality t

[2]Dimensionality does not affect the universality class if $d \geq d_c^+$, d_c^+ is the upper critical dimension.

and field h. If the system is close to a ferromagnetic phase transition, neighboring spins are mostly parallel. This implies that we can approximately replace a group of neighboring sites (or bonds) by a single site. Repeating this everywhere in the lattice leads to a new lattice of "block-spins" with a lattice constant lr_0 and modified distance from criticality t_l and field h_l. If we now rescale all lengths by a factor l, the free energy density changes by a factor l^{-d}. Further assuming that $t_l = l^x t$ and $h_l = l^y h$, we obtain the scaling form

$$f(t,h) = l^{-d} f(l^x t, l^y h) \tag{17}$$

for the free energy and the correlation length

$$\xi(t,h) = l\xi(l^x t, l^y h). \tag{18}$$

This implies that f and ξ are not functions of the two variables t, h independently. Instead, they can be combined to one relevant variable. For example, if we simply set l to $l = t^{-1/x}$, functional forms of the free energy and the correlation length are

$$f(t,h) \sim t^{d/x} f(ht^{-y/x}) \quad , \quad \xi(t,h) \sim t^{-1/x} \xi(ht^{-y/x}). \tag{19}$$

This is the scaling hypothesis.[3] [9, 10, 17, 16]. These relations were first found by Wilson [12, 13] on a phenomenological basis.

By taking the appropriate derivative of f, the scaling behavior of thermodynamic functions can be found. When $h = 0$, the two functions in Eq. (19) give the power-laws $f(t) \sim t^{d/x}$ and $\xi(t) \sim t^{-1/x}$ respectively. For the ferromagnetic phase transition, the spontaneous magnetization $m(t)$ is

$$m(t) \sim t^{(d-y)/x}, \tag{20}$$

because $m = \partial f / \partial h$. Comparing with $m(t) \sim t^{\beta}$ gives a relationship which is called the *scaling relation* [9, 10, 16]

$$\beta = \frac{d-y}{x} = (d-y)\nu \tag{21}$$

[3] Widom proposed that close to the critical point the singular part of the free energy density $f = F/V$ is a function of one rather than two arguments, see Refs. [16, 17].

with $\nu = 1/x$. The magnetization at the critical point ($t = 0$) with $l = h^{-1/y}$,

$$m \sim h^{(d-y)/y}, \tag{22}$$

gives another scaling relation which is called the *Widom scaling relation* [17],

$$\delta = \frac{y}{d-y}. \tag{23}$$

From the susceptibility and the specific heat, $\chi = (\partial m/\partial h)_T$, $C = -T(\partial^2 f/\partial t^2)_h$, two more scaling relations can be derived

$$\gamma = \frac{2y-d}{x} = (2y-d)\nu, \tag{24}$$

$$\alpha = \frac{2x-d}{x} = 2 - d\nu. \tag{25}$$

By using these scaling relations for the critical exponents, we can derive the *Rushbrook scaling law* [16] and the *Widom scaling law* [17, 18],

$$\alpha + 2\beta + \gamma = 2 \tag{26}$$

$$\alpha + \beta(\delta + 1) = 2. \tag{27}$$

1.3. PERCOLATION THEORY

Percolation concerns the movement of particles on randomly connected network systems [19, 20, 21]. Representative examples can be found in forest fires, oil fields, diffusion in disordered media, and random magnetism. For example, water moving through porous rocks is a well-known example of percolation phenomena in nature. In this case, the paths for water can be considered a random network. If one considers percolation on a lattice consisting of "sites" connected by "bonds", one can distinguish two different kinds of percolation problems. If the sites are randomly occupied or empty, we speak of a *site percolation* problem. In contrast, a bond percolation problem arises if the bonds can be present or absent with some probability. Percolation is a purely geometric problem in which *clusters* of connected sites or bonds are clearly defined static objects. Percolation theory treats and predicts the geometric properties of these clusters on the network mathematically.

Historically, Flory (1941) [19] and Stockmayer (1943) [22] developed the framework of percolation theory on the *Bethe lattice* (or Cayley tree model) to describe polymerization processes in which small molecules branch to macromolecules. In 1957, Broadbent and Hammersley [23] introduced the percolation problem into the

mathematics literature. The relations between percolation and critical phenomena have been studied in great detail since the 1970's [24, 25].

1.3.1. Site Percolation on A Lattice. Consider an infinite lattice system, with each site randomly occupied independent of its neighbors with probability p. When $p = 0$, all sites are in empty state, but empty sites are getting occupied at $p > 0$. All sites are occupied at $p = 1$. In the region $0 < p < 1$, the occupied sites form connected clusters, whose typical size increases with p. For small p, below some critical value p_c, called the percolation threshold, all clusters are of finite size, even in an infinite lattice. When p reaches p_c, an infinite cluster of connected sites starts to form which spans the entire sample. The phase transition occurring across p_c is called the percolation transition. Its order parameter is the probability $P_\infty(p)$ of a site to belong to the infinite cluster. The percolation transition is illustrated in Figs. 1.3 and 1.4. In the left panel of Fig. 1.3, the infinite cluster has not appeared yet, this corresponds to $P_\infty = 0$. At $p \geq p_c$ the infinite cluster appears (see right panel of Fig. 1.3) and $P_\infty \neq 0$. Close to p_c, the order parameter follows a power-law with the critical exponent β,

$$P_\infty \sim (p - p_c)^\beta \qquad p \to p_c^+, \tag{28}$$

analogous to the critical phenomena discussed in Subsecs 1.1 and 1.2. The critical exponent β is only dependent on the dimensionality and, as mentioned before, this is known as universality[4].

1.3.2. Distribution of Finite-size Clusters. An interesting question in percolation theory is the distribution of the sizes of the clusters, and how it changes with p. Since the probability of a site to be occupied is p, one can imagine that the s-cluster has s occupied sites with probability p^s and the occupied edge sites have empty neighboring sites with the probability $1 - p$ each. However, the number of these perimeter sites depends on the shape of the cluster. Therefore the number of clusters with s sites per lattice $n_s(p)$ is

$$n_s(p) = \sum_t g(s, t) p^s (1 - p)^t, \tag{29}$$

where $g(s,t)$ is a configuration factor[5] and t is a number of perimeter sites. The summation $\sum_t g(s, t)$ is proportional to $s^{-\theta} A^s$ on the condition of s being very large

[4]In this section we only treat a site percolation problem, but in agreement with universality, a bond percolation shows same critical behavior.

[5]The number of lattice animals (or configurations of finite clusters) with size s and perimeter t.

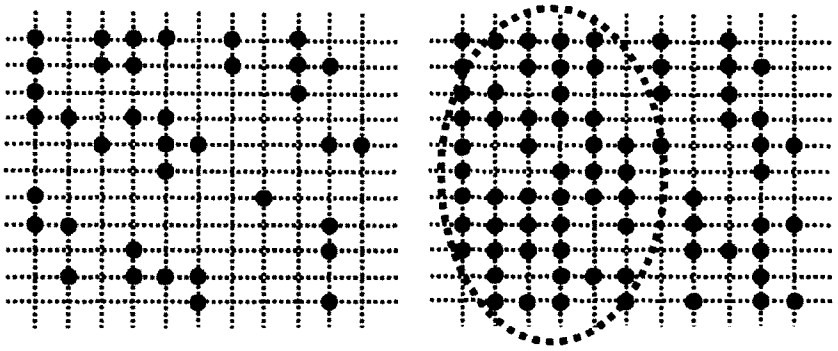

Figure 1.3. Example of site percolation on the square lattice. Left: At $p < p_c$, occupied sites form small finite-size clusters. Right: At $p \geq p_c$, an infinite cluster spanning the entire lattice emerges. Blue dashed oval shows the infinite cluster.

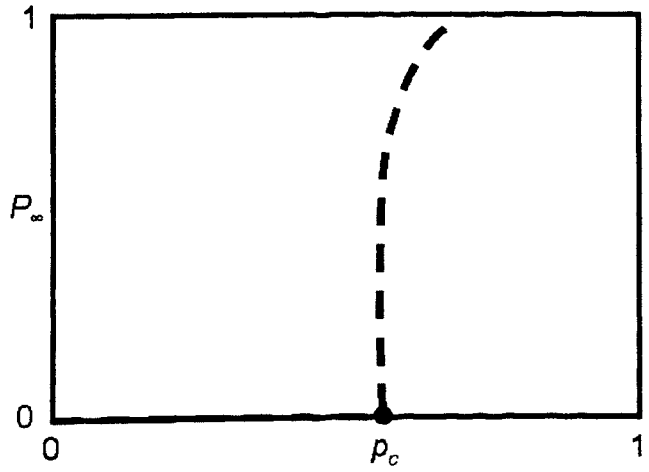

Figure 1.4. The behavior of the order parameter (P_∞) at the percolation transition. Here p_c is a percolation threshold (critical point).

[21, 25, 26],

$$g(s) = \sum_t g(s, t) \sim s^{-\theta} A^s, \tag{30}$$

where A is a constant and θ is an exponent[6] which is associated with the statistics of lattice animals [27, 28].

When $p \to 0$ under the condition of $s \to \infty$, this condition gives $(1-p)^t \simeq 1$ and therefore $n_s(p)$ is given by,

$$\begin{aligned} n_s(p &< p_c) \sim s^{-\theta} p^s A^s \\ &= s^{-\theta} \exp\left(-s \ln\left(\frac{1}{pA}\right)\right) \\ &\sim \exp\left(-c_1 s\right). \end{aligned} \tag{31}$$

When $p > p_c$, if p is close to 1, this condition gives $p^s \simeq 1$. Here, we can neglect the term for $g(s)$ because s is close to the system size. Thus $n_s(p)$ is given by

$$\begin{aligned} n_s(p &> p_c) \sim const \cdot (1-p)^t \\ &\sim B(s) \exp\left(-t \ln \frac{1}{1-p}\right) \sim \exp\left(-c_2 \cdot t\right). \end{aligned} \tag{32}$$

In d-dimensional hyper-cubic lattice, s is proportional to r^d, $s \sim r^d$, and t is proportional to r^{d-1}, $t \sim r^{d-1}$. Therefore by using

$$t \sim r^{d-1} = s^{1-1/d}, \tag{33}$$

we obtain the cluster size distribution

$$n_s(p > p_c) \sim \exp\left(-c_2 \cdot s^{1-1/d}\right). \tag{34}$$

The results of Eqs.(31) and (34) can be combined. Using the analogy between percolation and critical phenomena, we can postulate a scaling form for $n_s(p)$ close to the percolation threshold (this also follows from *Fisher's Ising droplet model*[7] [29]),

$$n_s(p) = s^{-\tau} f[s^{\sigma}(p - p_c)] \tag{35}$$

with

$$f(x) \sim \exp[-const \cdot x^{1/\sigma}] \qquad (x > 0) \tag{36}$$

[6]For examples: $\theta = 1\,(d = 2)$, $3/2\,(d = 3)$, and $5/2\,(d > 8)$ in the Bethe lattice.

[7]This model was first suggested by Essam and Fisher (1963) and extended by Fisher (1967). In this droplet model, $z \sim As^{\sigma}$ represents droplet's surface area where s is the number of molecules in the droplet and A is a constant of order unity to differentiate shapes of the droplet.

and

$$f(x) \sim \exp[-(const \cdot x^{1/\sigma})^{1-1/d}] \qquad (x < 0). \tag{37}$$

Here, σ and τ are critical exponents.

1.3.3. Criticality and Scaling of Percolating Clusters. In this subsection, we relate the scaling of the cluster number to other critical properties of the percolation problem. Each lattice site is either empty or occupied, and if it is occupied, it belongs either to a finite cluster or to the infinite cluster. The fraction $P_\infty(p)$ of sites belonging to the infinite cluster is thus given by,

$$P_\infty(p) = p - \sum_s n_s s. \tag{38}$$

Here, the sum over s gives the probability that an arbitrary chosen site belongs to any finite cluster. Thus, near the critical point p_c, the relative strength is $P_{\infty,rel}(p) = P_\infty(p) - P_{\infty,c}(p)$, but $P_{\infty,c}(p) = 0$ because $\sum_s n_s(p_c)s = p_c$. By using these relations we can show that the asymptotic behavior of $P_{\infty,rel}(p)$ is represented by the following

$$\begin{aligned} P_{\infty,rel}(p) &= P_\infty(p) - P_{\infty,c}(p) \\ &= \sum_s [n_s(p_c) - n_s(p)]\, s + O(p - p_c) \\ &\sim |p - p_c|^{\frac{\tau-2}{\sigma}} \int_0^\infty dz\, z^{-1-(\frac{\tau-2}{\sigma})}[f(z) - f(0)], \end{aligned} \tag{39}$$

where $z = |p - p_c|\, s^\sigma$ (or $z = |p - p_c|^{1/\sigma}\, s$) and the integration over z gives the gamma function. In this integration, only $z > 0$ could be considered, because the infinite cluster dose not exist in $p < p_c$. The integration converges to a finite value and the leading behavior of $P_\infty(p)$ is

$$P_\infty(p) \sim (p - p_c)^{\frac{(\tau-2)}{\sigma}}. \tag{40}$$

Therefore, from Eqs. (28) and (40), we obtain the relation for the critical exponent β,

$$\beta = \frac{\tau - 2}{\sigma}. \tag{41}$$

The average cluster size S is obtained by

$$\begin{aligned} S &= \sum_s \frac{n_s s^2}{\sum n_s s} \\ &\sim \int ds\, s^{2-\tau} \exp(-cs) \\ &\sim |p-p_c|^{\frac{(\tau-3)}{\sigma}} \int dz\, z^{-1+\frac{(3-\tau)}{\sigma}} f(z). \end{aligned} \tag{42}$$

Comparing with the definition $S \sim |p-p_c|^{-\gamma}$ which follows from the analogy between S and the susceptibility Eq.(6), we have

$$\gamma = \frac{3-\tau}{\sigma}. \tag{43}$$

The total number of clusters per site $M(p)$ is defined by

$$M(p) = \sum_s n_s(p) \tag{44}$$

and it is analogous to the free energy per site $F(T) \sim |T-T_c|^{2-\alpha}$. Therefore the critical exponent α is obtained by the following steps,

$$\begin{aligned} M &= \sum_s n_s \sim \int ds\, s^{-\tau} \exp(-cs) \\ &\sim |p-p_c|^{\frac{(\tau-1)}{\sigma}} \int dz\, z^{-1+\frac{(1-\tau)}{\sigma}} f(z), \end{aligned} \tag{45}$$

$$\alpha = 2 - \frac{\tau-1}{\sigma}. \tag{46}$$

By combining the three scaling laws above, Eqs. (41), (43), and (46), we can confirm the Rushbrooke scaling law

$$\alpha + 2\beta + \gamma = 2. \tag{47}$$

Now we need to investigate the correlation length ξ_p for the percolating cluster, in order to have a full set of critical exponents which describe the critical behavior. As we mentioned before, the correlation length is given by the average distance of two sites belonging to the same cluster. The correlation length follows a power-law

with the critical exponent ν,

$$\xi_p \sim |p - p_c|^{-\nu} . \tag{48}$$

1.3.4. Fractal Dimension of The Percolating Cluster. Close to the percolation threshold, the geometric structure of the spanning cluster is inhomogeneous. Right at p_c its structure is actually that of a fractal, a system of non-integer dimension d_f (called the *fractal dimension*). If $N(L)$ denotes the number of occupied sites in a spanning cluster, $N(L)$ is proportional to L^d for the homogeneous distribution. For the fractal case, however, $N(L)$ is proportional to L^{d_f} and d_f can take non-integer values.

Therefore, if one takes a sphere with radius R in the infinite cluster and then counts the number of occupied sites in that sphere, the count is proportional to R^{d_f}. Since the probability of an arbitrary occupied site to belong the infinite cluster is P_∞ , this gives the relation

$$P_\infty \sim \frac{R^{d_f}}{R^d} \sim \frac{\xi_p^{d_f}}{\xi_p^d} \tag{49}$$

(at $p \neq p_c$, the structure is fractal for length up to the correlation length ξ_p). By Eqs. (28) and (48), one obtains the scaling relation

$$d_f = d - \frac{\beta}{\nu} \tag{50}$$

which is only valid for $d < 6$ [21].

Now to consider the correlation length, we note that ξ^2 is the average distance of two sites belonging to the same cluster or, equivalently, the squared radius of a given cluster. If a site belongs with probability $n_s s$ to an s-cluster with radius R_s, ξ^2 is given by the average of R_s^2 over all clusters

$$\xi^2 = \frac{2\sum_s R_s^2 s^2 n_s}{\sum s^2 n_s} \sim |p - p_c|^{-2\nu} . \tag{51}$$

In the fractal region, $R_s \sim s^{1/d_f}$. Therefore Eq. (51) gives (See Ref. [21])

$$\frac{1}{d_f} = \sigma\nu \tag{52}$$

and, we obtain the scaling law which relates ν to the other exponents

$$d\nu = \gamma + 2\beta = 2 - \alpha = \frac{\tau - 1}{\sigma}. \tag{53}$$

1.4. NONEQUILIBRIUM PHASE TRANSITIONS

The preceding sections dealt with phase transitions in equilibrium systems. However, research has shown that abrupt transitions can also occur between different nonequilibirum steady states. These nonequilibrium phase transitions display large-scale fluctuations and collective behavior over large distances just like equilibrium phase transitions [30, 31, 32]. This section gives an introduction into the nonequilibrium phase transitions in *stochastic nonequilibrium lattice models* [33, 31, 32].

What is a nonequilibrium system? Recall that a thermodynamic equilibrium state is characterized by being time-independent and by the absence of macroscopic currents [34, 35]. Thus, one can broadly distinguish two classes of nonequilibrium systems. In one class are systems whose steady states are proper equilibrium states, but they are prepared in states far from equilibrium. The other class, nonequilibrium steady states, involve macroscopic currents. In the microscopic view, this can be understood by looking at the transition probabilities between microscopic states. Consider the master equation

$$\frac{dP_A(t)}{dt} = \sum_B W_{B\to A} P_B(t) - \sum_B W_{A\to B} P_A(t), \tag{54}$$

where $P_A(t)$ and $P_B(t)$ are the probabilities for each state and W is the transition rate between the two states. In equilibrium, they fulfill the so-called *detailed balance* condition [35], and the $P(t)$ are given by the Boltzmann distribution.

$$W_{B\to A} P_B(t) = W_{A\to B} P_A(t) \tag{55}$$

In contrast nonequilibrium steady states do not require detailed balance [31, 36]. As a result, the key point of difference between equilibrium and nonequilibrium is that the stationary probability distribution and the transition rates are known for the equilibrium, but for the nonequilibrium one must find the time-dependent solutions of the master equations.

In this section we treat nonequilibrium steady states, i.e., nonequilibrium systems of the 2nd kind.

1.4.1. The Contact Process. The *contact process* [37, 38, 39] which was proposed by T.E. Harris in 1974 is a prototype for nonequilibrium lattice models similar to the Ising model for equilibrium lattice models. It can be viewed as a model for describing *epidemic processes*[8] without immunity [31].

The contact process is defined on a d-dimensional hypercubic lattice. Each site can be occupied by a particle (active, denoted by A), or it can be empty (inactive, denoted by I). The time evolution of the contact process is a continuous-time *Markov process* [40] having two basic transitions. (i) Occupied sites can spontaneously become empty with a "healing" rate μ which can be set to unity. (ii) Empty sites get occupied ("infection") at a rate $n\lambda/(2d)$ where n is the number of occupied nearest neighbor sites, and λ is called the infection rate.

The value of λ controls the behavior of the contact process. For sufficiently small λ, the healing process dominates the state of the system. Thus, all sites will eventually become empty, resulting in a completely *inactive state.* For sufficiently large λ, the infection process dominates and a nonzero fraction of sites will remain occupied. This state is called *active state.*

The nonequilibrium phase transition between the inactive and active states which occurs at a critical value $\lambda_c$is a so-called "*absorbing-state*" transition: If the system is in the inactive state (the absorbing state), it cannot leave it anymore.

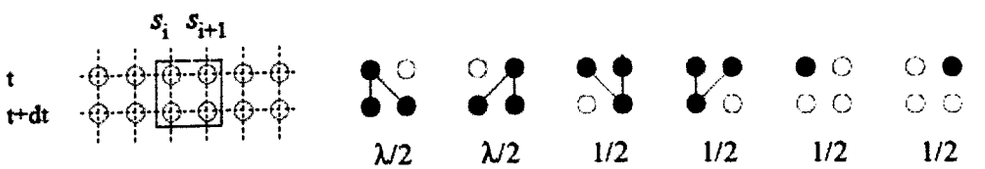

Figure 1.5. Schematic update for the contact process in $d = 1$. Infected-sites (occupied) infect their neighbors at rate $\lambda/2$ ($n = 1$, $d = 1$) and recover at rate 1. This figure is reprinted from Ref. [31]

1.4.2. Critical Phenomena of The Contact Process. The order parameter of the nonequilibrium phase transition in the contact process is the density of

[8]The representative model is the SIR(S) model, the contact process is a generalized version of it on lattices.

active sites ρ_A

$$\rho_A(t) =< \frac{1}{N} \sum_i s_i(t) >, \tag{56}$$

where N is the total number of sites, $s_i = 0, 1$ is the occupation number of site i, and $\langle \cdots \rangle$ denotes the average over the realizations of the Markov process. In the long time limit, if the system is in the active phase ($\lambda > \lambda_c$), ρ_A reaches a nonzero stationary value ρ_A^{stat}, and if the system is in the inactive phase ($\lambda < \lambda_c$), the stationary value of ρ_A is zero. Close to λ_c, the stationary value of the order parameter ρ_A follows a power-law

$$\rho_A^{stat} \sim (\lambda - \lambda_c)^{\beta}, \tag{57}$$

where β is the order parameter critical exponent.

Imagine the contact process starting from a single active site embedded in an otherwise inactive lattice. For $\lambda < \lambda_c$, we expect all activity to die out with time, while for $\lambda > \lambda_c$, activity will survive even for $t \longrightarrow \infty$ with a certain probability. This *survival probability* P_s is thus zero in the inactive phase, but nonzero in the active phase. Close to λ_c, P_s behaves as

$$P_\infty = \lim_{t \longrightarrow \infty} P_s(t) \sim (\lambda - \lambda_c)^{\beta'}, \tag{58}$$

where β' is another critical exponent.

In analogy with equilibrium critical points, one can introduce a correlation length

$$\xi_\perp \sim |\lambda - \lambda_c|^{-\nu_\perp}, \tag{59}$$

and a correlation time

$$\xi_\parallel \sim |\lambda - \lambda_c|^{-\nu_\parallel}, \tag{60}$$

which characterize the clusters of active sites. Here $\nu_\parallel$ and $\nu_\perp$are the critical exponents that characterize the divergence of the correlations in the vicinity of the critical point. The ratio of these two critical exponents produces the dynamical exponent $z = \nu_\parallel / \nu_\perp$,

thus

$$\xi_{\parallel} = \xi_{\perp}^{z}. \tag{61}$$

The four critical exponents, $\nu_{\parallel}$, $\nu_{\perp}$, β , and β', completely determine the universality class of a phase transition in a nonequilibrium lattice model.

In analogy to equilibrium critical phenomena, the behavior of observables close to λ_c is characterized by scaling. Let us discuss critical behavior and scaling properties of the contact process. If we set $\Delta = \lambda - \lambda_c$, the scaling form of the order parameter reads

$$\rho_A(t, \Delta) \sim t^{-\frac{\beta}{\nu_{\parallel}}} F(t^{\frac{1}{\nu_{\parallel}}}\Delta), \tag{62}$$

where F is a universal scaling function [31, 41]. At criticality, ρ_A is simplified to a time-dependent form,

$$\rho_A(t) \sim t^{-\alpha}, \tag{63}$$

where the critical exponent $\alpha = \beta/\nu_{\parallel}$ describes the time evolution of the density (for instance, starting from a fully occupied lattice). The survival probability has the analogous scaling form

$$P_s(t, \Delta) \sim t^{-\frac{\beta'}{\nu_{\parallel}}} \underline{F}(t^{\frac{1}{\nu_{\parallel}}}\Delta), \tag{64}$$

where $\underline{F}$ is another scaling function. Therefore the time evolution of this quantity is, at criticality,

$$P_s(t) \sim t^{-\delta}, \tag{65}$$

where the critical exponent $\delta = \beta'/\nu_{\parallel}$ describes the survival probability at criticality of a cluster starting from a single seed.

Next we study the pair connectedness function $C(x,t) = \langle s_x(t) \cdot s_0(0) \rangle$ which describes the probability that site x is active at time t when starting from a single active site at $x = 0$ and $t = 0$. This correlation function has a scaling form

$$C(x,t) \sim t^{\theta - \frac{d}{z}} X(xt^{-\frac{1}{z}}, \Delta t^{\frac{1}{\nu_{\parallel}}}), \tag{66}$$

where d is the dimensionality and θ is the so-called initial slip critical exponent. In the active phase, as mentioned, $\rho_A(t)$ and $P_s(t)$ both saturate in the long time limit. Therefore their product can be replaced by the autocorrelation

$$C(0,\infty) = \rho P_s \sim \Delta^{\beta+\beta'}. \tag{67}$$

Comparing with the scaling form Eq. (63) in the limit of $x \to 0$ gives

$$C(0,t) \sim t^{\theta-\frac{d}{z}} \underline{X}(\Delta t^{\frac{1}{\nu_\parallel}}). \tag{68}$$

Thus the time-independent form of Eq. (63) in the long time limit is

$$C(0,\infty) \sim \Delta^{-\nu_\parallel(\theta-\frac{d}{z})}. \tag{69}$$

Now we obtain the hyper scaling law, by using Eqs. (64) and (66),

$$\theta - \frac{d}{z} = -\frac{\beta+\beta'}{\nu_\parallel}, \tag{70}$$

which holds below the upper critical dimension d_c^+.

The number of occupied sites at time t when starting with a single occupied site at time 0 can be found from

$$N(t) = \int d^d\vec{x}\, C(\vec{x},t). \tag{71}$$

Therefore, at criticality, the number of occupied sites behaves as

$$N(t) \sim t^\theta. \tag{72}$$

For the contact process, the upper critical dimension can be determined by using the hyper scaling law. The initial slip exponent θ shows a non-zero positive value in this model [31, 42, 41, 43, 44], thus

$$\frac{d}{z} - \frac{\beta+\beta'}{\nu_\parallel} > 0, \tag{73}$$

and mean field values of critical exponents, i.e. $z = 2$, $\beta = \beta' = 1$, and $\nu_\parallel = 1$, give $d > 4$. So the upper critical dimension is

$$d_c^+ = 4. \tag{74}$$

Although a general absorbing state transition is characterized by four exponents, we will see it Subsubsec. 1.4.4 that for the contact process $\beta = \beta'$ and thus $\alpha = \delta$.

1.4.3. Mean-field Approximation for The Contact Process. A basic understanding of the contact process can be achieved by means of a mean-field approximation. To derive the mean-field equation, we replace the occupation number s_i of the neighbors of a given site by their average ρ_A. This gives

$$\frac{\partial \rho_A}{\partial t} = (\lambda - 1)\rho_A - \lambda \rho_A^2. \tag{75}$$

This equation has two stationary solutions, i.e., $\rho_A = 0$ and $\rho_A = (\lambda - 1)/\lambda$. The first one, $\rho_A = 0$ represents the inactive state, the second one represents the active state. The phase transition occurs at $\lambda = 1$, when the active solution first appears and the inactive one becomes unstable. Setting $\Delta = \lambda - \lambda_c = \lambda - 1$, we obtain

$$\rho_A \sim \Delta \simeq (\lambda - \lambda_c) = (\lambda - \lambda_c)^{\beta_{MF}} \tag{76}$$

in the vicinity of critical point. Thus the critical exponent β_{MF} has the value $\beta_{MF} = 1$.

The time evolution of the order parameter is given by

$$\rho_A(t) \sim t^{-1} \tag{77}$$

at the critical point. Close to the critical point, we instead obtain

$$\rho_A(t) = \frac{\Delta}{\lambda + (\frac{\Delta}{\rho_0} - \lambda)\exp(-\Delta t)}, \tag{78}$$

where $\rho_0 = \rho(0)$ is a constant. Asymptotically, $\rho_A(t)$ shows an exponential decay, i.e. $\rho_A(t) \sim e^{-|\Delta| t} \sim e^{-t/\xi_\parallel}$, independent of the sign[9] of Δ. From this asymptotic behavior, we can obtain the correlation time

$$\xi_\parallel \sim |\lambda - \lambda_c|^{-\nu_\parallel MF} \tag{79}$$

[9]For $\Delta > 0$, $\rho_A(t) \sim \frac{\Delta}{\lambda} + \frac{\Delta}{\lambda^2}\left(\lambda - \frac{\Delta}{\rho_0}\right) e^{-\Delta t}$ and for $\Delta < 0$, $\rho_A(t) \sim -\Delta\left(\lambda - \frac{\Delta}{\rho_0}\right)^{-1} e^{\Delta t}$

with $\nu_{\parallel MF} = 1$.

To discuss spatial correlations, we need to permit spatial variations and add a gradient term similar to Subsubsec. 1.1.2. Therefore the mean-field equation now is

$$\frac{\partial \rho_A}{\partial t} = (\lambda - 1)\rho_A - \lambda \rho_A^2 + D\nabla^2 \rho_A, \tag{80}$$

where $\rho_A = \rho_A(\vec{x}, t)$. Comparing space and time derivatives suggests [41]

$$\xi_\parallel \sim \xi_\perp^2, \tag{81}$$

where the dynamic exponent in the mean-field theory is $z_{MF} = 2$ and a critical exponent $\nu_{\perp MF} = 1/2$ for correlation length emerges via $z_{MF} = \nu_{\parallel MF}/\nu_{\perp MF}$.

1.4.4. Universality Class - Directed Percolation (DP). According to the so-called DP conjecture [45, 46], the contact process should belong to the directed percolation universality class. The DP conjecture was introduced by Jassen (1981) and Grassberger (1982). It states that a system is in the DP universality class if (*i*) it has a one-component order parameter and exhibits a continuous phase transition into a unique absorbing state, provided that (*ii*) the dynamic rules involve only short-range processes, and (*iii*) the system has no additional symmetries or quenched randomness [31, 45, 46].

What is directed percolation? In normal (isotropic) percolation, as discussed in Subsec 1.3, a site can be connected to its neighbors in all directions. In contrast, in directed percolation, only bonds in one direction are allowed, as illustrated in Fig. 1.6.

Epidemic process such as the contact process can be mapped onto DP by relating the time direction to the special direction in the DP problems.

1.4.5. Generalized Contact Process. In the previous sections we introduced the contact process which has a single absorbing-state and we found that its critical behavior falls into the directed percolation universality class. The common feature of lattice models belonging into the DP class is the existence of a single absorbing-state. According to the DP conjecture, if there are several symmetric absorbing states in the system, the critical behavior is expected to belong to a universality class other than DP.

Examples of universality classes with two absorbing-states are the *parity-conserving* (PC) universality class [47, 48, 49, 50] and the *Z_2-symmetric directed percolation* (DP2) universality class [31, 51] which coincide in 1*d* but are distinct classes in higher dimensions. The PC class is one of the ubiquitous classes for nonequilibrium lattice

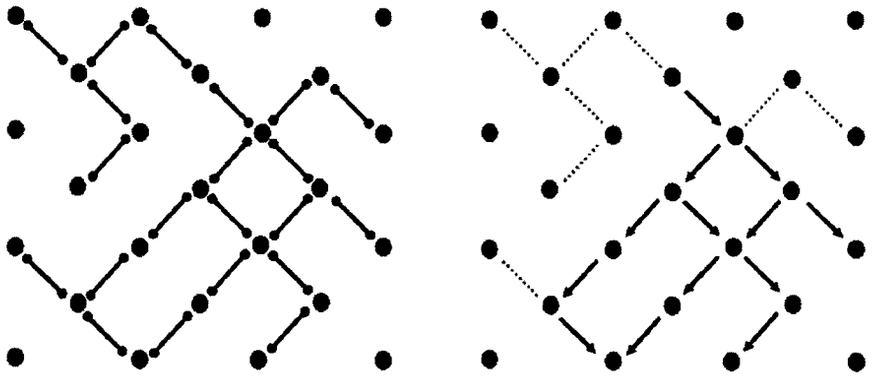

Figure 1.6. Difference between isotropic and directed percolation. Left : Bond percolation from a single seed (red dot) toward all directions. Right : Percolation (represented by arrows) is only allowed in downward direction, and dashed bonds represent forbidden directions in percolation process.

Table 1.2. Critical exponents of the directed percolation universality class: In $d = 1$, exponents $\nu_\perp$ and $\nu_\parallel$ are obtained from a series expansion by Jensen (1999). Exponents of other dimensions come from computational calculations which were performed by Voigt and Ziff for $d = 2$ (1997) and Jensen for $d = 3$ (1992) [42].

	MF	$d = 1$	$d = 2$	$d = 3$
$\beta = \beta'$	1	0.276486(8)	0.584(4)	0.81(1)
$\nu_\perp$	1/2	1.096854(4)	0.734(4)	0.581(5)
$\nu_\parallel$	1	1.733847(6)	1.295(6)	1.105(5)
z	2	1.580745(10)	1.76(3)	1.90(1)
$\alpha = \delta$	1	0.159464(6)	0.4505±0.0010	0.732±0.004
θ	0	0.313686(8)	0.2995±0.0010	0.114±0.004

models. One representative model is the *branching and annihilating random walk with an even number of offspring* (BARWe) [31, 32, 50], where the number of particles is conserved *mod* 2. The *generalized contact process* [31, 51] with two absorbing-states is a representative model in the DP2 class.

The generalized contact process was suggested by H. Hinrichsen in 1997 [51]. The difference between this model and the simple contact process is the number of absorbing states. While the simple contact process has a single absorbing state, the generalized contact process involves m symmetric absorbing states. The model is

defined on a lattice whose sites can now be in one of $m+1$ states, the active state A, or one of m inactive states I_k $(k = 1, \cdots, m)$. k is sometimes called the color index[10].

The dynamic rules of this model are defined by the transition rates $w\left(s_{i,t+dt}, s_{i+1,t+dt} | s_{i,t}, s_{i+1,t}\right)$ for pairs of nearest neighbor sites,

$$\begin{aligned} w\left(A, I_k | A, A\right) &= w\left(I_k, A | A, A\right) = \bar{\mu}/m, \\ w\left(I_k, I_k | I_k, A\right) &= w\left(I_k, I_k | A, I_k\right) = \mu_k, \\ w\left(A, A | I_k, A\right) &= w\left(A, A | A, I_k\right) = 1, \\ w\left(A, I_k | I_l, I_k\right) &= w\left(I_l, A | I_l, I_k\right) = 1, \end{aligned} \tag{82}$$

where $\bar{\mu}$ and μ_k are healing rates and the indices k and l denote different absorbing

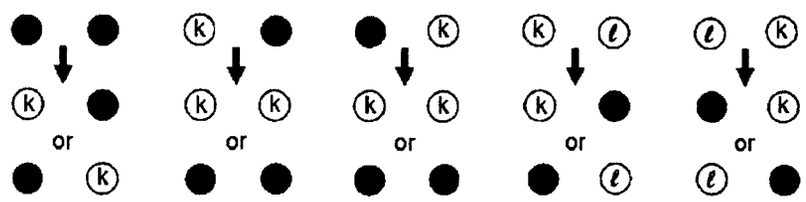

Figure 1.7. Schematic update of the generalized contact process. The occupied site is represented by the solid dot and different colored empty sites are labeled by k and l $(k \neq l)$.

states $k \neq l$. Full symmetry between the absorbing states requires the condition $\mu_1 = \mu_2 = \cdots = \mu_m = \mu$. Generally we may set $\bar{\mu} = \mu$, if there is no attractive or repulsive interaction between occupied sites. In the above dynamics, inactive sites with random colors are created within active islands but transformations between different colored states are not allowed. The first three rates in Eq. (79) are analogous to the simple contact process. The 4th rate prevents domains of different colors from sticking together. Instead, they can separate and move via the creation of active sites.

1.4.6. Universality Class of The Generalized Contact Process. According to the DP conjecture, a transition with a single absorbing state will be in the DP universality class. If the symmetry among different absorbing states does not exist in the generalized contact process (GCP), one of them will be dominant in the

[10]There is no deeper physical meaning here, this word is just used as an index to distinguish the m inactive states in Ref. [51].

Table 1.3. Critical exponents of DP2 universality class. For $d = 1$ all values coincide with the PC class and for $d = 2$ all exponents take mean-field values with logarithmic corrections according to the GV class [32].

	β	β'	θ	α	δ	z
$d = 1$	0.92(3)	0.92(3)	0.000(1)	0.285(5)	0.285(5)	1.747
$d = 2$	0	1	0	0	1	2

long time limit and we may expect DP critical behavior. However, the non-DP critical behavior is expected, if the symmetry exists. Especially if there are two symmetric absorbing states, the GCP belongs to the Z_2-symmetry directed percolation class (DP2 class). For the $d = 1$ this class coincides with the parity-conserving class (PC class) which is represented most prominently by branching annihilating walks with an even number of offspring (BAREe). This model is defined by particles diffusing and undergoing reactions

$$\begin{aligned} 2A &\xrightarrow{k_1} \varnothing \\ A &\xrightarrow{k_2} (n+1)A, \end{aligned} \tag{83}$$

where k_1 and k_2 are rates corresponding to annihilating and branching and $n = 2, 4, 6, ...$ indicates the number of offspring. The long-time dynamics of the GCP with two absorbing states can be mapped onto BARWe process in $1d$ by considering the domain walls I_1I_2 and I_2I_1 to be particles, $I_1I_2 = \Omega_{12}$ [51, 42]. The rates (79) then create the reactions

$$\begin{aligned} \Omega_{12}\Omega_{21} &\rightarrow \varnothing \\ \Omega_{12} &\rightarrow \Omega_{12}\Omega_{21}\Omega_{12}, \end{aligned} \tag{84}$$

corresponding to annihilation and branching of these particles. However in higher dimension systems, the interfaces[11] between differently colored inactive domains are lines, therefore we cannot treat the interface as a particle in mapping to the BARWe.

The values of the critical exponents of the DP2/PC universality class in $1d$ are known with high accuracy (see Table 1.3). In $2d$, the DP2 class is very close to its upper critical dimension. In fact, based on a conjecture by Dornic *et al.* [52], the

[11] We may think these interfaces as strings or walls of As. See Refs [31, 51].

$2d$ DP2 class maps onto the *generalized voter model*[12] (GV) class which is exactly at its upper critical dimension. This suggests that the upper critical dimension of DP2 universality class is $d_c^+ = 2$.

1.5. SUMMARY

In this section we introduced the background and theories to support the next sections. In first two subsections (Subsecs 1.1 and 1.2), we discussed equilibrium phase transitions based on the Ising model and its mean-field theory which were discussed via Landau theory. Although Landau theory is incorrect in low-dimensional systems, this theoretical approach to criticality still gives valuable insights into phase transitions. Going beyond mean-field theory, we then introduced the effects of fluctuations and the Ginzburg criterion. Finally, we discussed Widom's scaling assumption and the resulting scaling forms of physical quantities.

In Subsec 1.3, we introduced the classical percolation theory which concerns the movement of particles on randomly connected network systems. We mainly discussed a site percolation problem in order to apply it to site dilutions in sections 2 and 3.

In Subsec 1.4, we introduced two nonequilibrium lattice models, i.e., the contact process and the generalized contact process. Nonequilibrium phase transitions in these models are the primary topic of this dissertation. After explaining a key difference between equilibrium and nonequilibrium systems we introduced the nonequilibrium critical properties of the contact process. Then we discussed the generalized contact process which is not in the universality class of the contact process. Thus we showed two different kinds of universality classes for nonequilibrium lattice models.

The remainder of this thesis consists of reprints of four papers. Sections 2 and 3 deal with nonequilibrium phase transitions of the contact process and the generalized contact process on percolating lattices. Sections 4 and 5 explore the phase diagram and the phase transitions of the generalized contact process in more detail.

[12]The voter model is defined by spin-flip dynamics, but "opinions" is used instead of spin configurations. Two absorbing-states can be represented by two spins states (all spin up or down).

BIBLIOGRAPHY

[1] H. Stocker W. Greiner, L. Neise. *Thermodynamics and statistical mechanics.* Springer-Verlag, New York, 1995.

[2] Thomas Andrews. The bakerian lecture: On the continuity of the gaseous and liquid states of matter. *Philosophical Transactions of the Royal Society of London*, 159, 1869.

[3] H. Eugene Stanley. *Introduction to phase transitions and critical phenomena.* Oxford Univ. Press, Oxford, 1971.

[4] L. Landau. Theory of phase transformations. i. *Zh. Eksp. Teor. Fiz. Phys. Z. Sowjetunion*, 7 11:19 26, 1937 1937.

[5] L. Landau. Theory of phase transformations. ii. *Eksp. Teor. Fiz. Phys. Z. Sowjetunion*, 7 11:627 545, 1937 1937.

[6] L. Onsager. *Phys. Rev.*, 65:117–149, 1944.

[7] E. Ising. *Z. Physik*, 31:253, 1925.

[8] S. G. Brush. *Rev. Mod. Phys.*, 39:883–893, 1967.

[9] B. Bergersen M. Plischke. *Equilibrium statistical physics.* Prentice Hall, New Jersey, 1989.

[10] R. K. Pathria. *Statistical mechanics.* Butterworth Heinemann, Oxford, 1996.

[11] V. L. Ginzburg. *Sov. Phys. Sol. State.*, 2:1824, 1960.

[12] K. G. Wilson. *Phys. Rev. B*, 4:3174, 1971.

[13] K. G. Wilson. *Phys. Rev. B*, 4:3184, 1971.

[14] R. Sknepnek. *Magnetic and superconducting quantum critical behavior of itinerant electronic systems.* PhD thesis, Univ. of Missouri-Rolla, 2004.

[15] L. P. Kadanoff et. *Rev. Mod. Phys.*, 39:395, 1967.

[16] K. Huang. *Statistical mechanics.* John Wiley & Sons, New York, 1987.

[17] B. Widom. *J. Chem. Phys.*, 43:3892, 1965.

[18] L. E. Reichl. *A morden course in statistical physics.* John Wiley & Sons, New York, 1998.

[19] P. J. Flory. *J. Am. Chem. Soc.*, 63:3089, 1941.

[20] P. J. Flory. *Statistical mechanics of chain molecules.* Interscience Publisher, New York, 1969.

[21] D. Stauffer and A. Aharony. *Introduction to percolation theory.* Taylor & Francis, London, 1994.

[22] W. H. Stockmayer. *J. Chem. Phys.*, 11:45, 1943.

[23] J. Hammersley S. Broadbent. Percolation processes i. crystals and mazes. *Proceedings of the Cambridge Philosophical Society*, 53:629–641, 1957.

[24] J. W. Essam. *Rep. Prog. Phys.*, 43, 1980.

[25] K. M. Gwilym J. W. Essam. *J. Phys. C: Solid State Phys.*, 4:L228, 1971.

[26] A. J. McKane T. C. Lubensky. *J. Phys. A: Math. Gen.*, 14:L157–Ll61, 1981.

[27] E. Stoll C. Domb, T. Schneider. *J. Phys. A: Math. Gen.*, 9:L90, 1975.

[28] C. Domb. *J. Phys. A: Math Gen.*, 9:L141, 1976.

[29] M. E. Fisher. *Physics*, 3:225, 1967.

[30] T. Vojta. *J. Phys. A*, 39:R143–R205, 2006.

[31] H. Hinrichsen. *Adv.Phys.*, 49:815–958, 2000.

[32] G. Odor. *Rev. Mod. Phys.*, 76:663, 2004.

[33] T. Liggett. *Interacting particle systems.* Springer-Verlag, New York, 1985.

[34] F. Reif. *Fundamentals of statistical and thermal physics.* McGRAW-HILL, Singapore, 1985.

[35] D. Chandler. *Introduction to modern statistical mechanics.* Oxford university press, New York, 1987.

[36] R. Dickmann J. Marro. *Nonequilibrium Phase Transitions in Lattice Models.* Cambridge university press, Cambridge, 1999.

[37] T. E. Harris. *Ann. Prob.*, 2:969, 1974.

[38] A. de la Torre P. Grassberger. *Ann. Phys. (N.Y.)*, 122:373, 1979.

[39] R. Dickman. *Nonequilibrium Statistical Mechanics in One Dimension.* Cambridge University Press, Cambridge, England, 1997.

[40] A. A. Markov. *Theory of Algorithms.* Academy of Sciences of the USSR, 1954.

[41] S. Lubeck. *International Journal of Modern Physics B*, 18:3977, 2004.

[42] T. Vojta M. Y. Lee. *Phys. Rev. E*, 81:061128, 2010.

[43] J. Mast T. Vojta, A. Farquhar. *Phys. Rev. E*, 79:011111, 2009.

[44] I. Jensen. *Phys. Rev. A*, 45:R563–R566, 1992.

[45] H. K. Janssen. *Z. Phys. B*, 42:151–154, 1981.

[46] P. Grassberger. *Z. Phys. B*, 47:365–374, 1982.

[47] D. ben Avraham D. Zhong. *Phys. Lett. A*, 209:333–337, 1995.

[48] I. Jensen. *J. Phys. A*, 26:3921–3930, 1993.

[49] I. Jensen. *Phys. Rev. E*, 50:3623–3633, 1994.

[50] U. C. Tauber J. Cardy. *Phys. Rev. Lett.*, 77:4870, 1996.

[51] H. Hinrichsen. *Phys. Rev. E*, 55:219, 1997.

[52] J. Chave I. Dornic, H. Chate and H. Hinrichsen. *Phys. Rev. Lett.*, 87:045701, 2001.

2. NONEQUILIBRIUM PHASE TRANSITION ON A RANDOMLY DILUTED LATTICE

Thomas Vojta and Man Young Lee

Department of Physics, University of Missouri-Rolla, Rolla, MO 65409

Abstract[13]

We show that the interplay between geometric criticality and dynamical fluctuations leads to a novel universality class of the contact process on a randomly diluted lattice. The nonequilibrium phase transition across the percolation threshold of the lattice is characterized by unconventional activated (exponential) dynamical scaling and strong Griffiths effects. We calculate the critical behavior in two and three space dimensions, and we also relate our results to the recently found infinite-randomness fixed point in the disordered one-dimensional contact process.

[13]All of this section is reproduced from Physical Review Letters **96** 035701 (2006) and then reformatted and renumbered

Nonequilibrium systems can undergo continuous phase transitions between different steady states. These transitions are characterized by collective fluctuations over large distances and long times similar to the behavior of equilibrium critical points. Examples can be found in population dynamics and epidemics, chemical reactions, growing surfaces, and in granular flow and traffic jams (for recent reviews see, e.g., Refs. [1, 2, 3, 4, 5, 6]).

If a nonequilibrium process is defined on a randomly diluted spatial lattice, its dynamical fluctuations coexist with geometric fluctuations. Site or bond dilution defines a percolation problem for the lattice with a geometric phase transition at the percolation threshold [7]. In this Letter we address the question of how the interplay between geometric criticality due to percolation and dynamical fluctuations of the nonequilibrium process influences the properties of the phase transition.

Our starting point is the contact process [8], a prototypical system exhibiting a nonequilibrium phase transition. It is defined on a d-dimensional hypercubic lattice ($d \geq 2$). Each site can be active (occupied by a particle) or inactive (empty). In the course of the time evolution, active sites infect their neighbors, or they spontaneously become inactive. Specifically, the dynamics is given by a continuous-time Markov process during which particles are created at empty sites at a rate $\lambda n/(2d)$ where n is the number of active nearest neighbor sites. Particles are annihilated at unit rate. For small birth rate λ, annihilation dominates, and the absorbing state without any particles is the only steady state (inactive phase). For large birth rate λ, there is a steady state with finite particle density (active phase). The two phases are separated by a nonequilibrium phase transition in the directed percolation [9, 10] universality class at some $\lambda = \lambda_c^0$.

We introduce quenched site dilution [11] by randomly removing lattice sites with probability p. The resulting phase diagram of the site-diluted contact process is sketched in Fig. 2.1. For small impurity concentrations below the percolation threshold of the lattice, $p < p_c$, the active phase survives, but the critical birth rate increases with p (to compensate for the missing neighbors). Right at the percolation threshold the active phase survives on the infinite percolation cluster for $\lambda > \lambda_*$. The (multi) critical birthrate λ_* must be smaller than the critical birthrate of the one-dimensional (1D) contact process because the critical percolation cluster is connected, infinitely extended, and its fractal dimension is $D_f > 1$. For $p > p_c$, no active phase can exist because the lattice consists of disconnected clusters of finite size that do not support a steady state density of active sites.

The contact process on a site-diluted lattice therefore has two nonequilibrium phase transitions, separated by a multicritical point. For $p < p_c$, the transition (marked by "a" in Fig. 2.1) is expected to be in the universality class of the generic disordered contact process [12, 13, 14] which has reattracted considerable attention recently [15, 16]. In contrast, the phase transition across the percolation threshold p_c of the lattice for $\lambda > \lambda_*$ (transition "b" in Fig. 2.1) has received much less attention.

In this Letter, we show that the interplay between geometric criticality and dynamic fluctuations leads to a novel universality class for this nonequilibrium phase transition. Even though the transition is driven entirely by the geometry of the lattice, the dynamical fluctuations of the contact process enhance the singularities in all quantities involving dynamic correlations. Our results can be summarized as follows. The dynamical scaling is not of conventional power-law form but activated, i.e., the relation between correlation length $\xi_\perp$ and correlation time $\xi_\parallel$ is exponential,

$$\ln \xi_\parallel \sim \xi_\perp^\psi \tag{85}$$

with the critical exponent ψ being equal to the fractal dimension of the critical percolation cluster, $\psi = D_f$. As a result, the long-time decay of the density ρ of active sites at $p = p_c$ is ultra-slow,

$$\rho(t) \sim [\ln(t/t_0)]^{-\bar{\delta}} \, . \tag{86}$$

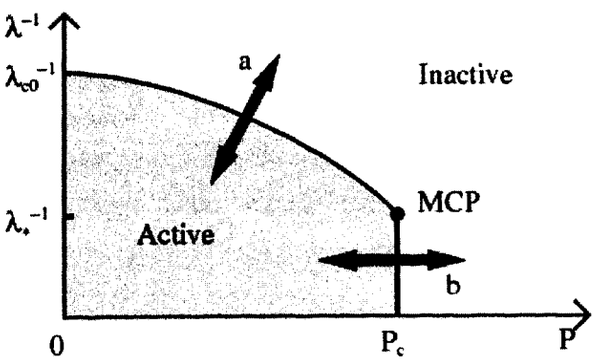

Figure 2.1. Schematic phase diagram of a site diluted contact process as function of impurity concentration p and birth rate λ. There is a multicritical point at $p = p_c$ and $\lambda = \lambda_*$. The phase transition (b) across the percolation threshold of the lattice is the topic of this Letter.

The exponent $\bar{\delta} = \beta_c/(\nu_c D_f)$ is determined by D_f together with the order parameter and correlation length exponents, β_c and ν_c, of the lattice percolation transition [17]. In contrast to the enhanced dynamical singularities, the exponents of static quantities like the steady state density ρ_{st} and the spatial correlation length $\xi_\perp$ are identical the corresponding lattice percolation exponents,

$$\rho_{st}(p) \sim |\Delta|^{\beta_c} \qquad (\Delta < 0) \;, \tag{87}$$

$$\xi_\perp \sim |\Delta|^{\nu_c} \;. \tag{88}$$

where $\Delta = p - p_c$ measures the distance from the percolation threshold. Off criticality, i.e., away from the percolation threshold, we find strong Griffiths effects [18] characterized by a non-exponential density decay [12],

$$\rho(t) \sim (t/t_0)^{-d/z'} \qquad (p > p_c) \tag{89}$$

$$\rho(t) - \rho_{st} \sim e^{-[(d/z'')\ln(t/t_0)]^{1-1/d}} \qquad (p < p_c) \;, \tag{90}$$

where the nonuniversal exponents z' and z'' diverge as $z', z'' \sim \xi_\perp^{D_f}$ for $p \to p_c$. In the remainder of the Letter we sketch the derivation of these results and calculate exponent values and additional observables. We also relate our results to the disordered 1D contact process [15, 16] and to the diluted quantum Ising model [19].

Let us start by considering the steady state density ρ_{st} of active sites (i.e.,the order parameter of the transition). A nonzero steady state density can only develop on the infinite percolation cluster; finite clusters do not contribute because they eventually go into the inactive state via a rare fluctuation. For $\lambda > \lambda_c$, the infinite cluster is in the active phase. The total steady state density is proportional to the number of sites in the infinite cluster, $\rho_{st} \sim P_\infty(p) \sim (p_c - p)^{\beta_c}$. The order parameter exponent of the nonequilibrium transition is therefore identical to that of the lattice percolation transition, $\beta = \beta_c$, as stated in (87). To determine the spatial correlation length $\xi_\perp$ we note that the correlations of the contact process cannot extend beyond the connectedness length ξ_c of the percolating lattice because sites on different percolation clusters are decoupled. On the other hand, for $\lambda > \lambda_*$, all sites on the same cluster are strongly correlated in space even though they collectively fluctuate in time. We thus conclude $\xi \sim \xi_c$ and $\nu = \nu_c$ in agreement with (88).

We now study the time dependence of the density $\rho(t)$ of active sites, starting from a completely active lattice. We first consider the contact process on a single percolation cluster of finite size (number of sites) s. For $\lambda > \lambda_*$ such a cluster is

locally in the active phase. It therefore has a metastable state with a nonzero density of active sites. This metastable state can decay into the inactive state only via a rare collective fluctuation involving all sites of the cluster. The probability for such a rare event decreases exponentially with the size s of the cluster. Therefore, the life time t_s of the metastable active state on a cluster increases exponentially with its size s,

$$t_s(s) \sim t_0 e^{A(\lambda)s} \,, \tag{91}$$

where t_0 is some microscopic time scale. The prefactor $A(\lambda)$ vanishes at the multicritical point, $A(\lambda_*) = 0$, and increases with increasing λ. The number of sites s of a percolation cluster is connected to its linear size R_s via $s \sim R_s^{D_f}$. Therefore, (91) establishes the exponential relation between length and time scales, $\ln t_s \sim R_s^{D_f}$ leading to activated dynamical scaling (85).

After having analyzed a single cluster we turn to the full percolation problem. From classical percolation theory, we know that close to p_c the number n_s of occupied clusters of size s per lattice site (excluding the infinite cluster for $p < p_c$) obeys the scaling form

$$n_s(\Delta) = s^{-\tau_c} f\left(s\Delta^{1/\sigma_c}\right). \tag{92}$$

The scaling function $f(x)$ behaves as

$$f(x) \sim \exp(-B_1 x) \qquad (p > p_c) \tag{93}$$

$$f(x) = \text{const} \qquad (p = p_c) \tag{94}$$

$$f(x) \sim \exp[-(B_2 x)^{1-1/d}] \qquad (p < p_c). \tag{95}$$

where B_1, B_2 are constants. The exponents τ_c and σ_c determine all critical exponents of the percolation transition of the lattice including the correlation length exponent $\nu_c = (\tau_c - 1)/(d\sigma_c)$, the order parameter exponent $\beta_c = (\tau_c - 2)/\sigma_c$, and the fractal dimension $D_f = d/(\tau_c - 1)$ of the percolating cluster [7].

In order to obtain the total density of active sites for the contact process on the diluted lattice, we sum the number of active sites over all percolation clusters. Combining the cluster size distribution (92) with the lifetime of the metastable active state (91) leads to

$$\rho(t, \Delta) \sim \int ds\; s\; n_s(\Delta) \exp[-t/t_s(s)] \tag{96}$$

Right at the percolation threshold, this reduces to

$$\rho(t,0) \sim \int ds\ s^{1-\tau_c} \exp[-(t/t_0 e^{As})] \ . \tag{97}$$

The leading behavior of this integral can be found by noticing that only islands with size $s > s_{\min}(t) = A^{-1} \ln(t/t_0)$ contribute at time t. The critical long-time dependence of the total density is thus given by

$$\rho(t,0) \sim [\ln(t/t_0)]^{2-\tau_c} \qquad (p = p_c). \tag{98}$$

This completes the derivation of (86) with the critical exponent $\bar{\delta}$ given by $\bar{\delta} = \tau_c - 2 = \beta_c/(\nu_c D_f)$ in agreement with general scaling arguments [15, 16].

We now consider the behavior of the density off criticality. In the inactive phase, $p > p_c$, the time dependence of the density is given by

$$\rho(t,\Delta) \sim \int ds s^{1-\tau_c} \exp[-B_1 s \Delta^{1/\sigma_c} - (t/t_0 e^{As})]. \tag{99}$$

For long times, the leading behavior of the integral can be calculated using the saddle-point method, giving

$$\rho(t,\Delta) \sim t^{-(B_1/A)\Delta^{1/\sigma_c}} \qquad (p > p_c) \tag{100}$$

equivalent to (89). The nonuniversal exponent z' is given by $z' = (Ad/B_1)\Delta^{-1/\sigma_c} \sim \xi_\perp^{D_f}$.

In the active phase, $p < p_c$, there is a nonzero steady state density ρ_{st} coming from the infinite percolation cluster. However, the approach of the density towards this value is still determined by the slow decay of the metastable states of the finite percolation clusters

$$\begin{aligned} &\rho(t,\Delta) - \rho_{st}(\Delta) \sim \\ &\sim \int ds s^{1-\tau_c} \exp\left[-\left(B_2 s |\Delta|^{1/\sigma_c}\right)^{1-1/d} - (t/t_0 e^{As})\right] \end{aligned} \tag{101}$$

Using the saddle point method to calculate the leading long-time behavior gives (for $p < p_c$)

$$\rho(t,\Delta) - \rho_{st}(\Delta) \sim e^{-\left[(B_2/A)|\Delta|^{1/\sigma_c} \ln(t/t_0)\right]^{1-1/d}} \ . \tag{102}$$

This completes the derivation of (90) with $z'' = (Ad/B_2)|\Delta|^{-1/\sigma_c} \sim \xi_\perp^{D_f}$. The non-exponential off-critical relaxation of the density (89,90) is characteristic of a Griffiths region in the contact process [12, 18]. We also point out that time and spatial correlation length enter these equations in the form of the combination $\ln(t)/\xi_\perp^{D_f}$ again characteristic of activated scaling.

We now turn to the influence of an external source field h that describes spontaneous particle creation at a rate h at each lattice site. To determine the steady state density as a function of h we again start by considering a single percolation cluster of size s. For $\lambda > \lambda_*$, the cluster is active if at least one particle has been spontaneously created on one of the s sites within the life time $t_s(s) = t_0 e^{As}$. For small h, the average number of particles created on a cluster of size s within time t_s is $M_s(h) = hst_s = hst_0 e^{As}$. If $M_s > 1$, the cluster is (almost) always active. If $M_s < 1$, it is active with a probability proportional to M_s. The total steady state density is obtained by summing over all clusters

$$\rho_{st}(h, \Delta) \sim \int ds\ s\ n_s(\Delta) \min[1, M_s(h)]\ . \tag{103}$$

Evaluating this integral analogously to the time-dependent density (96) yields, for small fields h,

$$\rho_{st}(h) \sim [\ln(h_0/h)]^{-\bar{\delta}} \qquad (p = p_c), \tag{104}$$

$$\rho_{st}(h) \sim (h/h_0)^{d/z'} \qquad (p > p_c), \tag{105}$$

$$\rho_{st}(h) \sim \exp\left[-(d/z'')\ln(h_0/h)\right]^{1-1/d} \quad (p < p_c)\ , \tag{106}$$

where $h_0 \sim 1/t_0$. At $p = p_c$, the relation between density and field is logarithmic, as expected from activated scaling. Off criticality, we find strong Griffiths effects similar to those in the time-dependence of the density.

The above results can also be derived from a scaling theory. In the active phase, the density is proportional to the number of sites in the infinite percolation cluster. Thus, its scale dimension must be β_c/ν_c. Time must enter via the scaling combination $\ln(t)b^{D_f}$ reflecting the exponential dependence of the life time (91) on the cluster size. The field h, being a rate, scales like inverse time. We therefore obtain the following scaling form:

$$\rho[\Delta, \ln(t), \ln(1/h)] = b^{\beta_c/\nu_c}\rho[\Delta b^{-1/\nu_c}, \ln(t)b^{\psi}, \ln(1/h)b^{\psi}] \tag{107}$$

Table 2.1. Critical exponents of the nonequilibrium phase transition at $p = p_c$ in two and three space dimensions.

Exponent	$d = 2$	$d = 3$
$\beta = \beta_c$	5/36	0.417
$\nu = \nu_c$	4/3	0.875
$\psi = D_f = d - \beta_c/\nu_c$	91/48	2.523
$\bar{\delta} = \beta_c/(\nu_c D_f)$	5/91	0.188

where b is an arbitrary (length) scale factor and $\psi = D_f$. This form is consistent with all our explicit results.

All critical exponents of the nonequilibrium phase transition are determined by the classical percolation exponents of the lattice. In two space dimensions, their values are known exactly and in three dimensions they are known numerically with high accuracy [7]. Table I shows numerical exponent values for these cases.

We also briefly comment on the early time behavior. For $\lambda > \lambda_*$ each percolation cluster is locally in the active phase. Starting from a single active seed, the cloud of active sites thus initially grows ballistically, i.e., the radius of the cloud grows linearly with time, until a metastable state is reached in which it covers the entire percolation cluster. The time required for this initial spreading on an island of size s is $t_i(s) \sim R_s \sim s^{1/D_f}$. As discussed above, the metastable state decays only at the much larger time scale $t_s(s) \sim e^{As}$. We thus arrive at the somewhat surprising conclusion that the early time behavior of the contact process on our diluted lattice is much faster than the logarithmically slow long-time decay of the density.

In the remaining paragraphs, we discuss the generality of our results, compare them to the transition in the diluted quantum Ising model [19] and to the recently found infinite-randomness critical point in a random 1D contact process [15, 16]. We also compare to a general classification of phase transitions with quenched disorder [20].

The logarithmic time and field dependencies (86) and (104) at the nonequilibrium phase transition at $p = p_c$ as well as the strong Griffiths effects in its vicinity are the direct result of combining the spectrum of percolation cluster sizes (92) with the exponential dependence (91) of the life time on the cluster size. We therefore expect similar behavior in other diluted equilibrium or nonequilibrium systems that share

this exponential relation between length and time scales. One example is the diluted transverse field Ising model [19]. In this system, the energy gap of a cluster decreases exponentially with its size. As a result, the scaling behavior at the quantum phase transition across the percolation threshold of the lattice is very similar to the one found in this paper.

Recently, the critical point of the 1D contact process with spatial disorder was found to be of infinite-randomness type [15, 16]. Analogous behavior is expected for the generic disordered directed percolation transition in higher dimensions, e.g., the transition at $p < p_c$ in the site-diluted contact process (transition a in Fig. 2.1). Our critical point at the percolation threshold shares some characteristics with these infinite-randomness critical points, notably the exponential relation between correlation length and time as well as the logarithmically slow decay of the total density. However, it belongs to a different universality class with novel critical exponents. Moreover, the early time behavior is different (logarithmically slow at the generic infinite randomness critical point but of power-law type at our transition).

Lastly, we point out that our results are in agreement with a general classification of phase transitions with quenched disorder (and short-range interactions) according to the effective dimensionality d_{eff} of the droplets or clusters [20]. Three cases can be distinguished: (i) If the clusters are below the lower critical dimension of the problem, $d_{eff} < d_c^-$, the critical behavior is of conventional power-law type and the Griffiths effects are exponentially weak. (ii) If $d_{eff} = d_c^-$, the critical point shows activated scaling accompanied by strong, power-law Griffiths effects. This case is realized in random transverse field Ising magnets [19, 21] as well as in our diluted contact process. (iii) If $d_{eff} > d_c^-$, the phase transition is smeared because locally ordered clusters can undergo the phase transition independently from the bulk. This occurs, e.g., for some metallic quantum magnets [22] or for the contact process with extended defects [23, 24].

In conclusion, we have shown that the contact process on a diluted lattice has unusual properties. The interplay between geometric criticality and dynamical fluctuations leads to a novel universality class with activated scaling and ultraslow dynamics. Interestingly, despite its ubiquity in theory, experimental observations of directed percolation scaling [25] are very rare. Our results suggest that peculiar disorder effects may be responsible for this in at least some of the experiments.

This work has been supported in part by the NSF under grant nos. DMR-0339147 and PHY99-07949, by Research Corporation and by the University of Missouri Research Board. Parts of this work have been performed at the Aspen Center for Physics and the Kavli Institute for Theoretical Physics, Santa Barbara.

[1] B. Schmittmann and R.K.P. Zia, in *Phase transitions and critical phenomena*, edited by C. Domb and J.L. Lebowitz, Vol. 17, (Academic, New York 1995), p. 1.

[2] J. Marro and R. Dickman, Nonequilibrium Phase Transitions in Lattice Models (Cambridge University Press, Cambridge, England, 1996).

[3] R. Dickman, in *Nonequilibrium Statistical Mechanics in One Dimension*, edited by V. Privman (Cambridge University Press, Cambridge, England, 1997), p. 51.

[4] H. Hinrichsen, Adv. Phys. **49**, 815 (2000).

[5] G. Odor, Rev. Mod. Phys. **76**, 663 (2004).

[6] U.C. Täuber, M. Howard, and B.P. Vollmayr-Lee, J. Phys. A **38**, R79 (2005).

[7] D. Stauffer and A. Aharony, *Introduction to Percolation Theory* (Taylor & Francis, London, 1994).

[8] T.E. Harris, Ann. Prob. **2**, 969 (1974).

[9] P. Grassberger and A. de la Torre, Ann. Phys. (NY) **122**, 373 (1979).

[10] H.K. Janssen, Z. Phys. B **42**, 151 (1981); P. Grassberger, Z. Phys. B **47**, 365 (1982).

[11] Our percolating lattice is externally given. This differs from the general epidemic process with immunization where the nonequilibrium process itself dynamically generates a percolation cluster of inaccesible sites [26].

[12] A.J. Noest, Phys. Rev. Lett **57**, 90 (1986); Phys. Rev. B **38**, 2715 (1988).

[13] H.K. Janssen, Phys. Rev. E **55**, 6253 (1997).

[14] A.G. Moreira and R. Dickman, Phys. Rev. E **54**, R3090 (1996); R. Dickman and A.G. Moreira, *ibid.* **57**, 1263 (1998).

[15] J. Hooyberghs, F. Igloi, C. Vanderzande, Phys. Rev. Lett **90**, 100601 (2003); Phys. Rev. E **69**, 066140 (2004).

[16] T. Vojta and M. Dickison, Phys. Rev. E **72**, 036126 (2005).

[17] In the following, lattice percolation exponents carry a subscript c while the exponents of the nonequilibrium transition of the contact process do not carry a subscript.

[18] R.B. Griffiths, Phys. Rev. Lett **23**, 17 (1969).

[19] T. Senthil and S. Sachdev, Phys. Rev. Lett **77**, 5292 (1996).

[20] T. Vojta and J. Schmalian, Phys. Rev. B **72**, 045438 (2005).

[21] D.S. Fisher, Phys. Rev. B **51**, 6411 (1995).

[22] T. Vojta, Phys. Rev. Lett **90** 107202 (2003).

[23] T. Vojta, Phys. Rev. E **70**, 026108 (2004).

[24] M. Dickison and T. Vojta, J. Phys. A **38**, 1999 (2005).

[25] H. Hinrichsen, Braz. J. Phys. **30**, 69 (2000).

[26] P. Grassberger, Math. BioSci. **63**, 157 (1982); J. Cardy, J. Phys. A **16**, L709 (1983); H.K. Jannssen, Z. Phys. B **58**, 311 (1985).

3. ABSORBING STATE PHASE TRANSITIONS ON PERCOLATING LATTICES

Man Young Lee and Thomas Vojta

Department of Physics, University of Missouri-Rolla, Rolla, MO 65409

Max-Planck-Institute for Physics of Complex Systems, Noethnitzer Str. 38, 01187 Dresden, Germany

Abstract[14]

We study nonequilibrium phase transitions of reaction-diffusion systems defined on randomly diluted lattices, focusing on the transition across the lattice percolation threshold. To develop a theory for this transition, we combine classical percolation theory with the properties of the supercritical nonequilibrium system on a finite-size cluster. In the case of the contact process, the interplay between geometric criticality due to percolation and dynamical fluctuations of the nonequilibrium system leads to a new universality class. The critical point is characterized by ultraslow activated dynamical scaling and accompanied by strong Griffiths singularities. To confirm the universality of this exotic scaling scenario we also study the generalized contact process with several (symmetric) absorbing states, and we support our theory by extensive Monte-Carlo simulations.

3.1. INTRODUCTION

In recent years, considerable effort has been directed towards identifying and classifying phase transitions far from thermal equilibrium. Such nonequilibrium transitions can be found in a wide variety of problems in biology, chemistry, and physics. Examples include population dynamics, the spreading of epidemics, surface chemical reactions, catalysis, granular flow, traffic jams as well as growing surfaces and

[14]All of this section is reproduced from Physical Review E **79** 041112 (2009) and then reformatted and renumbered. This paper is an extended version of PRL 96 035701 (2006), thus many parts of this section are overlapped in section 2

interfaces (see, e.g., [1, 2, 3, 4, 5, 6, 7, 8]). Nonequilibrium phase transitions are characterized by large scale fluctuations and collective behavior in space and time very similar to the behavior at equilibrium critical points.

A particularly interesting situation arises when an equilibrium or nonequilibrium many-particle system is defined on a randomly diluted lattice. Then, two distinct types of fluctuations are combined, *viz.* the dynamical fluctuations of the many-particle system and the static geometric fluctuations due to lattice percolation [9]. In equilibrium systems, their interplay gives rise to novel universality classes for the thermal [10, 11, 12] and quantum [13, 14, 16, 15] phase transitions across the lattice percolation threshold.

In this paper, we investigate the interplay between dynamical fluctuations and geometric criticality in nonequilibrium many-particle systems. We focus on a particularly well-studied type of transitions, the so-called absorbing state transitions, that separate active, fluctuating steady states from inactive (absorbing) states in which fluctuations cease completely. The generic universality class for absorbing state transitions is directed percolation (DP) [17]. It is conjectured [18, 19] to be valid for all absorbing state transitions with scalar order parameter and no extra symmetries or conservation laws. In the presence of symmetries and/or conservation laws, other universality classes can be realized, such as the DPn class in systems with n symmetric absorbing states [20].

For definiteness, we consider the contact process [21], a prototypical system in the DP universality class. We show that the contact process on a randomly site or bond diluted lattice has two different nonequilibrium phase transitions: (i) a generic disordered DP transition at weak dilutions (below the lattice percolation threshold) driven by the dynamic fluctuations of the contact process and (ii) the transition across the lattice percolation threshold driven by the geometric criticality of the lattice. The former transition has been investigated for a number of years [22, 23, 24, 25]; it has recently reattracted considerable attention because it is governed by an exotic infinite-randomness fixed point [26, 27, 28, 29]. In contrast, the latter transition has received much less attention.

Here, we develop a theory for the nonequilibrium transition across the lattice percolation threshold by combining classical percolation theory with the properties of the supercritical contact process on a finite-size cluster. We show that the critical point is characterized by ultraslow activated (exponential) dynamical scaling and accompanied by strong Griffiths singularities. The scaling scenario is qualitatively similar to the generic disordered DP transition, but with different critical exponent

values. To confirm the universality of this exotic scenario, we also investigate the generalized contact process with n (symmetric) absorbing states [20]. This is a particularly interesting problem because the generic transition of the disordered generalized contact process does *not* appear to be of infinite-randomness type [26, 27].

The paper is organized as follows. In Subec. 3.2, we introduce our models, the simple and generalized contact processes on a randomly diluted lattice. We also discuss the phase diagrams. In Subec. 3.3 we briefly summarize the results of classical percolation theory to the extent necessary for our purposes. Subsection 3.4 contains the main part of the paper, the theory of the nonequilibrium transition across the lattice percolation threshold. Subsection 3.5 is devoted to the question of the generality of the arising scaling scenario. We conclude in Subsec. 3.6. A short account of part of this work has already been published in Ref. [30].

3.2. SIMPLE AND GENERALIZED CONTACT PROCESSES ON DILUTED LATTICES

3.2.1. Contact Process. The clean contact process [21] is a prototypical system in the DP universality class. It is defined on a d-dimensional hypercubic lattice. (We consider $d \geq 2$ since we will be interested in diluting the lattice.) Each lattice site $\mathbf{r}$ can be active (infected, state A) or inactive (healthy, state I). During the time evolution of the contact process which is a continuous-time Markov process, each active site becomes inactive at a rate μ ("healing") while each inactive site becomes active at a rate $\lambda m/(2d)$ where m is the number of active nearest neighbor sites ("infection"). The infection rate λ and the healing rate μ are external parameters. Their ratio controls the behavior of the contact process.

For $\lambda \ll \mu$, healing dominates over infection, and the absorbing state without any active sites is the only steady state of the system (inactive phase). For sufficiently large infection rate λ, there is a steady state with a nonzero density of active sites (active phase). These two phases are separated by a nonequilibrium phase transition in the DP universality class at a critical value $(\lambda/\mu)_c^0$ of the ratio of the infection and healing rates.

The basic observable in the contact process is the average density of active sites at time t,

$$\rho(t) = \frac{1}{L^d} \sum_{\mathbf{r}} \langle n_{\mathbf{r}}(t) \rangle \tag{108}$$

where $n_{\mathbf{r}}(t) = 1$ if the site $\mathbf{r}$ is active at time t and $n_{\mathbf{r}}(t) = 0$ if it is inactive. L is the linear system size, and $\langle \ldots \rangle$ denotes the average over all realizations of the Markov process. The longtime limit of this density (i.e., the steady state density)

$$\rho_{\text{stat}} = \lim_{t \to \infty} \rho(t) \tag{109}$$

is the order parameter of the nonequilibrium phase transition.

3.2.2. Generalized Contact Process. Following Hinrichsen [20], we now generalize the contact process by introducing n different inactive states I_k with $k = 1 \ldots n$ ($n = 1$ corresponds to the simple contact process). Here, k is sometimes called the "color" label. The time evolution is again a continuous-time Markov process. The first two rates are equivalent to those of the simple contact process: An active site can decay into each of the inactive states I_k with rate μ/n, and a site in any of the inactive states becomes active at a rate $\lambda m/(2d)$ with m the number of active nearest-neighbor sites. To introduce competition between the different inactive states, we define a third rate: If two neighboring sites are in *different* inactive states, each can become active with a rate σ. This last rule prevents the boundaries between domains of different inactive states from sticking together infinitely. Instead they can separate, leaving active sites behind.

The properties of the clean generalized contact process have been studied in some detail in the literature [20, 31]. If the boundary activation rate σ vanishes, the behavior becomes identical to the simple contact process for all n. (This becomes obvious by simply dropping the color label and treating all inactive sites as identical.) For $\sigma > 0$, the system becomes "more active" than the simple contact process, and the universality class changes. In one space dimension, a phase transition exists for $n = 1$ (in the DP universality class) and for $n = 2$ (in the Z_2-symmetric directed percolation (DP2) class which coincides with the the parity-conserving (PC) class in one dimension [5]). For $n \geq 3$ the system is always in the active phase, and no phase transition exists at finite values of λ, μ and σ.

The generalized contact process in higher space dimensions presumably behaves in an analogous fashion: There is a DP transition for $n = 1$ while the properties for $n > 1$ are different. For sufficiently large n, the system is always active [15].

3.2.3. Lattice Dilution. We now introduce quenched site dilution by randomly removing each lattice site with probability p. (Bond dilution could be

[15] For $d = 2, n = 2$, Hinrichsen [20] finds a mean-field transition while our own simulations suggest that the system always active. Since this difference is of no importance for the present paper, it will be addressed elsewhere.

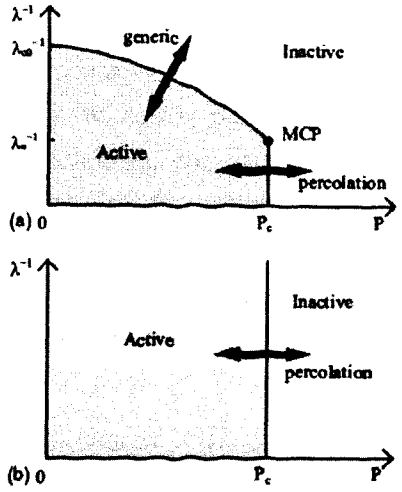

Figure 3.1. (Color online:) Schematic phase diagrams for the simple and generalized contact processes on a diluted lattice in dimensions $d \geq 2$ as a function of dilution p and inverse infection rate λ^{-1} (healing and boundary activation rates μ and σ are fixed). Case (a) applies to systems that display a phase transition at λ_c^0 in the absence of dilution. There is a multicritical point (MCP) at (p_c, λ_*) separating the generic transition from the lattice percolation transition. Case (b) is for systems that are always active in the absence of dilution.

introduced analogously.) As long as the vacancy concentration p remains below the lattice percolation threshold p_c, the lattice consists of an infinite connected cluster of sites accompanied by a spectrum of finite-size clusters. In contrast, at dilutions above p_c, the lattice consists of disconnected finite-size clusters only.

Figure 3.1 schematically shows the resulting phase diagrams of the nonequilibrium process as a function of the infection rate λ and dilution p, keeping the healing rate μ and the boundary activation rate σ, if any, constant. Depending on the properties of the clean undiluted system, there are two qualitatively different cases.

(a) If the undiluted system has a phase transition at a nonzero critical infection rate λ_c^0, the active phase survives for all vacancy concentrations below the percolation

threshold, $p < p_c$. It even survives at the percolation threshold p_c on the critical percolation cluster because it is connected, infinitely extended, and its fractal dimension D_f is larger than unity. The critical infection rate λ_c increases with increasing dilution p to compensate for the missing neighbors, reaching λ_* at p_c. The active phase cannot exist for $p > p_c$ because the lattice consists of finite-size clusters only, and the nonequilibrium process will eventually end up in one of the absorbing states on any finite-size cluster. Thus, in case (a), our system features two nonequilibrium phase transitions, (i) a generic (disordered) transition for dilutions $p < p_c$, driven by the dynamic fluctuations of the nonequilibrium process and (ii) the transition across the lattice percolation threshold driven by the geometric criticality of the lattice. They are separated by a multicritical point at (p_c, λ_*) which was studied numerically in Ref. [33].

(b) If the undiluted system is always active (as for the generalized contact process with a sufficiently high number of inactive states), the phase diagram is simpler. The active phase covers the entire region $p \leq p_c$ for all $\lambda > 0$ (λ_* is formally zero) while the inactive phase exists in the region $p > p_c$. There is no generic (disordered) nonequilibrium phase transition, only the transition across the lattice percolation threshold.

The focus of the present paper is the nonequilibrium phase transition across the lattice percolation threshold that exists in both cases. In order to develop a theory for this transition, we combine classical percolation theory with the properties of the nonequilibrium process on a finite-size cluster. In the next section we therefore briefly summarize key results of percolation theory.

3.3. CLASSICAL PERCOLATION THEORY

Consider a regular lattice in d dimensions. If each lattice site is removed with probability p [34], an obvious question is whether or not the lattice is still connected in the sense that there is a cluster of connected (nearest neighbor) sites that spans the entire system. This question defines the percolation problem (see Ref. [9] for an introduction).

In the thermodynamic limit of infinite system volume, there is a sharp boundary between the cases of a connected or disconnected lattice. If the vacancy concentration p stays below the percolation threshold p_c, an infinite cluster of connected sites exists (with a probability of unity). For $p > p_c$, an infinite cluster does not exist, instead, the lattice consists of many disconnected finite-size clusters.

The behavior of the lattice for vacancy concentrations close to the percolation threshold can be understood as a (geometric) continuous phase transition or critical phenomenon. The order parameter is the probability P_∞ of a site to belong to the infinite connected percolation cluster. It is obviously zero in the disconnected phase ($p > p_c$) and nonzero in the percolating phase ($p < p_c$). Close to p_c it varies as

$$P_\infty \sim |p - p_c|^{\beta_c} \qquad (p < p_c) \tag{110}$$

where β_c is the order parameter critical exponent of classical percolation. Note that we use a subscript c to distinguish quantities associated with the classical lattice percolation problem from those of the nonequilibrium phase transitions discussed later. In addition to the infinite cluster, we also need to characterize the finite clusters on both sides of the transition. Their typical size, the correlation or connectedness length ξ_c diverges as

$$\xi_c \sim |p - p_c|^{-\nu_c} \tag{111}$$

with ν_c the correlation length exponent. The average mass S_c (number of sites) of a finite cluster diverges with the susceptibility exponent γ_c according to

$$S_c \sim |p - p_c|^{-\gamma_c} \, . \tag{112}$$

The complete information about the percolation critical behavior is contained in the cluster size distribution n_s, i.e., the number of clusters with s sites excluding the infinite cluster (normalized by the total number of lattice sites). Close to the percolation threshold, it obeys the scaling form

$$n_s(\Delta) = s^{-\tau_c} f\left(\Delta s^{\sigma_c}\right). \tag{113}$$

Here $\Delta = p - p_c$, and τ_c and σ_c are critical exponents. The scaling function $f(x)$ is analytic for small x and has a single maximum at some $x_{\max} > 0$. For large $|x|$, it drops off rapidly

$$f(x) \sim \exp\left[-B_1 x^{1/\sigma_c}\right] \qquad (x > 0), \tag{114}$$

$$f(x) \sim \exp\left[-\left(B_2 x^{1/\sigma_c}\right)^{1-1/d}\right] \qquad (x < 0), \tag{115}$$

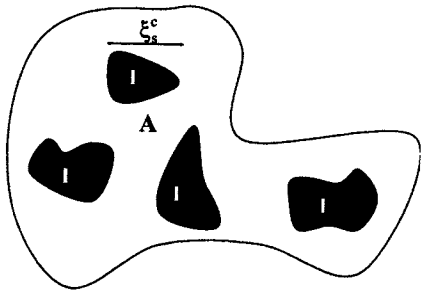

Figure 3.2. (Color online:) Schematic of the metastable state of the supercritical contact process on a single percolation cluster. A and I denote active and inactive sites, and ξ_s^c is the connected correlation length of the density fluctuations *on* the cluster.

where B_1 and B_2 are constants of order unity. All classical percolation exponents are determined by τ_c and σ_c including the correlation lengths exponent $\nu_c = (\tau_c - 1)/(d\sigma_c)$, the order parameter exponent $\beta_c = (\tau_c - 2)/\sigma_c$, and the susceptibility exponent $\gamma_c = (3 - \tau_c)/\sigma_c$.

Right at the percolation threshold, the cluster size distribution does not contain a characteristic scale. The structure of the critical percolation cluster is thus fractal with the fractal dimension being given by $D_f = d/(\tau_c - 1)$.

3.4. NONEQUILIBRIUM TRANSITION ACROSS THE LATTICE PERCOLATION THRESHOLD

3.4.1. Single-cluster Dynamics. To develop a theory of the nonequilibrium phase transition across the lattice percolation threshold, we first study the nonequilibrium process on a single connected finite-size cluster of s sites. For definiteness, this section focuses on the simple contact process. The generalized contact process will be considered in Subsec. 3.5.

The crucial observation is that on the percolation transition line (for $\lambda > \lambda_*$), the contact process is supercritical, i.e., the cluster is locally in the active phase. The time evolution of such a cluster, starting from a fully active lattice, therefore proceeds in two stages: Initially, the density ρ_s of active sites decays rapidly towards a metastable state (which corresponds to the steady state of the equivalent *infinite* system) with a nonzero density of active sites and islands of the inactive phase of linear size ξ_s^c (see Fig. 3.2). This metastable state can then decay into the inactive (absorbing) state

only via a rare collective fluctuation involving *all* sites of the cluster. We thus expect the long-time decay of the density to be of exponential form (suppressing subleading pre-exponential factors),

$$\rho_s(t) \sim \exp[-t/t_s(s)] \ , \tag{116}$$

with a long lifetime t_s that increases exponentially with the cluster size s

$$t_s(s) = t_0 \exp[A(\lambda)s] \tag{117}$$

for sufficiently large s. Here, t_0 is some microscopic time scale.

The lifetime increases the faster with s the further the cluster is in the active phase. This means, the prefactor $A(\lambda)$ which plays the role of an inverse correlation volume vanishes at the multicritical value λ_* and monotonically increases with increasing λ. Close to the multicritical point, the behavior of $A(\lambda)$ can be inferred from scaling. Since $A(\lambda)$ has the dimension of an inverse volume, it varies as

$$A(\lambda) \sim (\lambda - \lambda_*)^{\nu_* D_f} \tag{118}$$

where ν_* is the correlation length exponent of the multicritical point and D_f is the (fractal) space dimensionality of the underlying cluster.

Note that (117) establishes an exponential relation between length and time scales at the transition. Because the number of sites s of a percolation cluster is related to its linear size R_s via $s \sim R_s^{D_f}$, eq. (117) implies

$$\ln t_s \sim R_s^{D_f} \ . \tag{119}$$

Thus, the dynamical scaling is activated rather than power-law with the tunneling exponent being identical to the fractal dimension of the critical percolation cluster, $\psi = D_f$.

To confirm the above phenomenological arguments, we have performed extensive Monte-Carlo simulations of the contact process on finite-size clusters using clean one-dimensional and two-dimensional systems as well as diluted lattices. Our simulation method is based on the algorithm by Dickman [35] and described in detail in Refs. [28, 29].

A characteristic set of results is shown in Fig. 3.3. It shows the time evolution of the contact process on several one-dimensional clusters of different size s, starting

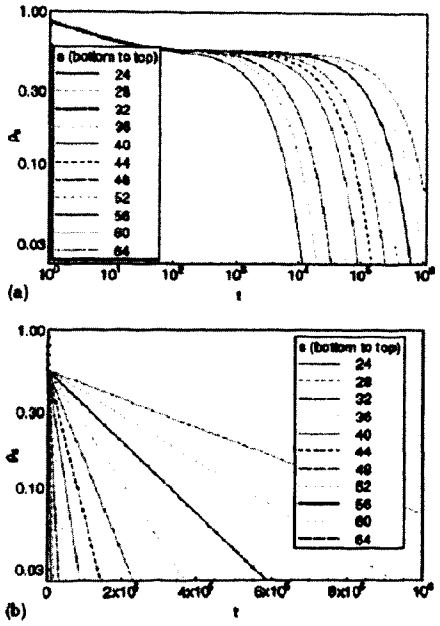

Figure 3.3. (Color online:) Contact process on one-dimensional clusters of size s, starting from a fully active lattice at $\lambda = 3.8, \mu = 1$ which is in the active phase. (a) Double-logarithmic plot of density vs. time showing the two-stage time-evolution via a metastable state. (b) Log-linear plot demonstrating that the long-time decay is exponential. All data are averages over 10^5 independent runs.

from a fully active lattice. The infection rate $\lambda = 3.8$ (we set $\mu = 1$) puts the clusters (locally) in the ordered phase, i.e., it is supercritical, since the critical value in one dimension is $\lambda_c = 3.298$. All data are averages over 10^5 independent trials. The double-logarithmic plot of density ρ_s vs. time t in Fig. 3.3a clearly shows the two-stage time evolution consisting of a rapid initial decay (independent of cluster size) towards a metastable state followed by a long-time decay towards the absorbing state which becomes slower with increasing cluster size. Replotting the data in log-linear form in Fig. 3.3b confirms that the long-time decay is exponential, as predicted in (116).

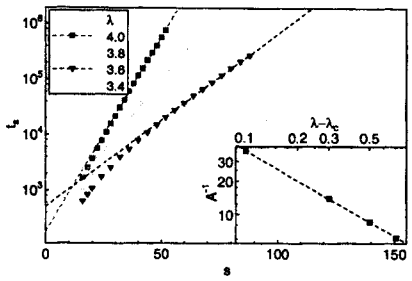

Figure 3.4. (Color online:) Lifetime t_s as a function of cluster size s for different values of the infection rate λ. The other parameters are as in Fig. 3.3. The dashed lines are fits of the large-s behavior to the exponential dependence (117). Inset: Correlation volume A^{-1} as a function of the distance from bulk criticality. The dashed line is a power-law fit.

The lifetime t_s of the contact process on the cluster can be determined by fitting the asymptotic part of the $\rho_s(t)$ curve to (116). Figure 3.4 shows the lifetime as a function of cluster size s for four different values of the infection rate λ. Clearly, for sufficiently large clusters, the lifetime depends exponentially on the cluster size, as predicted in (117). (The data for $\lambda = 3.4$ which is very close to the bulk critical point of $\lambda_c = 3.298$ have not fully reached the asymptotic regime as can be seen from the remaining slight curvature of the plot.) By fitting the large-s behavior of the lifetime curves to the exponential law (117), we obtain an estimate of the inverse correlation volume A. The inset of Fig. 3.4 shows this correlation volume as a function of the distance from the bulk critical point. In accordance with (118) it behaves as a power law. The exponent value of approximately 0.95 is in reasonable agreement with the prediction $\nu = 1.097$ for our one-dimensional clusters.

We have performed analogous simulations for various sets of two-dimensional clusters as well as finite-size diluted lattices. In all cases, the Monte-Carlo results confirm the phenomenological theory summarized in eqs. (116), (117), and (118).

3.4.2. Steady-state Density and Density Decay . We now consider the full problem, the contact process on a diluted lattice close to the percolation threshold. To obtain observables of the entire system, we must sum over all percolation clusters.

Let us start by analyzing static quantities such as the steady state density ρ_{st} of active sites (the order parameter of the nonequilibrium transition) and the spatial correlation length $\xi_\perp$. Finite-size percolation clusters do not contribute to the

steady-state density because the contact process eventually decays into the absorbing inactive state on any finite-size cluster. A steady-state density can thus exist only on the infinite percolation cluster for $p < p_c$. For $\lambda > \lambda_*$, the infinite cluster is supercritical, i.e., a finite fraction of its sites is active. Thus, the total steady-state density is proportional to the number of sites in the infinite cluster,

$$\rho_{\rm st} \sim P_\infty(p) \sim \begin{cases} |p-p_c|^{\beta_c} & (p<p_c) \\ 0 & (p>p_c) \end{cases} . \tag{120}$$

Consequently, the order parameter exponent β of the nonequilibrium transition is identical to the corresponding exponent β_c of the lattice percolation problem.

The (average) spatial correlation length $\xi_\perp$ of the nonequilibrium process can be found using a similar argument. On the one hand, the spatial correlations of the contact process cannot extend beyond the connectedness length ξ_c of the underlying diluted lattice because different percolation clusters are completely decoupled. This implies $\xi_\perp \lesssim \xi_c$. On the other hand, for $\lambda > \lambda_*$, all sites on the same percolation cluster are strongly correlated in space, implying $\xi_\perp \gtrsim \xi_c$. We therefore conclude

$$\xi_\perp \approx \xi_c \ , \tag{121}$$

and the correlation length exponent $\nu_\perp$ is also identical to its lattice percolation counterpart ν_c.

We now turn to the dynamics of the nonequilibrium transition across the percolation threshold. In order to find the time evolution of the total density of active sites (starting from a completely active lattice), we sum over all percolation clusters by combining the cluster size distribution (113) with the single-cluster time evolution (116). The total density is thus given by

$$\begin{aligned} \rho(t,\Delta) &= \int ds\, s\, n_s(\Delta)\, \rho_s(t) \\ &\sim \int ds\, s\, n_s(\Delta)\, \exp[-t/t_s(s)] \end{aligned} \tag{122}$$

In the following, we evaluate this integral at the transition as well as in the active and inactive phases.

Right at the percolation threshold, the scaling function in the cluster size distribution (113) is a constant, $f(0)$, and (122) simplifies to

$$\rho(t,0) \sim \int ds\; s^{1-\tau_c} \exp[-(t/t_0 e^{As})] \; . \tag{123}$$

To estimate this integral, we note that only sufficiently large clusters, with a minimum size of $s_{\min}(t) = A^{-1} \ln(t/t_0)$, contribute to the total density at time t,

$$\rho(t,0) \sim \int_{s_{\min}}^{\infty} ds\, s^{1-\tau_c} \sim s_{\min}^{2-\tau_c} \; . \tag{124}$$

The leading long-time dependence of the total density right at the percolation threshold thus takes the unusual logarithmic form

$$\rho(t,0) \sim [\ln(t/t_0)]^{-\bar{\delta}} \; , \tag{125}$$

again reflecting the activated dynamical scaling, with the critical exponent given by $\bar{\delta} = \tau_c - 2 = \beta_c/(\nu_c D_f)$.

In the disconnected, inactive phase ($p > p_c$) we need to use expression (114) for the scaling function of the cluster size distribution. The resulting integral for the time evolution of the density reads

$$\rho(t,\Delta) \sim \int ds s^{1-\tau_c} \exp[-B_1 s \Delta^{1/\sigma_c} - (t/t_0 e^{As})]. \tag{126}$$

For long times, the leading behavior of the integral can be calculated using the saddle-point method. Minimizing the exponent of the integrand shows that the main contribution at time t to the integral (126) comes from clusters of size $s_0 = -A^{-1} \ln[B_1 \Delta^{1/\sigma_c} t_0/(At)]$. Inserting this into the integrand results in a power-law density decay

$$\rho(t,\Delta) \sim (t/t_0)^{-d/z'} \qquad (p > p_c) \; . \tag{127}$$

The nonuniversal exponent z' is given by $z' = (Ad/B_1)\Delta^{-1/\sigma_c} \sim \xi_\perp^{D_f}$, i.e., it diverges at the critical point $p = p_c$.

In the percolating, active phase ($p < p_c$), the infinite percolation cluster contributes a nonzero steady state density $\rho_{\rm st}(\Delta)$ given by (120). However, the long-time approach of the density towards this value is determined by the slow decay of the

metastable states of large finite-size percolation clusters. To estimate their contribution, we must use the expression (115) for the scaling function of the cluster size distribution. The resulting integral now reads

$$\rho(t,\Delta) - \rho_{st}(\Delta) \sim \int ds\, s^{1-\tau_c} \exp\left[-(B_2 s|\Delta|^{1/\sigma_c})^{1-1/d} - (t/t_0 e^{As})\right] . \tag{128}$$

We again apply the saddle-point method to find the leading low-time behavior of this integral. Minimizing the exponent shows the main contribution coming from clusters of size $s_0 = -A^{-1}\ln[B_2|\Delta|^{1/\sigma_c}(d-1)/(Atd)]$. By inserting this into the integrand, we find a nonexponential density decay of the form

$$\rho(t,\Delta) - \rho_{st}(\Delta) \sim e^{-[(d/z'')\ln(t/t_0)]^{1-1/d}} \qquad (p < p_c) . \tag{129}$$

Here, $z'' = (Ad/B_2)|\Delta|^{-1/\sigma_c} \sim \xi_\perp^{D_f}$ is another nonuniversal exponent which diverges at the critical point.

The slow nonexponential relaxation of the total density on both sides of the actual transition as given in (127) and (129) is characteristic of a Griffiths phase [36] in the contact process [37]. It is brought about by the competition between the exponentially decreasing probability for finding a large percolation cluster off criticality and the exponentially increasing lifetime of such a cluster. Note that time t and spatial correlation length $\xi_\perp$ enter the off-critical decay laws (127) and (129) in terms of the combination $\ln(t/t_0)/\xi_\perp^{D_f}$ again reflecting the activated character of the dynamical scaling.

3.4.3. Spreading from A Single Seed. After having discussed the time evolution of the density starting from a completely infected lattice, we now consider the survival probability $P_s(t)$ for runs starting from a single random seed site. To estimate $P_s(t)$, we note that the probability of a random seed site to belong to a cluster of size s is given by $s\,n_s(\Delta)$. The activity of the contact process is confined to this seed cluster. Following the arguments leading to (116), the probability that this cluster survives is proportional to $\exp(-t/t_s)$. The average survival probability at time t can thus be written as a sum over all possible seed clusters,

$$P_s(t,\Delta) \sim \int ds\, s\, n_s(\Delta)\, \exp[-t/t_s(s)] . \tag{130}$$

This is exactly the same integral as the one governing the density decay (122). We conclude that the time dependence of the survival probability for runs starting from a single seed is identical to the time evolution of the density when starting from a fully infected lattice, as is expected for the contact process under very general conditions (see, e.g., Ref. [5]).

To determine the (average) total number $N(t)$ of active sites in a cloud spreading from a single seed, we observe that a supercritical cloud initially grows ballistically. This means its radius grows linearly with time, and the number of active sites follows a power law. This ballistic growth stops when the number of active sites is of the order of the cluster size s. After that, the number of active sites stays approximately constant. The number $N_s(t)$ of active sites on a percolation cluster of size s is thus given by

$$N_s(t) \sim \begin{cases} (t/t_0)^{D_f} & (t < t_i(s)) \\ s & (t > t_i(s)) \end{cases} \tag{131}$$

where $t_i(s) \sim R_s(s) \sim t_0 s^{1/D_f}$ is the saturation time of this cluster. Note that N_s decays to zero only after the much longer cluster lifetime $t_s(s) = t_0 \exp[A(\lambda)s]$ given in (117).

We now average over all possible positions of the seed site as in (130). This yields

$$N(t,\Delta) \sim \int_{s_{\min}}^{\infty} ds\, s\, n_s(\Delta)\, N_s(t) \tag{132}$$

with $s_{\min} \sim A^{-1} \ln(t/t_0)$. At criticality, this integral is easily evaluated, giving

$$N(t,0) \sim t^{D_f(3-\tau_c)} = t^{\gamma_c/\nu_c} \, . \tag{133}$$

The lower bound of the integral (i.e., the logarithmically slow long-time decay of the clusters) produces a subleading correction only. Consequently, we arrive at the somewhat surprising conclusion that the initial spreading follows a power-law and is thus much faster than the long-time density decay. In contrast, at the infinite-randomness critical point governing the generic ($p < p_c$) transition, both the initial spreading and the long-time decay follow logarithmic laws [26, 27, 28, 29]. Note that a similar situation occurs at the percolation quantum phase transition in the diluted transverse-field Ising model [13] where the temperature-dependence of the correlation length does not follow the naively expected logarithmic law.

3.4.4. External Source Field. In this subsection we discuss the effects of spontaneous activity creation on our nonequilibrium phase transition. Specifically, in addition to healing and infection, we now consider a third process by which an inactive site can spontaneously turn into an active site at rate h. This rate plays the role of an external "source field" conjugate to the order parameter.

To find the steady state density in the presence of such a source field, we first consider a single percolation cluster. As before, we are interested in the supercritical regime $\lambda > \lambda_*$. At any given time t, a cluster of size s will be active (on average), if at least one of the s sites has spontaneously become active within one lifetime $t_s(s) = t_0 e^{As}$ before t, i.e., in the interval $[t - t_s(s), t]$. For a small external field h, the average number of active sites created on a cluster of size s is $M_s(h) = hst_s(s) = hst_0 e^{As}$. This linear response expression is valid as long as $M_s \ll s$. The probability $w_s(h)$ for a cluster of size s to be active in the steady state is thus given by

$$w_s(h) \approx \begin{cases} M_s(h) & (M_s(h) < 1) \\ 1 & (M_s(h) > 1) \end{cases} . \tag{134}$$

Turning to the full lattice, the total steady state density is obtained by summing over all clusters

$$\rho_{\rm st}(h, \Delta) \sim \int ds\, s\, n_s(\Delta) \min[1, M_s(h)] . \tag{135}$$

This integral can be evaluated along the same lines as the corresponding integral (122) for the time-evolution of the zero-field density. For small fields h, we obtain

$$\rho_{\rm st}(h, 0) \sim [\ln(h_0/h)]^{-\bar{\delta}} \qquad (p = p_c), \tag{136}$$

$$\rho_{\rm st}(h, \Delta) \sim (h/h_0)^{d/z'} \qquad (p > p_c), \tag{137}$$

$$\delta\rho_{\rm st}(h, \Delta) \sim e^{[(d/z'')\ln(h/h_0)]^{1-1/d}} \qquad (p < p_c) , \tag{138}$$

where $\delta\rho_{\rm st}(h, \Delta) = \rho_{\rm st}(h, \Delta) - \rho_{\rm st}(0, \Delta)$ is the excess density due to the field in the active phase and $h_0 = 1/t_0$. At criticality, $p = p_c$, the relation between density $\rho_{\rm st}$ and field h is logarithmic because the field represents a rate (inverse time) and the dynamical scaling is activated. Off criticality, we find strong Griffiths singularities analogous to those in the time-dependence of the density. The exponents z' and z'' take the same values as calculated after eqs. (127) and (129), respectively.

3.4.5. Scaling Theory. In Subsubsecs 3.4.2 and 3.4.4, we have determined the critical behavior of the density of active sites by explicitly averaging the single

cluster dynamics over all percolation clusters. The same results can also be obtained from writing down a general scaling theory of the density for the case of activated dynamical scaling [28, 29].

According to (120), in the active phase, the density is proportional to the number of sites in the infinite percolation cluster. Its scale dimension must therefore be identical to the scale dimension of P_∞ which is β_c/ν_c. Time must enter the theory via the scaling combination $\ln(t/t_0)b^\psi$ with the tunneling exponent given by $\psi = D_f$ and b an arbitrary length scale factor. This scaling combination reflects the activated dynamical scaling, i.e., the exponential relation (119) between length and time scales. Finally, the source field h, being a rate, scales like inverse time. This leads to the following scaling theory of the density,

$$\begin{aligned}\rho[\Delta, \ln(t/t_0), \ln(h_0/h)] = \\ = b^{\beta_c/\nu_c}\rho[\Delta b^{-1/\nu_c}, \ln(t/t_0)b^\psi, \ln(h_0/h)b^\psi]\end{aligned} \tag{139}$$

This scaling theory is compatible with all our explicit results which can be rederived by setting the arbitrary scale factor b to the appropriate values.

3.5. GENERALITY OF THE ACTIVATED SCALING SCENARIO

In Subsec 3.4, we have developed a theory for the nonequilibrium phase transition of the simple contact process across the lattice percolation threshold and found it to be characterized by unconventional activated dynamical scaling. In the present section, we investigate how general this exotic behavior is for absorbing state transitions by considering the generalized contact process with several absorbing states.

This is a particularly interesting question because the generic transitions ($p < p_c$) of the diluted simple and generalized contact processes appear to behave differently. The generic transition in the simple contact process has been shown to be of infinite-randomness type with activated dynamical scaling using both a strong-disorder renormalization group [26, 27] and Monte-Carlo simulations [28, 29]. In contrast, the strong-disorder renormalization group treatment of the disordered generalized contact process [27] suggests more conventional behavior, even though the ultimate fate of the transition could not be determined.

To address the same question for our transition across the lattice percolation threshold, we note that any difference between the simple and the generalized contact processes must stem from the single-cluster dynamics because the underlying lattice

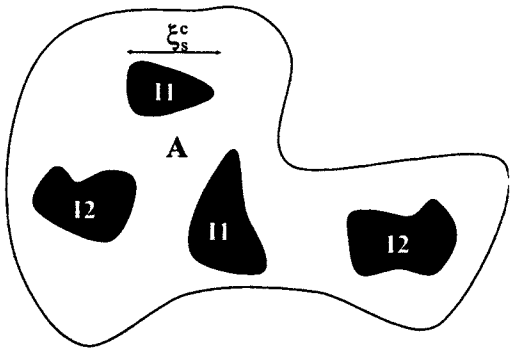

Figure 3.5. (Color online:) Schematic of the metastable state of the supercritical generalized contact process with two inactive states on a single percolation cluster. A denotes the active state, and I_1 and I_2 are the inactive states. ξ_s^c is the connected correlation length of the density fluctuations *on* the cluster.

is identical. In the following we therefore first give heuristic arguments for the single-cluster dynamics of the supercritical generalized contact process and then verify them by Monte-Carlo simulations.

If the percolation cluster is locally in the active phase ($\lambda > \lambda_*$), the density time evolution, starting from a fully active lattice, proceeds in two stages, analogously to the simple contact process. There is a rapid initial decay to a metastable state with a nonzero density of active sites and finite-size islands of each of the inactive phases (see Fig. 3.5). For this metastable state to decay into one of the n absorbing configurations, all sites must go into *the same* inactive state which requires a rare large density fluctuation. Let us assume for definiteness that the decay is into the I_1 state. The main difference to the simple contact process considered in Subsubsec. 3.4.1 is that sites that are in inactive states $I_2 \ldots I_n$ cannot directly decay into I_1. This means, each of the inactive islands in states $I_2 \ldots I_n$ first needs to be "eaten" by the active regions before the entire cluster can decay into the I_1 state. This can only happen via infection from the boundary of the inactive island and is thus a slow process. However, since the characteristic size of the inactive islands in the metastable state is finite (it is given by the connected density correlation length ξ_s^c on the cluster), this process happens with a nonzero rate that is independent of the size s of the underlying percolation cluster (for sufficiently large s).

The decay of the metastable state into one of the absorbing states is therefore brought about by the rare collective decay of a large number of *independent* correlation volumes just as in the simple contact process. As a result, the lifetime $t_s(s)$ depends exponentially on the number of involved correlation volumes, i.e., it depends exponentially on the cluster size s. We thus find that the long-time density decay of the generalized contact process on a single large percolation cluster is governed by the same equations (116) and (117) as the decay of the simple contact process.

To verify these phenomenological arguments, we have performed large-scale Monte-Carlo simulations of the generalized contact process with two and three absorbing states on clean and disordered one-dimensional and two-dimensional lattices. In all cases, we have first performed bulk simulations (spreading from a single seed) to find the bulk critical point. An example is shown in Fig. 3.6, details of the bulk critical behavior will be reported elsewhere.

After having determined the critical point, if any, we have selected several parameter sets in the bulk active phase and studied the long-time density decay of the generalized contact process on finite size clusters. As expected, the decay proceeds via the two stages discussed above. As in Subsubsec. 3.4.1, we extract the lifetime t_s from the slow exponential long-time part of the decay. Two characteristic sets of results are shown in Fig. 3.7. The figure confirms that the lifetime of the generalized contact process on a finite-size cluster depends exponentially on the number of sites in the cluster, as given in (117). We have obtained analogous results for all cases investigated, verifying the phenomenological theory given above.

Because the long-time dynamics of the generalized contact process on a single supercritical cluster follows the same behavior (116) and (117) as that of the simple contact process, we conclude that its nonequilibrium transition across the percolation threshold will also be governed by the theory developed on Subsec. 3.4. In other words, the lattice percolation transitions of the simple and generalized contact processes belong to the same universality class, irrespective of the number n of absorbing states.

3.6. CONCLUSIONS

In this final subsection of the paper, we first summarize our results, discuss their generality, and relate them to the behavior of certain quantum phase transitions on diluted lattices. We then compare the recently found infinite-randomness critical point at the generic transition ($p < p_c$) to the behavior at our lattice percolation transition. Finally, we relate our findings to a general classification of phase transitions with quenched spatial disorder [38].

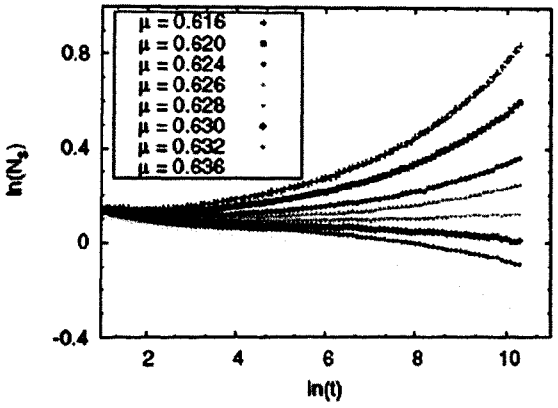

Figure 3.6. (Color online:) Bulk phase transition of the generalized contact process with two absorbing states in $d = 1$ measured via spreading from a single seed: Number N of active sites vs. time t for different healing rates μ. The infection and boundary activation rates are fixed, $\lambda = \sigma = 1$, and the data are averages over 10^6 runs. The critical point appears to be close to $\mu = 0.628$ in agreement with [20].

To summarize, we have investigated absorbing state phase transitions on randomly diluted lattices, taking the simple and generalized contact processes as examples. We have focused on the nonequilibrium phase transition across the lattice percolation threshold and shown that it can be understood by combining the time evolution of the supercritical nonequilibrium process on a finite-size cluster with results from classical lattice percolation theory. The interplay between geometric criticality and dynamic fluctuations at this transition leads to a novel universality class. It is characterized by ultraslow activated (i.e., exponential) rather than power-law dynamical scaling and accompanied by a nonexponential decay in the Griffiths regions. All

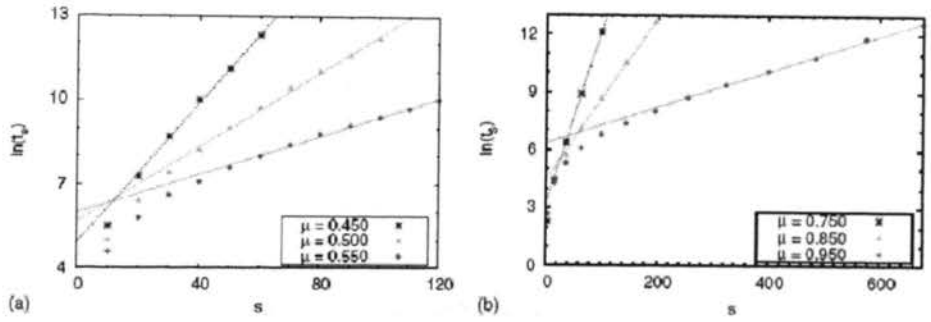

Figure 3.7. (Color online:) Lifetime t_s as a function of cluster size s for the generalized contact process with two inactive states at different values of the healing rate μ. The infection and boundary activation rates are fixed, $\lambda = \sigma = 1$, and the data are averages over 10^6 runs. (a) $d = 1$ where the bulk system has a transition, see Fig. 3.6. (b) $d = 2$, where we do not find a bulk transition because the system is always active [32]. The dashed lines are fits of the large-s behaviors to the exponential law (117).

critical exponents of the nonequilibrium phase transition can be expressed in terms of the classical lattice percolation exponents. Their values are known exactly in two space dimensions and with good numerical accuracy in three space dimensions; they are summarized in Table 3.1.

Thus, our transition in $d = 2$ provides one of the few examples of a nonequilibrium phase transition with exactly known critical exponents.

The logarithmically slow dynamics (125), (136) at criticality together with the small value of the exponent $\bar{\delta}$ make a numerical verification of our theory by simulations of the full diluted lattice a very costly proposition. The results of recent

Table 3.1. Critical exponents of the nonequilibrium phase transition across the percolation threshold in two and three space dimensions.

Exponent	$d = 2$	$d = 3$
$\beta = \beta_c$	5/36	0.417
$\nu = \nu_c$	4/3	0.875
$\psi = D_f = d - \beta_c/\nu_c$	91/48	2.523
$\bar{\delta} = \beta_c/(\nu_c D_f)$	5/91	0.188

Monte-Carlo simulations in two dimensions [29] at $p = p_c$ are compatible with our theory but not yet sufficient to be considered a quantitative verification. This remains a task for the future.

The unconventional critical behavior of our nonequilibrium phase transition at $p = p_c$ is the direct result of combining the power-law spectrum (113) of cluster sizes with the exponential relation (119) between length and time scales. We therefore expect other equilibrium or nonequilibrium systems that share these two characteristics to display similar critical behavior at the lattice percolation transition. One prototypical example is the transverse-field Ising model on a diluted lattice. In this system, the quantum-mechanical energy gap (which represents an inverse time) of a cluster decreases exponentially with the cluster size. Consequently, the critical behavior of the diluted transverse-field Ising model across the lattice percolation threshold is very similar to the one found in this paper [13]. Other candidates are magnetic quantum phase transitions in metallic systems or certain superconductor-metal quantum phase transitions [39, 40, 41, 42], even though a pure percolation scenario may be hard to realize in metallic systems.

Our work has focused on the nonequilibrium phase transition across the lattice percolation threshold. It is instructive to compare its critical behavior to that of the generic transition occurring for $p < p_c$ (see Fig. 3.1). Hooyberghs et al. [26, 27] applied a strong disorder renormalization group to the one-dimensional disordered contact process. They found an exotic infinite-randomness critical point in the universality class of the random-transverse field Ising model (which likely governs the transition for any disorder strength [43]). The same analogy is expected to hold in two space dimensions. Recently, these predictions were confirmed by large scale Monte-Carlo simulations [28, 29]. Our nonequilibrium transition across the lattice percolation

threshold shares some characteristics with these infinite-randomness critical points, in particular, the activated dynamical scaling which leads to a logarithmically slow density decay at criticality.

However, the generic and percolation transitions are in different universality classes with different critical exponent values. Moreover, the initial spreading from a single seed is qualitatively different (logarithmically slow at the generic infinite-randomness critical point but of power-law type at our percolation transition). Finally, at the percolation transition the simple and generalized contact processes are in the same universality class while this does not seem to be the case for the generic transition [27].

The results of this paper are in agreement with a recent general classification of phase transitions with quenched spatial disorder and short-range interactions [39, 38]. It is based on the effective dimensionality $d_{\rm eff}$ of the droplets or clusters. Three classes need to be distinguished: (a) If the clusters are below the lower critical dimension of the problem, $d_{\rm eff} < d_c^-$, the critical behavior is conventional (power-law scaling and exponentially weak Griffiths effects). This is the case for most classical equilibrium transitions. (b) If $d_{\rm eff} = d_c^-$, the dynamical scaling is activated and accompanied by strong Griffiths effects. This case is realized at the nonequilibrium transition considered here as well as the generic transition of the disordered contact process. It also applies to various quantum phase transitions [44, 13, 40]. (c) If $d_{\rm eff} > d_c^-$, a single supercritical cluster can undergo the phase transition independently of the bulk system. This leads to the smearing of the global phase transition; it occurs, e.g., in dissipative quantum magnets [45, 46] or in the contact process with extended defects [47].

In conclusion, our work demonstrates that absorbing state transitions on percolating lattices display unusual behavior. Interestingly, experimental verifications of the theoretically predicted critical behavior at (clean) absorbing state transitions are extremely rare [48]. For instance, to the best of our knowledge, the only complete verification of directed percolation scaling was found very recently in the transition between two turbulent states in a liquid crystal [49]. Our theory suggests that unconventional disorder effects may be responsible for the surprising absence of directed percolation scaling in at least some of the experiments.

Acknowledgements

This work has been supported in part by the NSF under grant no. DMR-0339147, by Research Corporation, and by the University of Missouri Research Board. We gratefully acknowledge discussions with J. Hoyos as well the hospitality of the Max-Planck-Institute for Physics of Complex Systems during part of this research.

[1] T. M. Liggett, Interacting Particle Systems Springer, Berlin, 1985.

[2] V. P. Zhdanov and B. Kasemo, Surf. Sci. Rep. **20**, 113 1994.

[3] B. Schmittmann and R. K. P. Zia, in Phase Transitions and Critical Phenomena, edited by C. Domb and J. L. Lebowitz Academic, New York, 1995, Vol. **17**, p. 1.

[4] J. Marro and R. Dickman, Nonequilibrium Phase Transitions in Lattice Models Cambridge University Press, Cambridge, England, 1999.

[5] H. Hinrichsen, Adv. Phys. **49**, 815 2000.

[6] G. Odor, Rev. Mod. Phys. **76**, 663 2004.

[7] S. Lbeck, Int. J. Mod. Phys. B **18**, 3977 2004.

[8] U. C. Tuber, M. Howard, and B. P. Vollmayr-Lee, J. Phys. A **38**, R79 2005.

[9] D. Stauffer and A. Aharony, Introduction to Percolation Theory CRC Press, Boca Raton, FL, 1991.

[10] T. K. Bergstresser, J. Phys. C **10**, 3381 1977.

[11] M. J. Stephen and G. S. Grest, Phys. Rev. Lett. **38**, 567 1977.

[12] Y. Gefen, B. B. Mandelbrot, and A. Aharony, Phys. Rev. Lett. **45**, 855 1980.

[13] T. Senthil and S. Sachdev, Phys. Rev. Lett. **77**, 5292 1996.

[14] A. W. Sandvik, Phys. Rev. Lett. **89**, 177201 2002.

[15] L. Wang and A. W. Sandvik, Phys. Rev. Lett. **97**, 117204 2006.

[16] T. Vojta and J. Schmalian, Phys. Rev. Lett. **95**, 237206 2005.

[17] P. Grassberger and A. de la Torre, Ann. Phys. N.Y. **122**, 373 1979.

[18] H. K. Janssen, Z. Phys. B: Condens. Matter **42**, 151 1981.

[19] P. Grassberger, Z. Phys. B: Condens. Matter **47**, 365 1982.

[20] H. Hinrichsen, Phys. Rev. E **55**, 219 1997.

[21] T. E. Harris, Ann. Probab. **2**, 969 1974.

[22] W. Kinzel, Z. Phys. B: Condens. Matter **58**, 229 1985.

[23] A. J. Noest, Phys. Rev. Lett. **57**, 90 1986.

[24] A. G. Moreira and R. Dickman, Phys. Rev. E **54**, R3090 1996.

[25] H. K. Janssen, Phys. Rev. E **55**, 6253 1997.

[26] J. Hooyberghs, F. Igloi, and C. Vanderzande, Phys. Rev. Lett. **90**, 100601 2003.

[27] J. Hooyberghs, F. Igloi, and C. Vanderzande, Phys. Rev. E **69**, 066140 2004.

[28] T. Vojta and M. Dickison, Phys. Rev. E **72**, 036126 2005.

[29] T. Vojta, A. Farquhar, and J. Mast, Phys. Rev. E **79**, 011111 2009.

[30] T. Vojta and M. Y. Lee, Phys. Rev. Lett. **96**, 035701 2006.

[31] J. Hooyberghs, E. Carlon, and C. Vanderzande, Phys. Rev. E **64**, 036124 2001.

[32] For d=2,n=2, Hinrichsen [20] finds a mean-field transition while our own simulations suggest that the system is always active. Since this difference is of no importance for the present paper, it will be addressed elsewhere.

[33] S. R. Dahmen, L. Sittler, and H. Hinrichsen, J. Stat. Mech. Theor. Exp. 2007, P01011.

[34] We define p as the fraction of sites removed rather than the fraction of sites present.

[35] R. Dickman, Phys. Rev. E **60**, R2441 1999.

[36] R. B. Griffiths, Phys. Rev. Lett. **23**, 17 1969.

[37] A. J. Noest, Phys. Rev. B **38**, 2715 1988.

[38] T. Vojta, J. Phys. A **39**, R143 2006.

[39] T. Vojta and J. Schmalian, Phys. Rev. B **72**, 045438 2005.

[40] J. A. Hoyos, C. Kotabage, and T. Vojta, Phys. Rev. Lett. **99**, 230601 2007.

[41] A. Del Maestro, B. Rosenow, M. Mller, and S. Sachdev, Phys. Rev. Lett. **101**, 035701 2008.

[42] T. Vojta, C. Kotabage, and J. A. Hoyos, Phys. Rev. B **79**, 024401 2009.

[43] J. A. Hoyos, Phys. Rev. E **78**, 032101 2008.

[44] D. S. Fisher, Phys. Rev. Lett. **69**, 534 1992.

[45] T. Vojta, Phys. Rev. Lett. **90**, 107202 2003.

[46] J. A. Hoyos and T. Vojta, Phys. Rev. Lett. **100**, 240601 2008.

[47] T. Vojta, Phys. Rev. E **70**, 026108 2004.

[48] H. Hinrichsen, Braz. J. Phys. **30**, 69 2000.

[49] K. A. Takeuchi, M. Kuroda, H. Chate, and M. Sano, Phys. Rev. Lett. **99**, 234503 2007.

4. PHASE TRANSITIONS OF THE GENERALIZED CONTACT PROCESS WITH TWO ABSORBING STATES

Man Young Lee and Thomas Vojta

Physics, Missouri University of Science and Technology, Rolla, MO 65409, USA

Abstract[16]

We investigate the generalized contact process with two absorbing states in one space dimension by means of large-scale Monte-Carlo simulations. Treating the creation rate of active sites between inactive domains as an independent parameter leads to a rich phase diagram. In addition to the conventional active and inactive phases we find a parameter region where the simple contact process is inactive, but an *infinitesimal* creation rate at the boundary between inactive domains is sufficient to take the system into the active phase. Thus, the generalized contact process has two different phase transition lines. The point separating them shares some characteristics with a multicritical point. We also study in detail the critical behaviors of these transitions and their universality.

4.1. INTRODUCTION

Many systems in physics, chemistry, and biology are far from thermal equilibrium, even if they are in time-independent steady states. In recent years, continuous phase transitions between different nonequilibrium steady states have attracted lots of attention. Just as in equilibrium, these transitions are characterized by large-scale fluctuations and collective behavior over large distances and long times. Examples can be found, e.g., in surface growth, granular flow, chemical reactions, population dynamics, and even in traffic jams [1, 2, 3, 4, 5, 6, 7].

Continuous nonequilibrium phase transitions can be divided into different universality classes according to their critical behavior, and considerable effort has been

[16] All of this section is reproduced from Physical Review E **81** 061128 (2010) and then reformatted and renumbered.

devoted to categorizing the variety of known transitions. A well-studied type of nonequilibrium phase transitions separates fluctuating (active) steady states from absorbing (inactive) states where fluctuations stop completely. The generic universality class for these so-called absorbing state transitions is directed percolation (DP) [8]. More specifically, it was conjectured by Janssen and Grassberger [9, 10] that all absorbing state transitions with a scalar order parameter and short-range interactions belong to this class as long as there are no extra symmetries or conservation laws. While nonequilibrium transitions in the DP universality class are ubiquitous in both theory and computer simulations, experimental verifications were only found rather recently in ferrofluidic spikes [11] and in the transition between two turbulent states in a liquid crystal [12].

Absorbing state transitions in universality classes different from DP can occur in the presence of additional symmetries or conservation laws. Hinrichsen [13] introduced nonequilibrium lattice models with $n \geq 2$ absorbing states. In the case of two symmetric absorbing states ($n = 2$), he found the transition to be in a new universality class, the Z_2-symmetric directed percolation class (DP2). If the symmetry between the absorbing states is broken, the critical behavior reverts back to DP. In one dimension, the DP2 universality class coincides [4] with the parity-conserving PC class [14] which is observed, e.g., in the branching-annihilating random walk with an even number of offspring (BARWE) [15].

In this paper, we revisit one of the stochastic lattice models introduced in Ref. [13], the generalized contact process with two absorbing states in one space dimension. Compared to the simple contact process [16], this model contains an additional dynamical process, *viz.*, the creation of active sites at the boundary between domains of different inactive states. By treating the rate for this process as an independent parameter we uncover a rich phase diagram with two different types of phase transitions, separated by a special point that shares many characteristics with a multicritical point. We perform large-scale Monte-Carlo simulations of this model to study in detail the critical behavior of these transitions.

Our paper is organized as follows. We introduce the generalized contact process with several absorbing states in Subsec. 4.2. In Subsec. 4.3, we summarize the mean-field theory for this system. Subsec. 4.4 is devoted to the results and interpretation

of our Monte-Carlo simulations. We conclude in Subsec. 4.5.

4.2. THE GENERALIZED CONTACT PROCESS WITH SEVERAL ABSORBING STATES

The contact process [16] is a paradigmatic model in the DP universality class. It is defined on a d-dimensional hypercubic lattice. Each lattice site $\mathbf{r}$ can be in one of two states, namely A, the active (infected) state or I, the inactive (healthy) state. Over the course of the time evolution, active sites can infect their nearest neighbors, or they can become inactive spontaneously. More precisely, the contact process is a continuous-time Markov process during which active sites turn inactive at a rate μ, while inactive sites become infected at a rate $\lambda m/(2d)$ where m is the number of active nearest neighbors. The healing rate μ and the infection rate λ are external parameters whose ratio determines the behavior of the system.

If $\mu \gg \lambda$, healing dominates over infection. All infected sites will eventually become inactive, leaving the absorbing state without any active sites the only steady state. Thus, the system is in the inactive phase. In the opposite limit, $\lambda \gg \mu$, the infection survives for infinite times, i.e., there is a steady state with a nonzero density of active sites. This is the active phase. The nonequilibrium phase transition between these two phases at a critical value of the ratio λ/μ is in the DP universality class.

In 1997, Hinrichsen [13] introduced a generalization of the contact process. Each lattice site can now be in one of $n+1$ states, the active state A or one of the n different inactive states I_k ($k = 1 \ldots n$). k is sometimes called the "color" index. The dynamics of the generalized contact process is defined via the following rates for transitions of pairs of nearest-neighbor sites,

$$w(\mathrm{AA} \to \mathrm{AI}_k) = w(\mathrm{AA} \to \mathrm{I}_k\mathrm{A}) = \bar{\mu}/n \,, \tag{140}$$

$$w(\mathrm{AI}_k \to \mathrm{I}_k\mathrm{I}_k) = w(\mathrm{I}_k\mathrm{A} \to \mathrm{I}_k\mathrm{I}_k) = \mu_k \,, \tag{141}$$

$$w(\mathrm{AI}_k \to \mathrm{AA}) = w(\mathrm{I}_k\mathrm{A} \to \mathrm{AA}) = \lambda \,, \tag{142}$$

$$w(\mathrm{I}_k\mathrm{I}_l \to \mathrm{I}_k\mathrm{A}) = w(\mathrm{I}_k\mathrm{I}_l \to \mathrm{AI}_l) = \sigma \,, \tag{143}$$

with $k, l = 1 \ldots n$ and $k \neq l$. All other rates vanish. We are mostly interested in the fully symmetric case, $\mu_k \equiv \mu$ for all k. For $n = 1$ and $\bar{\mu} = \mu$, the so defined generalized contact process coincides with the simple contact process discussed above. One of the rates $\bar{\mu}, \mu, \lambda$, and σ can be set to unity without loss of generality, thereby fixing the unit of time. We choose $\lambda = 1$ in the following. Moreover, to keep the parameter

space manageable, we focus on the case $\bar{\mu} = \mu$ in the bulk of the paper. The changes for $\bar{\mu} \neq \mu$ will be briefly discussed in Subsec. 4.5.

The process (143) prevents inactive domains of different color (different k) to stick together indefinitely. They can separate, leaving active sites in between. Thus, this transition allows the domain walls to move through space. It is important to realize that without the process (143), i.e., for $\sigma = 0$, the color of the inactive sites becomes unimportant, and all I_k can be identified. Consequently, for $\sigma = 0$, the dynamics of the generalized contact process reduces to that of the simple contact process for all values of n.

Hinrichsen [13] studied the one-dimensional generalized contact process by means of Monte-Carlo simulations, focusing on the case $\sigma = \lambda = 1$. For $n = 2$, he found a nonequilibrium phase transition at a finite value of μ which separates the active and inactive phases. The critical behavior of this transition coincides with that of the PC universality class. For $n \geq 3$, he found the model to be always in the active phase. The Monte-Carlo simulations were later confirmed by means of a non-hermitian density-matrix renormalization group study [17].

Motivated by a seeming discrepancy between these results and simulations that we performed during our study of absorbing state transitions on a percolating lattice [18], we revisit the one-dimensional generalized contact process with two inactive states. In contrast to the earlier works we treat the rate σ of the process (143) as an independent parameter (rather than fixing it at $\sigma = \lambda = 1$).

4.3. MEAN-FIELD THEORY

To get a rough overview over the behavior of the generalized contact process with two inactive states, we first perform a mean-field analysis. Denoting the probabilities for a site to be in state A, I_1, and I_2 with P_A, P_1, and P_2, respectively, the mean-field equations read:

$$dP_A/dt = (1-\mu)P_A - P_A^2 + 2\sigma P_1 P_2 \,, \tag{144}$$

$$dP_1/dt = \mu P_A/2 - P_A P_1 - \sigma P_1 P_2 \,, \tag{145}$$

$$dP_2/dt = \mu P_A/2 - P_A P_2 - \sigma P_1 P_2 \,. \tag{146}$$

Let us begin by discussing the steady states which are given by the fixed points of the mean-field equations. There are two trivial, inactive fixed points $P_1 = 1, P_A = P_2 = 0$ and $P_2 = 1, P_A = P_1 = 0$. They exist for all values of the parameters μ and σ and correspond to the two absorbing states. In the case of $\sigma = 0$, these fixed points are

unstable for $\mu < 1$ and stable for $\mu > 1$. In contrast, for $\sigma > 0$, they are always unstable.

The active fixed point is given by $P_1 = P_2$ and fulfills the equation

$$0 = (1-\mu)P_A - P_A^2 + \sigma(1-P_A)^2/2 \; . \tag{147}$$

For $\sigma = 0$, this equation reduces to the well-known mean-field equation of the simple contact process, $0 = (1-\mu)P_A - P_A^2$ with the solution $P_A = 1-\mu$ for $\mu < 1$. Thus, for $\sigma = 0$, the nonequilibrium phase transition of the generalized contact process occurs at $\mu = \mu_c^{cp} = 1$. This means, it coincides with the transition of the simple contact process, in agreement with the general arguments given in Subsec. 4.2. In the general case, $\sigma \neq 0$, the steady state density of active sites, P_A, is given by the positive solution of

$$P_A = \frac{1}{2-\sigma}\left(1-\mu-\sigma \pm \sqrt{\mu^2 - 2\mu + 1 + 2\mu\sigma}\right) \; . \tag{148}$$

We are particularly interested in the behavior of P_A for small σ. As long as $\mu < \mu_c^{cp} = 1$ (i.e., in the active phase of the simple contact process), a small, nonzero σ only provides a subleading correction to P_A. At $\mu = \mu_c^{cp} = 1$, the density of active sites vanishes as $P_A \sim \sqrt{\sigma}$ with $\sigma \to 0$. Finally, for $\mu > \mu_c^{cp} = 1$, the density of active sites vanishes as $P_A \sim \sigma/(\mu - 1)$.

We thus conclude that within mean-field theory, the generalized contact process with two inactive states is in the active phase for any nonzero σ. This agrees with older mean-field results but disagrees with more sophisticated methods which predict a nonequilibrium transition at a finite value of μ [13, 17]. The mean-field dynamics can be worked out in a similar fashion. We find that the approach to the stationary state is exponential in time anywhere in parameter space except for the critical point of the simple contact process at $\mu = 1, \sigma = 0$. However, it is known that mean-field theory does not reflect the correct long-time dynamics of the generalized contact process which is of power-law type [13]. Therefore, we do not analyze the mean-field dynamics in detail.

4.4. MONTE CARLO SIMULATIONS

4.4.1. Method and Overview. We now turn to the main part of the paper, *viz.*, large-scale Monte-Carlo simulations of the one-dimensional generalized contact process with two inactive states. We perform two different types of calculations: (i) decay runs and (ii) spreading runs. Decay runs start from a completely active lattice;

we monitor the time evolution of the density $\rho(t)$ of active sites as well as the densities $\rho_1(t)$ and $\rho_2(t)$ of sites in inactive states I_1 and I_2, respectively. Spreading simulations start from a single active (seed) site embedded in a system of sites in state I_1. (From a domain wall point of view, the spreading runs are therefore in the even parity sector.) Here we measure the survival probability $P_s(t)$, the number of sites in the active cloud $N_s(t)$ and the mean-square radius of this cloud, $R^2(t)$.

In each case, the simulation proceeds as a sequence of events. In each event, a pair of nearest-neighbor sites is randomly selected from the active region. For the spreading simulations, the active region initially consists of the seed site and its neighbors; it is updated in the course of the simulation according to the actual size of the active cluster. For the decay runs, the active region comprises the entire sample. The selected pair than undergoes one of the possible transitions according to eqs. (140) to (143) with probability τw. Here the time step τ is a constant which we have fixed at 1/2. The time increment associated with the event is τ/N_{pair} where N_{pair} is the number of nearest-neighbor pairs in the active region.

Using this method we studied systems with sizes up to $L = 10^6$ lattice sites and times up to $t_{max} = 10^8$, exploring the parameter space $0 \leq \mu \leq 1$ and $0 \leq \sigma \leq 1$. The $\sigma - \mu$ phase diagram resulting from our simulations is displayed in Fig. 4.1. This phase diagram shows that the crossover from DP critical behavior at $\sigma = 0$ to DP2 (or, equivalently, PC) critical behavior at $\sigma > 0$ occurs in an unusual fashion. The phase boundary $\sigma_c(\mu)$ between the active and inactive phases does not terminate at the critical point of the simple contact process located at $(\mu, \sigma) = (\mu_c^{cp}, 0) \approx (0.30325, 0)$. Instead, it ends at the point $(\mu, \sigma) = (\mu^*, 0) \approx (0.552, 0)$. In the parameter range $\mu_c^{cp} < \mu < \mu^*$, the system is inactive at $\sigma = 0$, but an infinitesimally small nonzero σ takes it to the active phase.

Thus, the one-dimensional generalized contact process with two inactive states has two types of phase transitions, (i) the generic transition occurring at $\mu > \mu^*$ and $\sigma = \sigma_c(\mu) > 0$ (marked by the dashed blue line and arrows in Fig. 4.1) and (ii) the transition occurring for $\mu_c^{cp} < \mu < \mu^*$ as σ approaches zero (solid red line and arrows). We note in passing that our critical healing rate for $\sigma = 1$ is $\mu_c = 0.628(1)$, in agreement with Ref. [13]

In the following subsections we first discuss in detail the simulations that lead to this phase diagram, and then we present results on the critical behavior of both transitions as well as special point $(\mu^*, 0) \approx (0.552, 0)$ that separates them.

4.4.2. Establishing The Phase Diagram. We first performed a number of spreading simulations at $\sigma = 0$ and various μ for maximum times up to 3×10^4.

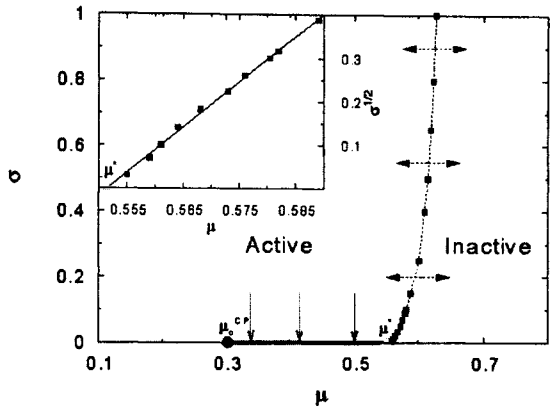

Figure 4.1. (Color online) Phase diagram of the 1D generalized contact process as function of the healing rate μ and the boundary rate σ. A line of DP2 (PC) transitions (blue dashed line) separates the active and inactive phases. For $\sigma \to 0$, this line does not terminate in the simple contact process critical point at $\mu_c^{cp} \approx 0.30325$ and but at $\mu^* \approx 0.552$. For $\mu_c^{cp} < \mu < \mu^*$, the system is inactive at $\sigma = 0$ (thick solid red line), but an infinitesimal σ takes it to the active phase. Inset: Close to the endpoint at μ^*, the phase boundary behaves roughly as $\sigma_c \sim (\mu - \mu^*)^2$.

The resulting number $N_s(t)$ of active sites in the cluster is shown in Fig. 4.2. The figure demonstrates that the transition between the active and inactive phases occurs at $\mu = 0.30325(25)$. A fit of the critical curve to $N_s \sim t^{\Theta_{cp}}$ yields $\Theta_{cp} = 0.315(5)$. As expected from the general arguments in Subsec. 4.2, both the critical healing rate and the initial slip exponent Θ_{cp} agree very well with the results of the simple contact process (see, e.g., Ref. [19] for accurate estimates of the DP exponents). Thus, at $\sigma = 0$, the generalized contact process undergoes a transition in the directed percolation universality class at $\mu = \mu_c^{cp} = 0.30325(25)$.

We now turn to nonzero σ. Because the domain boundary process (143) creates extra active sites, it is clear that the phase boundary between the active and inactive phases has to shift to larger healing rates μ with increasing σ. In the simplest crossover scenario, the phase boundary $\sigma_c(\mu)$ would behave as $\sigma_c \sim (\mu - \mu_c^{cp})^{1/\phi}$ where ϕ is a crossover exponent. To test this scenario, we performed spreading simulations for times up to 10^7 at several fixed $\mu > \mu_c^{cp}$ in which we vary σ to locate the transition. Examples of the resulting $N_s(t)$ curves for several σ at $\mu = 0.428$ and $\mu = 0.6$ are shown in Fig. 4.3. The set of curves for $\mu = 0.6$ (Fig. 4.3b) behaves as expected:

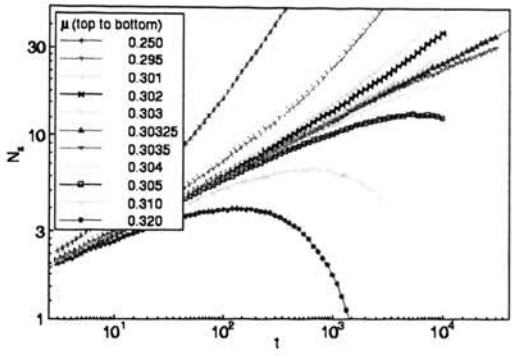

Figure 4.2. (Color online) Spreading simulations at $\sigma = 0$: Number N_s of active sites as a function of time t. The solid line for $\mu = 0.30325$ represents a fit to $N_s \sim t^{\Theta_{cp}}$ yielding $\Theta_{cp} = 0.315(5)$. The data are averages over 25000 runs.

Initially, $N_s(t)$ follows the behavior of the simple contact process at this μ. At later times, the curves with $\sigma \gtrapprox 0.25$ curve upwards implying that the system is in the active phase. The curves for $\sigma \lessapprox 0.25$ curve downward, indicating that the system is in the inactive phase. Thus, $\sigma_c(\mu = 0.6) \approx 0.25$.

In contrast, the set of curves for $\mu = 0.428$ (Fig. 4.3a) behaves very differently. After an initial decay, $N_s(t)$ curves strongly upwards for all values of σ down to the smallest value studied, $\sigma = 10^{-4}$. This suggests that at $\mu = 0.428$, any nonzero σ takes the generalized contact process to the active phase. The phase transition thus occurs at $\sigma = 0$.

We determined analogous sets of curves for many different values of the healing rate in the interval $\mu_c^{cp} = 0.30325 < \mu < 0.65$. We found that the phase transition to the active phase occurs at $\sigma = 0$ for $\mu_c^{cp} < \mu < \mu^* = 0.552$, while it occurs at a nonzero σ for healing rates $\mu > \mu^*$. This establishes the phase diagram shown in Fig. 4.1. The phase boundary thus does *not* follow the simple crossover scenario outlined above. In the following subsections, we analyze in detail the critical behavior of the different nonequilibrium phase transitions.

4.4.3. Generic Transition. We first consider the generic transition occurring at $\mu > \mu^* \approx 0.552$ and nonzero σ (the blue dashed line in Fig. 4.1). Figure 4.4 shows a set of spreading simulations at $\sigma = 0.1$ and several μ in the vicinity of the phase boundary. The data indicate a critical point at $\mu \approx 0.582$. We performed

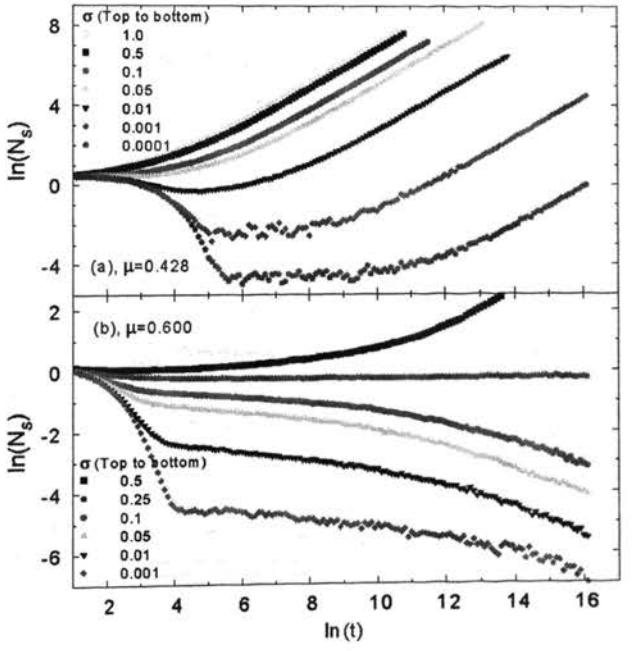

Figure 4.3. (Color online) Spreading simulations: Number N_s of active sites as a function of time t for several σ at fixed $\mu = 0.428$ (panel a) and $\mu = 0.6$ (panel b). The data are averages over 10^3 (at the smallest σ) to 10^5 runs.

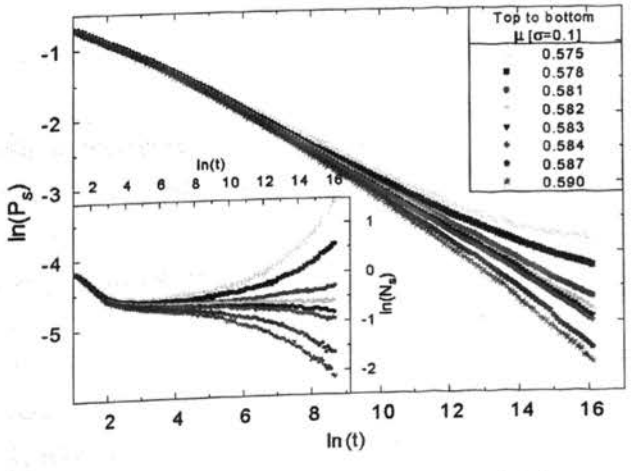

Figure 4.4. (Color online) Spreading simulations at $\sigma = 0.1$ for several μ close to the phase boundary. Main panel: Survival probability P_s as a function of time t. The data are averages over 10^5 runs. Inset: Number N_s of active sites as a function of time t.

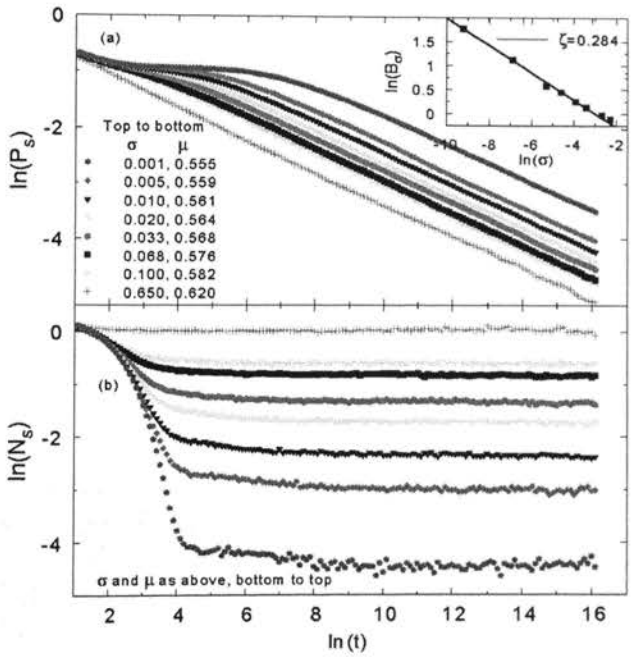

Figure 4.5. (Color online) Critical spreading simulations: Survival probability P_s and number of active sites N_s as functions of t for several points (μ, σ) located on the generic phase boundary. The inset shows the prefactor B_σ of the critical power law $P_s = B_\sigma t^{-\delta}$ as a function of σ. The solid line is a fit to $B_\sigma \sim \sigma^{-\zeta}$ which gives $\zeta = 0.284$.

analogous simulations for several points on the phase boundary. Figure 4.5 shows the survival probability P_s and number N_s of active sites as functions of time for all the respective critical points. In log-log representation, the N_s and P_s curves for different σ and μ are perfectly parallel, i.e., they represent power-laws with the same exponent. Fits of the asymptotic long-time behavior to $P_s = B_\sigma t^{-\delta}$ and $N_s = C_\sigma t^{\Theta}$ give estimates of $\delta = 0.289(5)$ and $\Theta = 0.000(5)$. Moreover, we measured (not shown) the mean-square radius $R^2(t)$ of the active cloud as a function of time. Its long time behavior follows a universal power law. Fitting to $R^2(t) \sim t^{2/z}$ gives $2/z = 1.145(5)$ ($z = 1.747(7)$). Here $z = \nu^{\parallel}/\nu^{\perp}$ is the dynamical exponent, i.e., the ratio between the correlation time exponent $\nu_{\parallel}$ and the correlation length exponent $\nu_{\perp}$.

In addition to the spreading simulations, we also performed density decay simulations for several (μ, σ) points on the phase boundary. Characteristic results are

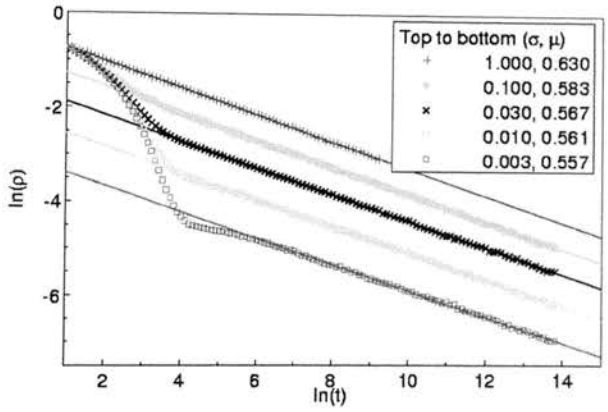

Figure 4.6. (Color online) Critical density decay simulations: Density ρ_A of active sites as function of t for several points (μ, σ) on the generic phase boundary. The solid lines are fits to a power law $\rho_A = \bar{B}_\sigma t^{-\alpha}$ giving $\alpha = 0.285(5)$. The data represent averages of 400 runs with system size $L = 10^4$.

presented in Fig. 4.6. The figure shows that the density ρ_A of active sites at criticality follows a universal power law, $\rho_A = \bar{B}_\sigma t^{-\alpha}$ at long times. The corresponding fits give $\alpha = 0.285(5)$ which agrees (within the error bars) with our value of the survival probability exponent δ. We thus conclude that the generic transition of our system is characterized by three independent exponents (for instance $\nu_\perp, z$ and δ) rather than four (as could be expected for a general absorbing state transition [4]). We point out, however, that even though P_s and ρ_A show the same power-law time dependence at criticality, the behavior of the prefactors differs. Specifically, the prefactor $\bar{B}_\sigma$ of the density is increasing with increasing σ while the prefactor B_σ of the survival probability decreases with increasing σ.

All the exponents of the generic transition do not depend on μ or σ, implying that the critical behavior is universal. Moreover, their values are in excellent agreement with the known values of the PC (or DP2) universality class (see, e.g., Ref. [4, 5]). We therefore conclude that the critical behavior of the generic transition of generalized contact process with two inactive states is universally in this class.

4.4.4. Transition at $\sigma = 0$. After discussing the generic transition, we now turn to the line of transitions at $\mu_c^{cp} < \mu < \mu^*$ and $\sigma = 0$. To investigate these

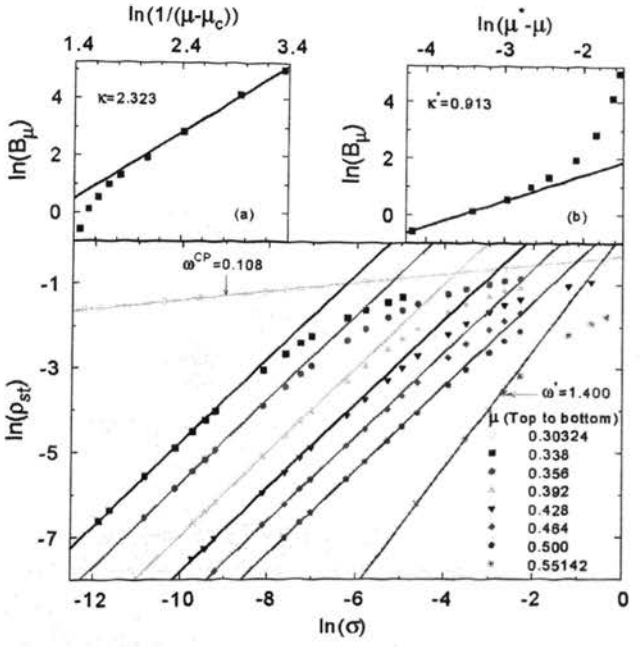

Figure 4.7. (Color online) Density decay simulations. Main panel: stationary density ρ_{st} as a function of the boundary rate σ for various healing rates μ. For $\mu_c^{cp} < \mu < \mu^*$, the solid lines are fits of the low-σ behavior to $\rho_{st} = B_\mu \sigma$. At the simple contact process critical point, $\mu = \mu_c^{cp} = 0.30324$, and at the endpoint, $\mu = \mu^* = 0.552$, we fit to power-laws $\rho_{st} \sim \sigma^\omega$ which gives exponents of $\omega_{cp} = 0.108(2)$ and $\omega^* = 1.4(1)$. The data are averages over 50 to 200 runs with system sizes $L = 2000$ to 5000. Inset a: prefactor B_μ of the linear σ dependence as a function of $\mu - \mu_c^{cp}$. A fit to a power law gives $B_\mu \sim (\mu - \mu_c^{cp})^{-\kappa}$ with $\kappa = 2.32(10)$. Inset b: prefactor B_μ as a function of $\mu^* - \mu$. A fit to a power law gives $B_\mu \sim (\mu^* - \mu)^{\kappa^*}$ with $\kappa^* = 0.91$.

transitions more closely, we performed both spreading and density decay simulations at fixed μ and several σ-values approaching $\sigma = 0$ (as indicated by the solid (red) arrows in the phase diagram, Fig. 4.1).

Let us start by discussing the density decay simulations. Figure 4.7 shows the stationary density ρ_{st} of active sites as a function of σ for several values of the healing rate μ. Interestingly, the stationary density depends linearly on σ for all healing rates $\mu_c^{cp} < \mu < \mu^*$, in seeming agreement with mean-field theory. This means $\rho_{st} = B_\mu \sigma^\omega$ with $\omega = 1$ and B_μ being a μ-dependent constant. We also analyzed, how the prefactor B_μ of the mean-field-like behavior depends on the distance from the simple contact

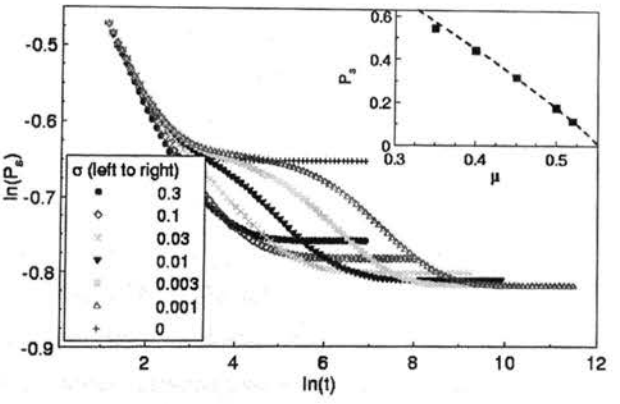

Figure 4.8. (Color online) Spreading simulations: Survival probability P_s as a function of time t at $\mu = 0.4$ for various values of the boundary rate σ. The data are averages over 100000 runs. Inset: Low-σ limit of the stationary P_s as a function of μ. The dashed line is a fit to $P_s \sim (\mu^* - \mu)^\beta$ with $\mu^* = 0.552$ and $\beta = 0.87(5)$ in agreement with the PC universality class (see, e.g., Refs. [4, 5]).

process critical point. As inset a) of Fig. 4.7 shows, B_μ diverges as $(\mu - \mu_c^{cp})^{-\kappa}$ with $\kappa = 2.3(1)$.

At the critical healing rate μ_c^{cp} of the simple contact process, the stationary density displays a weaker σ-dependence. A fit to a power-law $\rho_{st} \sim \sigma^{\omega_{cp}}$ gives an exponent value of $\omega_{cp} = 0.108(2)$. In contrast, at the endpoint at healing rate μ^*, the corresponding exponent $\omega^* = 1.4(1)$ is larger than 1.

These results of the density decay simulations must be contrasted with those of the spreading simulations. Figure 4.8 shows the time dependence of the survival probability P_s for $\mu = 0.4$ and several σ. At early times, all curves follow the $\sigma = 0$ data due to the small values of the rate of the boundary activation process (143). (Note that the $\sigma = 0$ curve does *not* reproduce the survival probability of the simple contact process. This is because in our generalized contact process, a sample is surviving as long as not every site is in state I_1 even if there are no active sites.) In the long-time limit, the P_s curves approach nonzero constants, as expected in an active phase. However, in contrast to the stationary density ρ_{st} (Fig. 4.7), the stationary value of P_s does not go to zero with vanishing boundary σ. Instead, it approaches a

σ-independent constant. We performed similar sets of simulations at other values of μ in the range $\mu_c^{cp} < \mu < \mu^*$, with analogous results. We therefore conclude that – somewhat surprisingly – the survival probability and the stationary density of active sites display qualitatively different behavior at the $\sigma = 0$ phase transition.

We now show that the properties of these quantities can be understood within a simple domain wall theory. The relevant long-time degrees of freedom at $\mu > \mu_c^{cp}$ and $\sigma \ll 1$ are the domain walls between I_1 and I_2 domains. These domains are formed during the early time evolution when the system follows the simple contact process dynamical rules (140) to (142). At late times, the domain walls can hop, they can branch (one wall branching into three), and they can annihilate (two walls vanish if the meet on the same bond between two sites). This means, the domain wall dynamics follows the branching-annihilating random walk with two offspring (BARW2).

In our case, the BARW2 dynamics is controlled by two rates, the domain wall hopping rate Γ and the branching rate Ω (annihilation occurs with certainty if two walls meet). These two rates depend on the underlying generalized contact process dynamics. In the limit $\sigma \ll 1$ they are both linear in the boundary rate, $\Gamma = \sigma F_\Gamma(\mu)$, $\Omega = \sigma F_\Omega(\mu)$ because a single boundary activation event is sufficient to start a domain wall hop or branching (F_Γ and F_Ω are nontrivial functions of μ). Because both rates are linear in σ, their ratio is σ-independent, thus the steady state of the domain walls does not depend on σ in the limit $\sigma \ll 1$. This explains why the survival probability P_s of the generalized contact process saturates at a nonzero, σ-independent value in Fig. 4.8. It also explains the σ-dependence of the stationary density ρ_{st} of active sites in the following way: For $\sigma \ll 1$ and $\mu > \mu_c^{cp}$, active sites are created mostly at the domain walls at rate σ. Consequently, their stationary density is proportional to both σ and the stationary domain wall density ρ_{dw}, i.e., $\rho_{st} \sim \sigma\rho_{dw}$, in agreement with Fig. 4.7. (The linear σ-dependence of ρ_{st} is thus *not* due to the validity of mean-field theory.)

These results imply that the phase transition line at $\sigma = 0$ between μ_c^{cp} and μ^* is *not* a true critical line because there is no (nontrivial) diverging length scale. It only appears critical because the stationary density of active sites vanishes with σ. Note that this is also reflected in the fact that the system is not behaving like a critical system right on the phase transition line $\sigma = 0$ (no power-law time dependencies, for instance). Instead, the physics of this transition line is controlled by the BARW2 dynamics of the domain walls with a finite correlation length for all $\mu_c^{cp} < \mu < \mu^*$.

4.4.5. Scaling at The Contact Process Critical Point $(\mu_c^{cp}, 0)$. Even though the generalized contact process is not critical at $\sigma = 0$ and $\mu > \mu_c^{cp}$, its

behavior close to the critical point of the simple contact process can be understood in terms of a phenomenological scaling theory.

Let us assume that the stationary density of active sites close to $(\mu_c^{cp}, 0)$ fulfills the homogeneity relation

$$\rho_{st}(\Delta\mu, \sigma) = b^{\beta_{cp}/\nu_{cp}^{\perp}} \rho_{st}(\Delta\mu\, b^{-1/\nu_{cp}^{\perp}}, \sigma b^{-y_{cp}}) \tag{149}$$

where $\Delta\mu = \mu - \mu_c^{cp}$ and b denotes an arbitrary scale factor. β_{cp} and $\nu_{cp}^{\perp}$ are the usual order parameter and correlation length exponents and y_{cp} denotes the scale dimension of σ at this critical point. Setting $b = \sigma^{1/y_{cp}}$ then gives rise to the scaling form

$$\rho_{st}(\Delta\mu, \sigma) = \sigma^{\beta_{cp}/(\nu_{cp}^{\perp} y_{cp})} X\left(\Delta\mu\, \sigma^{-1/(\nu_{cp}^{\perp} y_{cp})}\right) \tag{150}$$

where X is a scaling function. At criticality, $\Delta\mu = 0$, this leads to $\rho_{st}(0, \sigma) \sim \sigma^{\beta_{cp}/(\nu_{cp}^{\perp} y_{cp})}$ (using $X(0) = \text{const}$). Thus, $\omega_{cp} = \beta_{cp}/(\nu_{cp}^{\perp} y_{cp})$. For $\sigma \to 0$ at nonzero $\Delta\mu$, we need the large-argument limit of the scaling function X. On the active side of the critical point, $\Delta\mu < 0$, the scaling function must behave as $X(x) \sim |x|^{\beta_{cp}}$ to reproduce the correct critical behavior of the density, $\rho_{st} \sim |\mu - \mu_c^{cp}|^{\beta_{cp}}$.

More interesting is the behavior on the inactive side of the critical point, i.e., for $\Delta\mu > 0$ and $\sigma \to 0$. Here, we assume the scaling function to behave as $X(x) \sim x^{-\kappa}$. In this limit, we thus obtain $\rho_{st} \sim (\Delta\mu)^{-\kappa}\sigma^{\omega}$ (just as observed in Fig. 4.7) with $\omega = (\beta_{cp} + \kappa)/(\nu_{cp}^{\perp} y_{cp})$. As a result of our scaling theory, the exponents ω, ω_{cp} and κ are not independent, they need to fulfill the relation $\omega_{cp}(\beta_{cp} + \kappa) = \beta_{cp}\omega$. Our numerical values, $\omega = 1$, $\omega_{cp} = 0.108(2)$ and $\kappa = 2.32(10)$ fulfill this relation in very good approximation, indicating that they represent asymptotic exponents and validating the homogeneity relation (149). Using $\beta_{cp} = 0.2765$ and $\nu_{cp}^{\perp} = 1.097$ [19], the resulting value for the scale dimension y_{cp} of σ at the simple contact process critical point is $y_{cp} = 2.34(4)$.

4.4.6. The Endpoint $(\mu^*, 0)$. Finally, we turn to the point $(\mu^*, \sigma) = (0.552, 0)$ where the generic phase transition line terminates on the μ axis. At first glance, one might suspect this point to be a multicritical point because it is located at the intersection of two phase transition lines. However, we argued in Subsubsec. 4.4.4 (based on the domain wall theory) that the transition line at $\sigma = 0$ and $\mu_c^{cp} < \mu < \mu^*$ is not critical. This implies that the endpoint $(\mu^*, 0)$ is not multicritical but a simple critical point in the same universality class (*viz.*, the PC class) as the generic transition at $\mu > \mu^*$. In fact, the endpoint can be understood as the critical point of the BARW2 domain wall dynamics in the limit $\sigma \to 0$.

To test this hypothesis, we first study the survival probability and density of active sites as μ^* is approached along the μ axis. The inset of Fig. 4.8 shows the stationary survival probability (more precisely, its saturation value for $\sigma \to 0$) as a function of μ. The data can be well fitted by a power-law $P_s \sim (\mu^* - \mu)^\beta$ with $\beta = 0.87(5)$. The corresponding information on the stationary density of active sites can be obtained from inset b) of Fig. 4.7. It shows the prefactor B_μ of the linear σ-dependence $\rho_{st} = B_\mu \sigma$ as a function of $\mu^* - \mu$. Sufficiently close to μ^*, their relation can be fitted by a power law $B_\mu \sim (\mu^* - \mu)^{\kappa^*}$ with $\kappa^* = 0.91$. Thus both β and κ^* agree with the order parameter exponent of the PC universality class within their error bars. This confirms the validity of the domain wall theory of Subsubsec. 4.4.4 at μ^*.

The discussion of the σ-dependence of P_s and ρ_{st} right at μ^* is somewhat more complicated because it is determined by the *subleading* σ-dependencies of the domain-wall rates Γ and Ω. Moreover, because the dynamics is extremely slow at $\mu \approx \mu^*$ and $\sigma \ll 1$, our numerical results close to the endpoint are less accurate then our other results. According to the domain wall theory of Subsubsec. 4.4.4, the stationary survival probability should fulfill the homogeneity relation

$$P_s(\Delta\mu, \sigma) = b^{\beta/\nu^\perp} P_s(\Delta\mu\, b^{-1/\nu^\perp}, \sigma\, b^{-y^*}) \tag{151}$$

where $\Delta\mu = \mu - \mu^*$ while β and $\nu^\perp$ are the order parameter and correlation length exponents of the BARW2 transition (PC universality class). The only unknown exponent is y^*. The same homogeneity relation should hold for the domain wall density, but *not* the density of active sites.

Setting the scale factor to $b = \sigma^{1/y^*}$ gives the scaling form

$$P_s(\Delta\mu, \sigma) = \sigma^{\beta/(\nu^\perp y^*)} Y(\Delta\mu\, \sigma^{-1/(\nu^\perp y^*)}) \; . \tag{152}$$

Right at the endpoint, $\Delta\mu = 0$, this gives $P_s \sim \sigma^{\beta/(\nu^\perp y^*)}$. To test this power-law relation and to determine y^*, we performed spreading simulations at $\mu = \mu^*$ and several σ between 0.03 and 1. The low-σ behavior (not shown) can indeed be fitted by a power law in σ with an exponent $\beta/(\nu^\perp y^*) = 0.5(1)$. Using the well-known values $\beta = 0.92$ and $\nu^\perp = 1.83$ of the PC universality class, we conclude $y^* = 1.0(2)$. Within the domain wall theory, $\rho_{DW} \sim P_s$ and the stationary density of active sites is $\rho_{st} \sim \sigma \rho_{DW} \sim \sigma^{\omega^*}$ with $\omega^* = 1 + \beta/(\nu^\perp y^*) = 1.5(1)$. This agrees well with the numerical estimate of 1.4(1) obtained from the density decay simulations in Fig. 4.7.

The scaling form (152) can also be used to determine the shape of the phase boundary at $\mu > \mu^*$. The phase boundary corresponds to a singularity of the scaling function Y at some nonzero value of its argument. Thus, the phase boundary follows the power law $\sigma \sim (\mu - \mu^*)^{\nu_\perp y^*}$. At fit of the data in Fig. 4.1 leads to $\nu_\perp y^* = 1.8(2)$ which implies $y^* = 1.0(1)$ in agreement with the above estimate from the spreading simulation data.

To investigate the time dependence of P_s close to the endpoint, the homogeneity relation (151) can be generalized to include a time argument. On the right hand side, it appears in the scaling combination $(t/t_0)b^z$ with t_0 the basic microscopic time scale. It is important to realize that this *microscopic* scale diverges as σ^{-1} with $\sigma \to 0$ (independent of any criticality at μ^*). Thus, the right scaling combination is actually $t\sigma b^z$. We used the resulting scaling theory to discuss the power-law decay of P_s on the phase boundary shown in Fig. 4.5a. The scaling theory predicts $P_s \sim \sigma^{-\zeta} t^{-\delta}$ with $\zeta \equiv \delta$ as the endpoint is approached. This agrees with our numerical data (shown in the inset of Fig. 4.5a) which give $\zeta \approx 0.284$

In summary, all our simulation data support the notion that the endpoint $(\mu^*, 0)$ is a not a true multicritical point but a simple critical point in the same universality class (PC) as the entire generic phase boundary at $\mu \geq \mu^*$. The behavior of some observables makes it appear multicritical, though, because the microscopic time scale of the domain wall dynamics diverges with $\sigma \to 0$.

4.5. CONCLUSIONS

In summary, we have studied the phase transitions of the generalized contact process with two absorbing states in one space dimension by means of large-scale Monte-Carlo simulations. We have found that this model has two different nonequilibrium phase transitions, (i) the generic transition occurring for sufficiently hight values $\mu > \mu^*$ of the healing rate and nonzero values of the boundary activation rate σ, and (ii) a transition at exactly $\sigma = 0$ for $\mu_c^{cp} < \mu < \mu^*$.

The generic transition is in the parity-conserving (PC) universality class (which coincides with the DP2 class in one dimension) everywhere on the $\mu \geq \mu^*$ phase boundary, in agreement with earlier work [13, 17]. In contrast, the $\sigma = 0$ transition turned out to be *not* critical. The density of active sites rather goes to zero with the vanishing boundary activation rate σ while the survival probability remains finite for $\sigma \to 0$. Its behavior is controlled by the BARW2 dynamics of the domain walls between different inactive domains (which is not critical for $\mu_c^{cp} < \mu < \mu^*$). It is

interesting to note that the behavior of our model at $\sigma \equiv 0$ differs qualitatively from the $\sigma \to 0$ limit of the finite-σ behavior in the entire parameter region $\mu_c^{cp} < \mu < \mu^*$.

As a result, the crossover between directed percolation (DP) critical behavior at $\sigma \equiv 0$ and parity conserving (PC) critical behavior for $\sigma > 0$ does not take the naively expected simple scaling form. In particular, the generic ($\sigma > 0$) phase boundary does not continuously connect to the critical point of the $\sigma \equiv 0$ theory (the simple contact process critical point). Instead, it terminates at a separate endpoint $(\mu^*, 0)$ on the μ-axis. While this point shares some characteristics with a multicritical point, it is actually just a simple critical point in the same universality class (PC) as the entire generic phase boundary.

We emphasize that the crossover between the DP and PC universality classes as a function of σ in our model is very different from that investigated by Odor and Menyhard [20]. These authors started from the PC universality class and introduced perturbations that destroy the symmetry between the absorbing states or destroy the parity conservation in branching and annihilating random walk models. They found more conventional behavior that can be described in terms of crossover scaling. In contrast, the transition rates (140) to (143) of our model do not break the symmetry between the two inactive states anywhere in parameter space.

Crossovers between various universality classes of absorbing state transitions have also been investigated by Park and Park [21, 22, 23]. They found a discontinuous jump in the phase boundary similar to ours along the so-called excitatory route from infinitely many absorbing states to a single absorbing state [21]. Moreover, there is some similarity between our mechanism and the so-called channel route [22] from the PC universality class to the DP class which involves an infinite number of absorbing states characterized by an auxiliary density. In our case, at $\sigma \equiv 0$ (but not at any finite σ), any configuration consisting of I_1 and I_2 only can be considered absorbing because active sites cannot be created. The density of I_1-I_2 domain walls then plays the role of the auxiliary density; it vanishes at the endpoint $(\mu^*, 0)$. However, our crossover occurs in the opposite direction than that of Ref. [22]: The small parameter σ takes the system from the DP universality class to the PC class. Note that an unexpected survival of active sites has also been observed in a version of the nonequilibrium kinetic Ising model with strong disorder. Here, the disorder can completely segment the system, and in odd-parity segments residual particles cannot decay [24].

The generalized contact process as defined in eqs. (140) to (143) is characterized by *three* independent rates (one rate can be set to one by rescaling the time unit). In the bulk of our paper, we have focused on the case $\bar{\mu} = \mu$ for which our system reduces

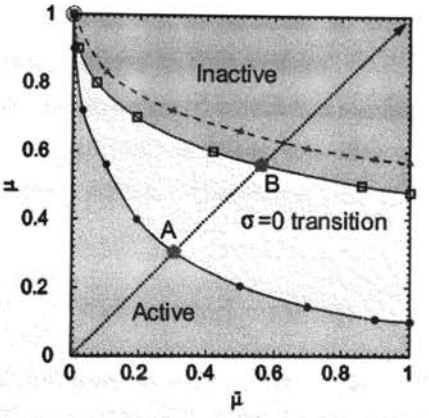

Figure 4.9. (Color online) Projection of the phase diagram of the generalized contact process on the $\bar{\mu} - \mu$ plane. The individual symbols show the locations of the phase boundaries as determined from our simulations: solid blue circles – transition for $\sigma \equiv 0$ (simple contact process), solid red triangles – generic transition for $\sigma = 1$, open squares – approximate location of the endpoint of the generic transition ($\sigma \to 0$) estimated from the transition at $\sigma = 0.01$. The lines are guides to the eye only. Points A and B are the simple contact process critical point and the endpoint investigated in the main part of the paper.

to the usual contact process in the limit of $\sigma \to 0$. In order to study how general our results are, we have performed a few simulation runs for $\bar{\mu} \neq \mu$ focusing on the fate of the endpoint that separates the generic transition from the $\sigma = 0$ transition. The results of these runs are summarized in Fig. 4.9 which shows the phase diagram projected on the $\bar{\mu} - \mu$ plane.

The figure shows that the line of endpoints of the generic phase boundary remains distinct from the simple contact process ($\sigma = 0$) critical line in the entire $\bar{\mu} - \mu$ plane. The two lines only merge at the point $\bar{\mu} = 0, \mu = 1$ where the system behaves as compact directed percolation [13].

Our study was started because simulations at $\mu \gtrsim \mu_c^{cp}$ and $\sigma \ll 1$ [18] seemed to suggest that the generalized contact process with two absorbing states is always active for any nonzero σ. The detailed work reported in this paper shows that this is *not* the case; a true inactive phase appears, but only at significantly higher $\mu > \mu^*$. Motivated by this result, we also carefully reinvestigated the generalized contact process with $n = 3$ absorbing states which has been reported to be always active (for any nonzero

σ) in the literature [13, 17]. However, in contrast to the two-absorbing-states case, we could not find any inactive phase in this system.

Let us close by posing the question of whether a similar splitting between the $n = 1$ critical point and the $n = 2$ phase transition line also occurs in *other* microscopic models with several absorbing states. Answering this questions remains a task for the future.

Acknowledgements

We acknowledge helpful discussions with Geza Odor and Ronald Dickman. This work has been supported in part by the NSF under grant no. DMR-0339147 and DMR-0906566 as well as by Research Corporation.

[1] V. P. Zhdanov and B. Kasemo, Surf. Sci. Rep. **20**, 113 1994.

[2] B. Schmittmann and R. K. P. Zia, in Phase Transitions and Critical Phenomena, edited by C. Domb and J. L. Lebowitz Academic, New York, 1995, Vol. **17**, p. 1.

[3] J. Marro and R. Dickman, Nonequilibrium Phase Transitions in Lattice Models Cambridge University Press, Cambridge, England, 1999.

[4] H. Hinrichsen, Adv. Phys. **49**, 815 2000.

[5] G. Odor, Rev. Mod. Phys. **76**, 663 2004.

[6] S. Lbeck, Int. J. Mod. Phys. B **18**, 3977 2004.

[7] U. C. Tuber, M. Howard, and B. P. Vollmayr-Lee, J. Phys. A **38**, R79 2005.

[8] P. Grassberger and A. de la Torre, Ann. Phys. N.Y. **122**, 373 1979.

[9] H. K. Janssen, Z. Phys. B **42**, 151 1981.

[10] P. Grassberger, Z. Phys. B **47**, 365 1982.

[11] P. Rupp, R. Richter, and I. Rehberg, Phys. Rev. E **67**, 036209 2003.

[12] K. A. Takeuchi, M. Kuroda, H. Chate, and M. Sano, Phys. Rev. Lett. **99**, 234503 2007.

[13] H. Hinrichsen, Phys. Rev. E **55**, 219 1997.

[14] P. Grassberger, F. Krause, and T. von der Twer, J. Phys. A **17**, L105 1984.

[15] D. Zhong and D. B. Avraham, Phys. Lett. A **209**, 333 1995.

[16] T. E. Harris, Ann. Probab. **2**, 969 1974.

[17] J. Hooyberghs, E. Carlon, and C. Vanderzande, Phys. Rev. E **64**, 036124 2001.

[18] M. Y. Lee and T. Vojta, Phys. Rev. E **79**, 041112 2009.

[19] I. Jensen, J. Phys. A **32**, 5233 1999.

[20] G. Odor and N. Menyhard, Phys. Rev. E **78**, 041112 2008.

[21] S.-C. Park and H. Park, Phys. Rev. E **76**, 051123 2007.

[22] S.-C. Park and H. Park, Phys. Rev. E **78**, 041128 2008.

[23] S.-C. Park and H. Park, Phys. Rev. E **79**, 051130 2009.

[24] G. Odor and N. Menyhard, Phys. Rev. E **73**, 036130 2006.

5. GENERALIZED CONTACT PROCESS WITH TWO SYMMETRIC ABSORBING STATES IN TWO DIMENSIONS

Man Young Lee and Thomas Vojta

Physics, Missouri University of Science and Technology, Rolla, MO 65409, USA

Abstract[17]

We explore the two-dimensional generalized contact process with two absorbing states by means of large-scale Monte-Carlo simulations. In part of the phase diagram, an infinitesimal creation rate of active sites between inactive domains is sufficient to take the system from the inactive phase to the active phase. The system therefore displays two different nonequilibrium phase transitions. The critical behavior of the generic transition is compatible with the generalized voter (GV) universality class, implying that the symmetry-breaking and absorbing transitions coincide. In contrast, the transition at zero domain-boundary activation rate is not critical.

5.1. INTRODUCTION

Phase transitions between different nonequilibrium steady states are a topic of great current interest in statistical physics. These transitions display large-scale fluctuations and collective behavior over large distances and long times just as equilibrium phase transition. They occur, for example, in surface growth, granular flow, chemical reactions, population dynamics, and even in traffic jams [1, 2, 3, 4, 5, 6, 7].

The so-called absorbing state transitions are a particularly well-studied type of nonequilibrium phase transitions. They separate fluctuating (active) steady states from absorbing (inactive) states where fluctuations stop completely. Generically, absorbing state transitions are in the directed percolation (DP) [8] universality class; Janssen and Grassberger [9, 10] conjectured that all absorbing state transitions with a scalar order parameter and short-range interactions belong to this class as long

[17]All of this section is reproduced from the manuscript (e-printed version, arXiv: 1010.3298) which is accepted for publication in Physical Review E.

as there are no extra symmetries or conservation laws. This conjecture has been confirmed in countless theoretical and computer simulation studies. Experimental verifications were found in ferrofluidic spikes [11] and in the transition between two turbulent states in a liquid crystal [12].

In recent years, significant attention has focused on absorbing state transitions in universality classes different from DP that can occur if the system features additional symmetries or conservation laws. In 1997, Hinrichsen [13] suggested several nonequilibrium stochastic lattice models with $n \geq 2$ absorbing states. In the case of two symmetric absorbing states ($n = 2$), he found the transition to be in a different universality class, the Z_2-symmetric directed percolation (DP2) class which is sometimes also called directed Ising (DI) class. If the symmetry between the absorbing states is broken, the critical behavior reverts back to DP.

Recently, we revisited [14] one of the stochastic lattice models introduced in Ref. [13], *viz.*, the generalized contact process with two absorbing states in one space dimension. By employing large-scale Monte-Carlo simulations, we found a rich phase diagram featuring two different nonequilibrium phase transitions separated by a special point that shares some characteristics with a multicritical point. The generic transition occurs at nonzero values of the infection, healing and domain-boundary activation rates. It belongs to the DP2 universality class which coincides [4] with the parity-conserving (PC) class [15] (occurring, e.g., in the branching-annihilating random walk with an even number of offspring (BARWE) [16]). In addition, we found an unusual line of phase transitions at zero domain-boundary activation rate which turned out to be non-critical.

Here, we consider the generalized contact process with two symmetric absorbing states in *two* space dimensions. The purpose of this paper is twofold. First, we wish to investigate whether the two-dimensional generalized contact process also displays the above-mentioned rich phase diagram having two nonequilibrium phase transitions. Second, we wish to study the critical behavior of these transitions and their universality. According to a conjecture by Dornic *et al.* [17], the DP2 universality class in two dimensions should coincide with the generalized voter (GV) universality class for which the upper critical dimension is exactly two. Alternatively, the transition could split into a symmetry-breaking Ising transition and a DP transition [18, 19]. To address these questions, we perform large-scale Monte-Carlo simulations.

Our paper is organized as follows. We introduce the generalized contact process with several absorbing states in Subsec. 5.2. Subsec. 5.3 is devoted to the results and interpretation of our Monte-Carlo simulations. We conclude in Subsec. 5.4.

5.2. GENERALIZED CONTACT PROCESS WITH SEVERAL ABSORBING STATES

We first define the simple contact process [20], one of the prototypical models in the DP universality class. Each site $\mathbf{r}$ of a d-dimensional hypercubic lattice can be in one of two states, either A, the active (infected) state or I, the inactive (healthy) state. During the time evolution of the contact process, active sites infect their nearest neighbors, or they heal (become inactive) spontaneously. More rigorously, the contact process is a continuous-time Markov process during which active sites become inactive at a rate μ, while inactive sites turn active at a rate $\lambda m/(2d)$ where m is the number of active nearest neighbor sites. The healing rate μ and the infection rate λ are external parameters.

The long-time state of the contact process is determined by the ratio of these two rates. If $\mu \gg \lambda$, healing occurs much more often than infection. Thus, all infected sites will eventually become inactive, and the absorbing state without any active sites is the only steady state. Consequently the system is in the inactive phase for $\mu \gg \lambda$. In the opposite limit, $\lambda \gg \mu$, the infection survives for infinite times, i.e., there is a steady state with a nonzero density of active sites. This is the active phase. These two phases are separated by a nonequilibrium phase transition in the DP universality class occurring at some critical value of the ratio λ/μ.

Following Hinrichsen [13], we now generalize the contact process to n absorbing states. Each lattice site can now be in one of $n+1$ states, the active state A or one of the n different inactive states I_k ($k = 1 \ldots n$). k is sometimes referred to as the "color" index. The Markov dynamics of the generalized contact process is defined via the following transition rates for pairs of nearest-neighbor sites,

$$w(\mathrm{AA} \to \mathrm{AI}_k) = w(\mathrm{AA} \to \mathrm{I}_k\mathrm{A}) = \bar{\mu}/n \;, \tag{153}$$

$$w(\mathrm{AI}_k \to \mathrm{I}_k\mathrm{I}_k) = w(\mathrm{I}_k\mathrm{A} \to \mathrm{I}_k\mathrm{I}_k) = \mu_k \;, \tag{154}$$

$$w(\mathrm{AI}_k \to \mathrm{AA}) = w(\mathrm{I}_k\mathrm{A} \to \mathrm{AA}) = \lambda \;, \tag{155}$$

$$w(\mathrm{I}_k\mathrm{I}_l \to \mathrm{I}_k\mathrm{A}) = w(\mathrm{I}_k\mathrm{I}_l \to \mathrm{AI}_l) = \sigma \;, \tag{156}$$

with $k, l = 1 \ldots n$ and $k \neq l$. All other transition rates vanish. We are mostly interested in the fully symmetric case, $\mu_k \equiv \mu$ for all k. For $n = 1$ and $\bar{\mu} = \mu$,

the so defined generalized contact process coincides with the simple contact process discussed above. One of the rates $\bar{\mu}, \mu, \lambda$, and σ can be set to unity without loss of generality, thereby fixing the unit of time. We choose $\lambda = 1$ in the following. Moreover, to keep the parameter space manageable, we focus on the case $\bar{\mu} = \mu$ [18].

The rate (156) is responsible for the new physics in the generalized contact process. It prevents inactive domains of different color (different k) to stick together indefinitely. By creating active sites at the domain wall, the two domains can separate. Thus, the rate (156) allows the domain walls to move through space. We emphasize that without the process (156), i.e., for $\sigma = 0$, the color of the inactive sites becomes unimportant, and all I_k can be identified. Consequently, for $\sigma = 0$, the dynamics of the generalized contact process reduces to that of the simple contact process for all values of n. In the main part of this paper, we shall focus on the case of $n = 2$ inactive states.

Before we turn to our Monte-Carlo simulations of the two-dimensional generalized contact process, let us briefly summarize the simulation results in one dimension [14] for comparison. For $\sigma = 0$, i.e., in the absence of the boundary activation process (156), the system undergoes an absorbing state transition at a healing rate $\mu = \mu_c^{cp} \approx 0.303$, which agrees with the critical healing rate of the simple contact process. In agreement with the general arguments above, this transition is in the DP universality class. For healing rates between μ_c^{cp} and $\mu^* \approx 0.552$, the system is inactive if $\sigma = 0$ but an infinitesimal nonzero σ takes it to the active phase. Finally, for $\mu > \mu^*$, the transition occurs at a finite nonzero value of σ. The one-dimensional generalized contact process with two inactive states thus has two lines of phase transitions, (i) the generic transition occurring at $\mu > \mu^*$ and $\sigma = \sigma_c(\mu) > 0$ and (ii) the transition occurring for $\mu_c^{cp} < \mu < \mu^*$ as σ approaches zero.

5.3. MONTE-CARLO SIMULATIONS

5.3.1. Method and Phase Diagram. In order to address the two main problems raised in the introduction, *viz*, the phase diagram of the two-dimensional generalized contact process with two inactive states and the critical behavior of its phase transitions, we performed two types of large-scale Monte Carlo simulations, (i) decay runs and (ii) spreading runs. Decay runs start from a completely active lattice; we measure the time evolution of the density $\rho(t)$ of active sites as well as the

[18] We studied the phase diagram for $\bar{\mu} \neq \mu$ in one space dimension in Ref. [14]. We found that the qualitative behavior is the same as in the $\bar{\mu} = \mu$ case. We expect the same to be true in two space dimensions.

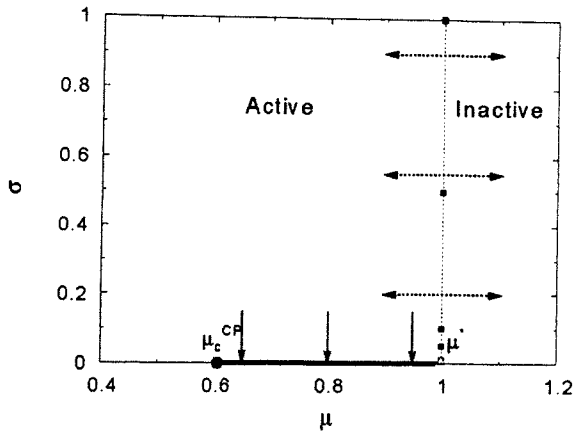

Figure 5.1. (Color online) Phase diagram of the two-dimensional generalized contact process with two inactive states as function of the healing rate μ and the domain-boundary activation rate σ. For $\mu < \mu_c^{cp} = 0.6066$, the system is in the active phase for any σ. For $\mu_c^{cp} < \mu < \mu^* = 1.0000$, the system is inactive at $\sigma = 0$ (thick solid red line), but an infinitesimal σ takes it to the active phase. For $\mu > \mu^*$, the system is inactive for any σ.

densities $\rho_1(t)$ and $\rho_2(t)$ of sites in inactive states I_1 and I_2, respectively. Spreading simulations start from a single active (seed) site embedded in a system of sites in state I_1. Here we monitor the survival probability $P_s(t)$, the number of sites in the active cloud $N_s(t)$ and the mean-square radius of this cloud, $R^2(t)$.

In both types of runs, the simulation is a sequence of individual events. In each event, a pair of nearest-neighbor sites is randomly selected from the active region. For the spreading simulations, the active region initially consists of the seed site and its neighbors; it is updated in the course of the simulation according to the actual size of the active cluster. For the decay runs, the active region comprises the entire sample. The selected pair than undergoes one of the possible transitions according to eqs. (153) to (156) with probability τw. Here the time step τ is a constant which we fix at 1/2. The time increment associated with the event is τ/N_{pair} where N_{pair} is the number of nearest-neighbor pairs in the active region.

Using this procedure, we investigated the parameter region $0.5 \leq \mu \leq 1.2$ and $0 \leq \sigma \leq 1$. We simulated samples with sizes up to 20000×20000 sites for times up to $t_{max} = 3 \times 10^6$. The $\sigma - \mu$ phase diagram that emerged from these calculations is shown in in Fig. 5.1.

In many respects, it is similar to the phase diagram of the one-dimensional generalized contact process [14]. In the absence of the domain-boundary activation process (i.e., for $\sigma = 0$), the transition from the active phase to the inactive phase occurs at a healing rate of $\mu = \mu_c^{cp} = 0.6066(2)$ which agrees well with the critical point of the simple contact process (see, e.g., Refs. [22, 23]). For healing rates in the interval $\mu_c^{cp} < \mu < \mu^* = 1.0000(2)$, the generalized contact process is inactive at $\sigma = 0$, but an infinitesimal nonzero σ takes it to the active phase. Thus, we find a line a phase transitions at $\mu_c^{cp} < \mu < \mu^*$ and $\sigma = 0$. In addition to this line of $\sigma = 0$ absorbing state transitions, we also find a line of generic (nonzero σ and μ) transitions. In contrast to one space dimension, this line is exactly "vertical" within our accuracy, i.e., the critical healing rate $\mu_c = 1.0000(2)$ does *not* depend on σ for all $\sigma > 0$. We note in passing that our critical healing rate is in agreement with the estimate $\mu_c \approx 0.99(1)$ obtained in Ref. [13] for $\sigma = 1$.

In the following subsections we shall discuss in detail the properties of both phase transition lines as well as special point $(\mu^*, 0)$ that separates them.

5.3.2. Generic Transition. In order to identify the generic transition and to study its critical behavior, we performed sets of spreading simulations at constant domain-boundary activation rate $\sigma = 0.01, 0.05, 0.1, 0.5$ and 1. For each σ, we have varied the healing rate μ varying from 0.8 to 1.1. Figure 5.2 shows the resulting time evolution of the survival probability P_s and the number of sites in the active cloud $N_s(t)$ for $\sigma = 0.1$ and several μ. The data indicate a critical healing rate of $\mu_c = 1.0000(2)$ for this σ value. Analogous simulations for $\sigma = 0.01, 0.05, 0.5$ and 1 yielded, somewhat surprisingly, exactly the same critical healing rate. We thus conclude that in the two-dimensional generalized contact process, the critical healing rate μ_c is independent of σ for all $\sigma > 0$.

Figure 5.3 shows the survival probability P_s and number N_s of active sites as functions of time for all the respective critical points. In log-log representation, the long-time parts of the N_s and P_s curves for different σ are perfectly parallel within their statistical errors, i.e., they differ only by constant factors, confirming that the critical behavior of the generic transition is universal. Fits of the long-time behavior to the pure power laws $P_s = B_\sigma t^{-\delta}$ and $N_s = C_\sigma t^{\Theta}$ give estimates of $\delta = 0.900(15)$ and $\Theta = -0.100(25)$. These values are very close to the mean-field values $\delta_{MF} = 1$ and $\Theta_{MF} = 0$. According to the conjecture by Dornic *et al.* [17], the generic transition should be in the GV universality class. Because the upper critical dimension of this universality class is exactly two, this conjecture corresponds to mean-field behavior with logarithmic corrections.

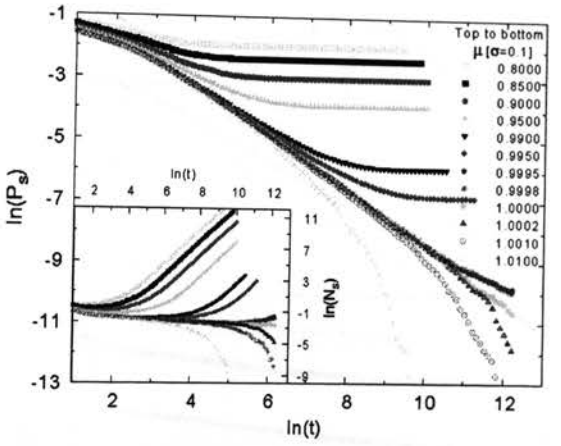

Figure 5.2. (Color online) Spreading simulations at $\sigma = 0.1$ for several μ close to the phase boundary. Main panel: Number N_s of active sites as a function of time t. Inset: Survival probability P_s as a function of time t. The data close to criticality are averages over 10^6 runs on a 4000×4000 system, smaller numbers of runs were used away from criticality.

To test this prediction we compare in Fig. 5.4 plots of $\ln(P_s t)$ vs. $\ln(t)$ (straight lines corresponds to power laws) and $P_s t$ vs. $\ln(t)$ (straight lines correspond to logarithmic behavior). Although both functional forms describe the long-time data reasonably well, the curves in the $\ln(P_s t)$ vs. $\ln(t)$ plot show a systematic downward curvature. Moreover, the semi-logarithmic plot, $P_s t$ vs. $\ln(t)$, leads to straight lines over a longer time interval which we take as evidence for GV critical behavior. We performed an analogous analysis for number of active sites N_s. Again, both a simple power law and mean-field behavior with logarithmic corrections describe the data reasonably well, with the quality of fits being somewhat higher for the latter case. We also measured (not shown) the mean-square radius $R^2(t)$ of the active cloud as a function of time. A pure power-law fit of its long time behavior, $R^2(t) \sim t^{2/z}$, gives $2/z = 0.97(4)$ ($z = 2.06(8)$). The data can be described equally well by mean-field behavior $R^2(t) \sim t$ with logarithmic corrections.

In addition to the spreading runs, we also performed density decay runs at the generic phase boundary. The resulting density of active sites ρ as a function of time can be fitted with a pure power law $\rho(t) \sim t^{-\alpha}$ giving a very small value of $\alpha = 0.080(4)$. A better fit is achieved with the simple logarithmic time dependence

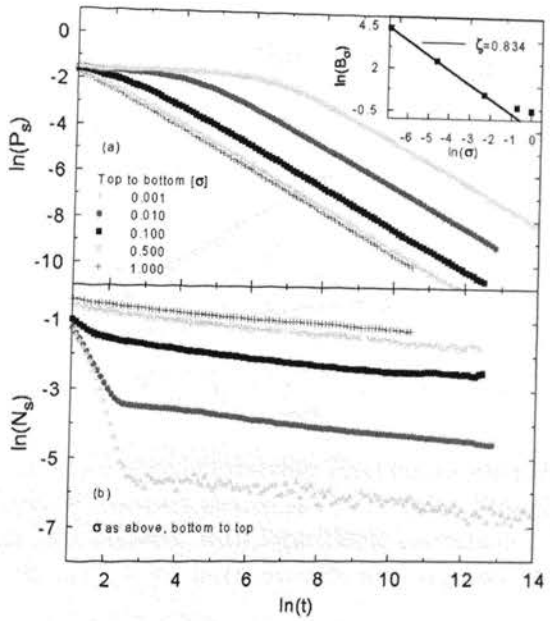

Figure 5.3. (Color online) Survival probability P_s and number of active sites N_s as functions of t for several points located on the generic phase boundary $\mu = 1.0000$ (2×10^6 to 10^7 runs used). Inset: prefactor B_σ vs. σ. The straight line is a fit to a power-law $B_\sigma \sim \sigma^{-\zeta}$.

$\rho(t) \sim 1/\ln(t/t_0)$ (with t_0 a microscopic time scale) expected for the GV universality class. This type of behavior is demonstrated in Fig. 5.5.

In summary, although all our results for the generic transition can be fitted both by pure power laws and by mean-field behavior with logarithmic corrections, the latter functional forms yield fits of somewhat higher quality. We also note that the critical exponents resulting from the pure power-law fits approximately fulfill the hyperscaling relation $\Theta - d/z = -\alpha - \delta$. However, the agreement is not very good (in particular, it is significantly worse than in one dimension [14]), indicating that the measured pure power-laws are not the true asymptotic behavior. Our results thus support the conjecture that the generic transition of the two-dimensional generalized contact process with two inactive states is in the GV universality class.

5.3.3. Transition at $\sigma = 0$. After addressing the generic transition, we now discuss in more detail the line of phase transitions occurring at $\sigma = 0$ and

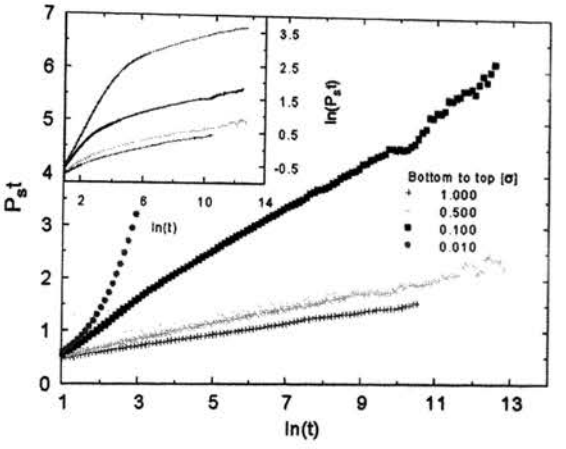

Figure 5.4. (Color online) Survival probability $P_s(t)$ for several points located on the generic phase boundary plotted as $P_s\, t$ vs. $\ln(t)$. Straight lines correspond to mean-field behavior with logarithmic corrections. Inset: Same data plotted as $\ln(P_s)\, t)$ vs. $\ln(t)$. Straight lines represent pure power laws.

$\mu_c^{cp} < \mu < \mu^*$. To study these transitions, we carried out several sets of simulations for fixed healing rate μ and several σ values approaching $\sigma = 0$.

We start by discussing the density decay runs. Figure 5.6 shows the stationary density ρ_{st} of active sites (reached at long times) as function of σ for several values of the healing rate μ. The figure shows that the stationary density depends linearly on σ for all healing rates in the interval $\mu_c^{cp} < \mu < \mu^*$, i.e., $\rho_{st} = B_\mu \sigma^\omega$ with $\omega = 1$ and B_μ being a μ-dependent constant. We also analyzed how the prefactor B_μ of this mean-field-like behavior depends on the distances from the simple contact process critical point and from the special point at $\mu = \mu^*$ and $\sigma = 0$. As inset (a) of Fig. 5.6 shows, B_μ diverges as $(\mu - \mu_c^{cp})^{-\kappa}$ with $\kappa = 1.56(5)$. According to inset (b), it vanishes as $(\mu^* - \mu)^{\kappa^*}$ with $\kappa^* \approx 0.23$ when approaching μ^*.

At the critical healing rate μ_c^{cp} of the simple contact process, the stationary density displays a weaker σ-dependence. A fit to a power-law $\rho_{st} \sim \sigma^{\omega_{cp}}$ gives an exponent value of $\omega_{cp} = 0.274(5)$.

Let us now compare these results with the behavior of spreading simulations in the same parameter region. Figure 5.7 shows the survival probability $P_s(t)$ and the number of active sites $N_s(t)$ for a fixed healing rate of $\mu = 0.8$ and several values of the boundary rate σ. After an initial decay, the number of active sites grows with time for all σ values, establishing that the system is in the active phase for

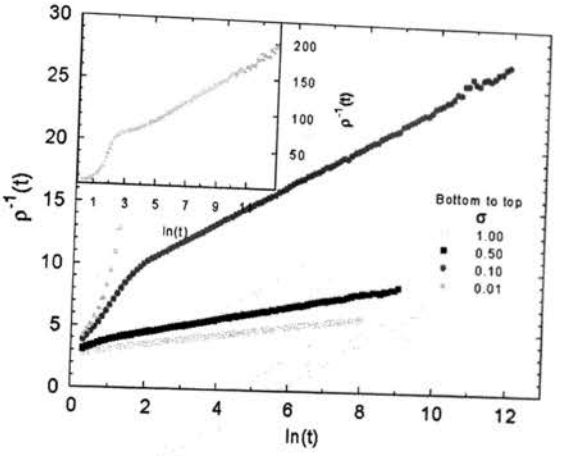

Figure 5.5. (Color online) Density of active sites plotted as $\rho^{-1}(t)$ vs. $\ln(t)$ for several points located on the generic phase boundary. The data are averages over 100 runs with system size 500 × 500. The curve for $\sigma = 0.01$ is shown in the inset because its density values are much smaller than those of the other curves.

all $\sigma > 0$. In agreement with this, the survival probability approaches a nonzero constant in the long-time limit. Remarkably, this stationary survival probability does *not* approach zero with vanishing σ. Instead, it approaches a σ-independent constant. We performed similar sets of simulations at other values of μ in the range $\mu_c^{cp} < \mu < \mu^*$, with analogous results.

We thus conclude that the behavior at the $\sigma = 0$ transition of the two-dimensional generalized contact process is very similar to the one-dimensional case. It can be understood in terms of the domain-wall motion as follows [14]. The relevant long-time degrees of freedom at $\mu > \mu_c^{cp}$ and $\sigma \ll 1$ are the domain walls between I_1 and I_2 domains. These walls can hop, branch and annihilate. The crucial observation is that the rates which control the domain wall dynamics are all proportional to σ for $\sigma \ll 1$, implying that their ratios are σ-independent. Consequently, the stationary state of the domain walls does not depend on σ for $\sigma \ll 1$. This explains why the survival probability P_s saturates at a nonzero, σ-independent value in Fig. 5.7. It also explains the σ-dependence of the stationary density ρ_{st} because active sites are created mostly at the domain walls at rate σ. Therefore, their stationary density is proportional to both σ and the stationary domain wall density ρ_{dw}, i.e., $\rho_{st} \sim \sigma\rho_{dw}$, in agreement with Fig. 5.6. Based on this argument, the exponent κ^* in inset (b)

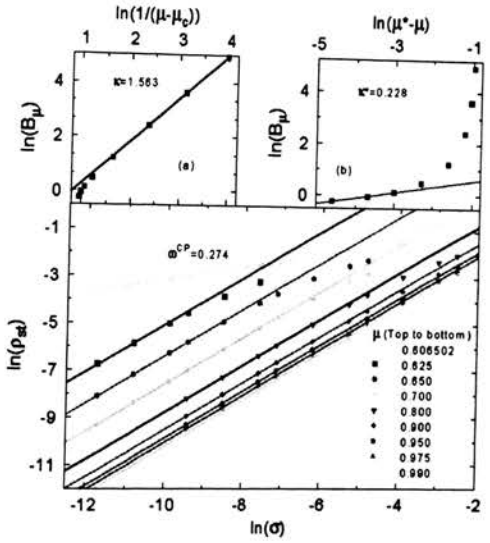

Figure 5.6. (Color online) Density decay simulations. Main panel: stationary density ρ_{st} as a function of the boundary rate σ for various healing rates μ. For $\mu_c^{cp} < \mu < \mu^*$, the solid lines are fits of the low-σ behavior to $\rho_{st} = B_\mu \sigma$. At the simple contact process critical point, $\mu = \mu_c^{cp} = 0.6066$, we fit to the power-law $\rho_{st} \sim \sigma^{\omega_{cp}}$ which gives an exponent of $\omega_{cp} = 0.274(5)$. The data are averages over 300 to 600 runs with system sizes 100×100. Inset a: prefactor B_μ of the linear σ dependence as a function of $\mu - \mu_c^{cp}$. A fit to a power law gives $B_\mu \sim (\mu - \mu_c^{cp})^{-\kappa}$ with $\kappa = 1.56(5)$. Inset b: prefactor B_μ as a function of $\mu^* - \mu$. A fit to a power law gives $B_\mu \sim (\mu^* - \mu)^{\kappa^*}$ with $\kappa^* \approx 0.23$.

of Fig. 5.6 should be identical to the exponent β of the generic transition line [14], which vanishes in mean-field theory. Our value, $\kappa^* \approx 0.23$ is thus somewhat too high which we attribute to it not representing the asymptotic behavior, in agreement with the significant curvature of the data in inset (b) of Fig. 5.6.

Just as in one dimension, the phase transition line at $\sigma = 0$ and $\mu_c^{cp} < \mu < \mu^*$ is thus not a true critical line. It only appears critical because the stationary density ρ_{st} (trivially) vanishes with σ. Correspondingly, the time evolution right on the transition line $\sigma = 0$ does not display critical power laws. also implies that the point $(\mu, \sigma) = (\mu^*, 0)$ is not a multicritical point, but a simple critical point in the same universality class as the generic transition.

5.3.4. Scaling of ρ_{st} at The Contact Process Critical Point $(\mu_c^{cp}, 0)$. The behavior of the stationary density of active sites ρ_{st} close to the simple contact process

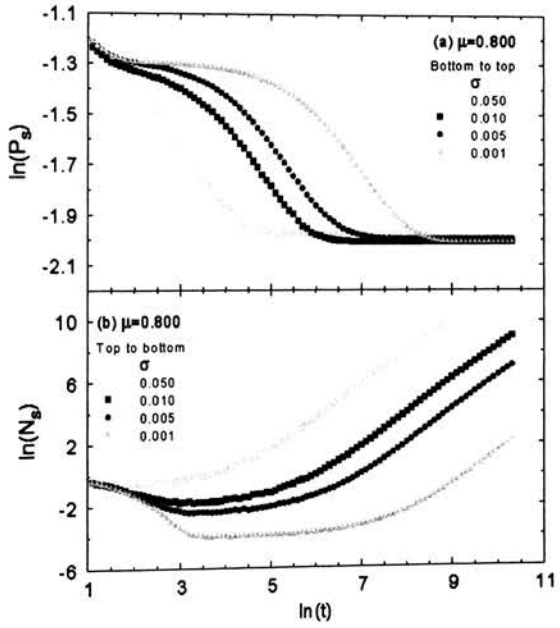

Figure 5.7. (Color online) Spreading simulations: Survival probability P_s and number of active sites N_s as functions of time t for a fixed healing rate of $\mu = 0.8$ and several σ. The data are averages over 2000 to 10000 runs on a 4000×4000 system.

critical point at $\mu = \mu_c^{cp}$ and $\sigma = 0$ can be understood in terms of a phenomenological scaling theory. We assume the homogeneity relation

$$\rho_{st}(\Delta\mu, \sigma) = b^{\beta_{cp}/\nu_{cp}^{\perp}} \rho_{st}(\Delta\mu\, b^{-1/\nu_{cp}^{\perp}}, \sigma b^{-y_{cp}}) \tag{157}$$

where $\Delta\mu = \mu - \mu_c^{cp}$, and b is an arbitrary scale factor. $\beta_{cp} = 0.584$ and $\nu_{cp}^{\perp} = 0.734$ are the usual order parameter and correlation length exponents of the two-dimensional contact process [22, 23], and y_{cp} denotes the scale dimension of σ at this critical point. Setting $b = \sigma^{1/y_{cp}}$ gives rise to the scaling form

$$\rho_{st}(\Delta\mu, \sigma) = \sigma^{\beta_{cp}/(\nu_{cp}^{\perp} y_{cp})} X\left(\Delta\mu\, \sigma^{-1/(\nu_{cp}^{\perp} y_{cp})}\right) \tag{158}$$

where X is a scaling function. At criticality, $\Delta\mu = 0$, this leads to $\rho_{st}(0, \sigma) \sim \sigma^{\beta_{cp}/(\nu_{cp}^{\perp} y_{cp})}$ (using $X(0) = \text{const}$). Thus, $\omega_{cp} = \beta_{cp}/(\nu_{cp}^{\perp} y_{cp})$. For $\sigma \to 0$ at nonzero

$\Delta\mu$, we need the large-argument limit of the scaling function X. On the active side of the critical point, $\Delta\mu < 0$, the scaling function behaves as $X(x) \sim |x|^{\beta_{cp}}$ to reproduce the correct critical behavior of the density, $\rho_{st} \sim |\mu - \mu_c^{cp}|^{\beta_{cp}}$.

On the inactive side of the critical point, i.e., for $\Delta\mu > 0$ and $\sigma \to 0$, we assume the scaling function to behave as $X(x) \sim x^{-\kappa}$. We thus obtain $\rho_{st} \sim (\Delta\mu)^{-\kappa}\sigma^{\omega}$ (just as observed in Fig. 5.6) with $\omega = (\beta_{cp} + \kappa)/(\nu_{cp}^{\perp} y_{cp})$. As a result of our scaling theory, the exponents ω, ω_{cp} and κ are not independent, they need to fulfill the relation $\omega_{cp}(\beta_{cp} + \kappa) = \beta_{cp}\omega$. Our numerical values, $\omega = 1$, $\omega_{cp} = 0.274$ and $\kappa = 1.56$ fulfill this relation in very good approximation, indicating that they represent asymptotic exponents and validating the homogeneity relation (157). The resulting value for the scale dimension y_{cp} of σ at the simple contact process critical point is $y_{cp} = 2.9(1)$.

5.4. CONCLUSIONS

To summarize, we investigated the two-dimensional generalized contact process with two inactive states by means of large-scale Monte-Carlo simulations. Its global phase diagram is very similar to that of the corresponding one-dimensional model. In particular, the generic ($\sigma > 0$) phase boundary between the active and inactive phases does not continuously connect to the critical point of the $\sigma = 0$ problem, i.e., the critical point $(\mu_c^{cp}, 0)$ of the simple contact process. Instead, it terminates at a separate end point $(\mu^*, 0)$ on the μ axis. As a result, the two-dimensional generalized contact process has two nonequilibrium phase transitions. In addition to the generic transition occurring for $\sigma > 0$, there is a line of transitions at $\sigma = 0$ and $\mu_c^{cp} < \mu < \mu^*$. We note that there is one interesting difference between the phase diagrams in one and two dimensions. In one dimension, the critical healing rate μ_c increases with increasing boundary rate σ. In contrast, the results of this paper show that the critical healing rate in two dimensions is completely independent of σ. The reason for this difference is presently an open question.

To determine the critical behavior of the generic transition, we performed simulations at and close to several points on the generic ($\sigma > 0$) phase boundary. We found the same critical behavior for all of these points, i.e, it is universal. Our data can be fitted reasonably well with pure power laws, giving the exponents $\Theta = -0.100(25)$, $\delta = 0.900(15)$, $\alpha = 0.080(4)$, and $z = 2.06(8)$. However, fits of equal and sometimes even better quality over longer ranges of time can be obtained by fitting to mean-field critical behavior, $\Theta = 0$, $\delta = 1$, $\alpha = 0$, and $z = 2$ with logarithmic corrections. We thus conclude that our results support the conjecture [17] that the critical behavior of the two-dimensional generalized contact process is in the generalized voter (GV)

universality class which is right at its upper critical dimensions. (In other words, the DP2 class coincides with the GV class in two dimensions). We also note that our simulations showed no indications of the transition being split into a symmetry-breaking transition and a separate DP transition as found in some absorbing-state Potts models [18].

As in one space dimension, the line of transitions at $\sigma = 0$ and $\mu_c^{cp} < \mu < \mu^*$ is not a critical line. The survival probability P_s remains finite when approaching this line. The density ρ of active sites vanishes, but simply because the domain-boundary activation rate σ vanishes. The behavior in the vicinity of the transition line is controlled by the dynamics of the I_1-I_2 domain walls which is not critical for $\mu_c^{cp} < \mu < \mu^*$.

Crossovers between various universality classes of absorbing state transitions in *one dimension* have been investigated by several authors [24, 25, 26, 27]. Some of the scenarios lead to conventional crossover scaling (of the type $\sigma_c \sim (\mu - \mu_c^{cp})^{1/\phi}$). Park and Park [25] found a discontinuous jump in the phase boundary along the so-called excitatory route from infinitely many absorbing states to a single absorbing state. There also is some similarity between our mechanism and the so-called channel route [26] from the PC universality class to the DP class which involves an infinite number of absorbing states characterized by an auxiliary density (which is density of I_1-I_2 domain walls in one-dimensional the generalized contact process [14]). To the best of our knowledge, a similarly systematic investigation of crossovers between absorbing state universality classes in two space dimensions has not yet been performed.

As our results suggest that the two-dimensional generalized contact process is right at the upper critical dimensions, the critical behavior of its (generic) phase transition in dimensions $d > 2$ should be governed by mean-field theory.

Acknowledgements

We acknowledge helpful discussions with Ronald Dickman, Geza Odor and Hyunggyu Park. This work has been supported in part by the NSF under grant no. DMR-0339147 and DMR-0906566 as well as by Research Corporation.

[1] V. P. Zhdanov and B. Kasemo, Surf. Sci. Rep. **20**, 113 1994.

[2] B. Schmittmann and R. K. P. Zia, in Phase Transitions and Critical Phenomena, edited by C. Domb and J. L. Lebowitz Academic, New York, 1995, Vol. **17**, p. 1.

[3] J. Marro and R. Dickman, Nonequilibrium Phase Transitions in Lattice Models Cambridge University Press, Cambridge, England, 1999.

[4] H. Hinrichsen, Adv. Phys. **49**, 815 2000.

[5] G. Odor, Rev. Mod. Phys. **76**, 663 2004.

[6] S. Lbeck, Int. J. Mod. Phys. B **18**, 3977 2004.

[7] U. C. Tuber, M. Howard, and B. P. Vollmayr-Lee, J. Phys. A **38**, R79 2005.

[8] P. Grassberger and A. de la Torre, Ann. Phys. N.Y. **122**, 373 1979.

[9] H. K. Janssen, Z. Phys. B **42**, 151 1981.

[10] P. Grassberger, Z. Phys. B **47**, 365 1982.

[11] P. Rupp, R. Richter, and I. Rehberg, Phys. Rev. E **67**, 036209 2003.

[12] K. A. Takeuchi, M. Kuroda, H. Chate, and M. Sano, Phys. Rev. Lett. **99**, 234503 2007.

[13] H. Hinrichsen, Phys. Rev. E **55**, 219 1997.

[14] M. Y. Lee and T. Vojta, Phys. Rev. E **81**, 061128 (2010).

[15] P. Grassberger, F. Krause, and T. von der Twer, J. Phys. A **17**, L105 1984.

[16] D. Zhong and D. B. Avraham, Phys. Lett. A **209**, 333 1995.

[17] I. Dornic, H. Chate, J. Chave, and H. Hinrichsen, Phys. Rev. Lett. **87**, 045701 (2001).

[18] [18] M. Droz, A. L. Ferreira, and A. Lipowski, Phys. Rev. E **67**, 056108 (2003).

[19] [19] O. Al Hammal, H. Chate, I. Dornic, and M. A. Munoz, Phys. Rev. Lett. **94**, 230601 (2005).

[20] T. E. Harris, Ann. Probab. **2**, 969 1974.

[21] We studied the phase diagram for $\bar{\mu} \neq \mu$ in one space dimension in Ref. [14]. We found that the qualitative be- havior is the same as in the $\bar{\mu} = \mu$ case. We expect the same to be true in two space dimensions.

[22] R. Dickman, Phys. Rev. E **60**, R2441 (1999).

[23] T. Vojta, A. Farquhar, and J. Mast, Phys. Rev. E **79**, 011111 (2009)

[24] G. Odor and N. Menyhard, Phys. Rev. E **78**, 041112 2008.

[25] S.-C. Park and H. Park, Phys. Rev. E **76**, 051123 2007.

[26] S.-C. Park and H. Park, Phys. Rev. E **78**, 041128 2008.

[27] S.-C. Park and H. Park, Phys. Rev. E **79**, 051130 2009.

VITA

Man Young Lee was born on April 01, 1972 in Seoul, Korea(South of). He received his bachelor degree in physics from Soongsil University, Seoul, Korea in Feb 1998. In the same year he joined the group of Prof. Dr. Cha-Hwan Oh as a graduate student at the Physics Department, Hanyang University, Seoul, Korea. His research topic for a master degree was for development of a small gamma camera and study for characteristics of scintillation crystals. In August 2004, he started his Ph. D program in the Department of Physics, Missouri University of Science and Technology (formerly University of Missouri-Rolla). From on August 2005, he was supervised by Dr. Thomas Vojta.